Offshore Hydrogen Production

Analysis of Different methods of hydrogen production using offshore wind

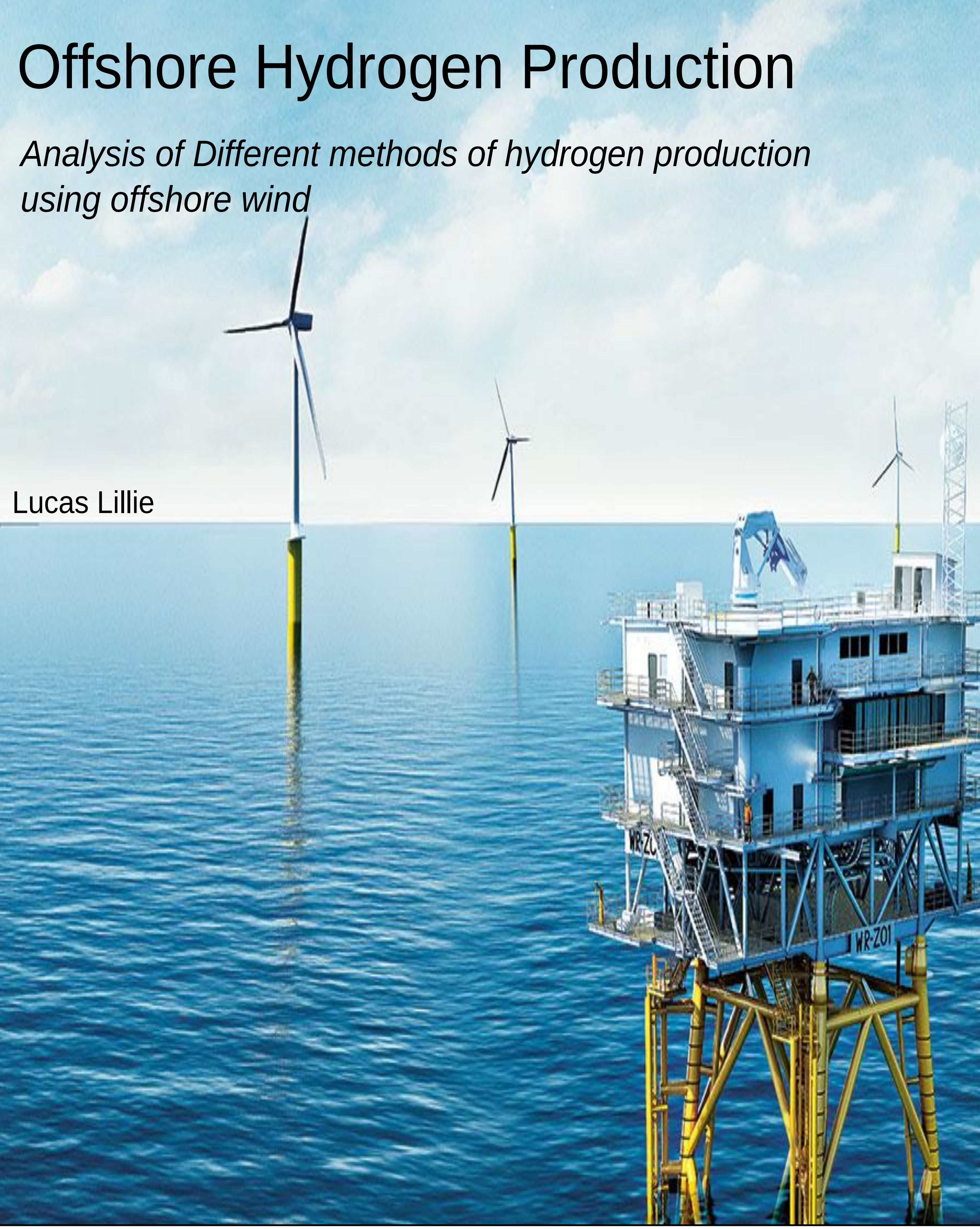

Lucas Lillie

NTNU
Norwegian University of Science and Technology

TU Delft

NTNU
Kunnskap for en bedre verden

Department of Marine Technology

Analysis of different methods of hydrogen production using offshore wind

Author:
Lucas Lillie

Advisors:

Bart Ummels

Zhen Gao

Svein Saevik

Committee Chair:

Andrei Metrikine

TU Delft

October, 2022

Table of Contents

List of Figures

List of Tables

Abstract

With an increasing shift to renewable energies, solutions are required to overcome that variability and unpredictability of power production that comes with it. Hydrogen is one solution that can overcome this issue since it can be produced using renewable energy through electrolysis, it can be transported to shore efficiently by pipelines and it can be stored, similar to natural gas. Not only can hydrogen be used as a way to store energy, it can also be used directly as a basis for steel production and for long-distance transport.

Using wind energy, specifically offshore wind farms, as the source for hydrogen is an idea that is gaining attention. Currently, wind turbines are electrically connected, bringing their electricity to shore by high-voltage cables, allowing hydrogen to be produced onshore. Hydrogen could however also be produced at a central location in the offshore wind farm or at each individual offshore wind turbine, removing the need for high-voltage cables. The purpose of this research is to explore different methods of hydrogen production and validate a model that can simulate each method. The goal is to be able to compare the different methods and quantify the losses of producing hydrogen offshore as opposed to onshore.

A time-based simulation model has been developed to represent an offshore wind farm, which would either produce electricity or hydrogen, which eventually arrives onshore. High-resolution wind data are used to correctly include short-term fluctuations in wind output. The N.O. Jensen wake model is implemented to capture the wake effects. Since wake is typically modelled steady-state, specific attention has been given to include the moving of the wake through the wind park. The power outputs for each turbine in the model could be accurately determined based on the incoming wind data. It is found that the spatial effect reduces max wind power variations at the wind farm level to about 22% of first turbine in the sting, as expected.

The output of the simulation model compares the power losses of producing hydrogen through four scenarios. This model uses a total of eleven wind turbine strings of seven 10 MW wind turbines each. The power output calculated would then be used to determine the amount of hydrogen produced. By applying electrical power loss equations and calculating the pressure drops for hydrogen traveling in a pipeline by assuming steady-state and isothermal, the losses are calculated for each scenario. A sensitivity study is performed to see the effects of changing model parameters on each of the different scenarios.

The model developed in this thesis allows for comparison of electricity production and hydrogen production by offshore wind turbines. It is found that producing hydrogen at the wind farm level and then transporting hydrogen to the shore (Scenario 2) has lower overall energy losses (kg of hydrogen available on shore) than using electrical cables. The same goes for individual offshore hydrogen production (Scenario 3). A high-level exploration of the economics indicates that both scenarios 2 and 3 are more economically feasible when only looking at transportation costs. It is recommended that further research is done to be able to determine which method of hydrogen production would be the most effective by taking the transportation losses and economics into account.

Preface

This thesis was the final obstacle to obtain my master's degree in Offshore and Dredging Engineering from Delft University of Technology in combination with graduating from Norwegian University of Science and Technology.

From TU Delft, I would like to personally thank Bart Ummels for his help and passion for my thesis. He taught me skills to use in both my engineering studies and life. I fear to think how my thesis would have turned out without his help.

From NTNU, I would like to personally thank Zhen Gao for his availability and support for any questions/concerns I had for my thesis. Without him, this thesis could not have been started. I would also like to thank my family and friends for their endless support whenever I needed them which helped me mentally.

Lastly, I would like to thank Opeth and Alice in Chains, two bands I would listen to on repeat, to calm my nerves and offered me a much-needed distraction be able to complete my thesis.

Lucas Lillie

TU Delft, October 12

Nomenclature

α	Wake Decay coefficient [-]
ϵ	Surface Roughness [mm]
μ	kinematic Viscosity [Pa s]
ρ	Density [kg/m^3]
A	Cross-sectional Area of Pipe [m^2]
D	Pipe Diameter [m]
f	Friction Factor [-]
g	Gravitational constant [m/s^2]
L	Pipe Length [m]
M	Mass Flow Rate [kg/s]
P	Power [MW]
p	Pressure [Pa]
Q	Volumetric flow rate [m^3/s]
R	Universal Gas constant [J/kg K]
Re	Reynolds Number [-]
T	Temperature [℃]
w	Fluid Velocity [m/s]
MEUR	Millions of Euro

1 Introduction

There is a rapid shift over the past 10 years to move away from fossil fuels and into the field of renewable energy for a variety of reasons [35]. One big factor is to fight climate change by lowering carbon emissions and reaching climate goals stated by the Paris Agreement that the United Nations have defined. One sector that is growing is harnessing the power of wind to produce electricity.The need for the switch to renewable energy is urgent to combat global warming [18]. Besides its massive impact of producing zero emissions, renewable energy such as wind power does have its drawbacks. Unlike oil, that can be stored and transported very easily, electricity can't or at least not in the same way. Also, renewables such as solar and wind power is intermittent since it depends on environmental conditions. There could be periods of low wind speeds meaning that electricity from wind would not be enough to supply the demand. Or there could be periods of time where there is too much supply of electricity than there is demand for it. This would mean that excess electricity would be a waste. few solutions for the storage of electricity could exist in:

- Battery
- Pumped Water storage
- Hydrogen

The first logical choice to choose as a storage device for energy from wind power would be the use of batteries as people typically associate battery and electricity together. However, with current technology, batteries are not the best choice as they are expensive and are not able to store large amounts of electricity. Pumped water storage uses a large dam with a body of water attached to it. The dam stores energy in the form of pumping water to a larger height. Most of the world's energy storage is done this way. The downside of this method of storage is the fact that is has a very large dependency in power systems based on geographical features, so building this type of structure is not feasible where these geographical conditions do not exist [49]. Since hydro power is well developed and with further growth in the renewable sector, a vast amount of new storage capacity will be needed, so additional options need to be implemented. Hydrogen is a new alternative form for energy storage and will be the focus of this literature review and Thesis.

1.1 Onshore and Offshore Wind

Wind energy and Solar PV are widely used forms of renewable energy. When it comes to wind energy, there are two categories: offshore and onshore wind turbines and each have their own disadvantages and disadvantages. Because of this push for electricity from renewable energy sources, this made the cost of renewable energy considerably cheaper over the years.

For onshore wind farms commissioned in 2018, it reached an average cost of electricity that was 13% lower than in 2017 and 35% lower than in 2010. For Solar PV, the levelized cost of energy decreased by 77%. In Europe, Offshore wind farms are increasingly competing at wholesale electricity prices [19]. Because of the decreasing prices of renewable energy, more wind farms are being built and are reaching larger sizes, in the order of 1000 MW. This has led to an increase of turbine sizes to exploit more of the wind resource available.

1.1.1 Onshore Wind Turbine

As the names implies, Onshore Wind Turbines are those that are placed on land. Onshore wind turbines are the oldest and most common source for wind energy today. The reason for its popularity could be attributed to multiple reasons. The cost of installing an onshore wind turbine is relatively cheap compared to offshore wind turbines since there are lower costs for operation and maintenance, there are infrastructures for energy transmission is already existent. Because of the profitability of offshore wind energy available, there has been an increase of the average onshore turbine rated power, from an average of 1.42 [MW] in the year 2005 to around 2.47 [MW] in the year 2014. [11]

However, there are downsides to building wind turbines onshore. Since there are many structures on land either natural or manmade, areas to install wind farms that experience wind uninterrupted from these structures are harder to find unless the turbine is larger. Another big disadvantage would be of visual pollution that comes with an onshore wind farm, as they are unsightly to people and causes local opposition for the construction of wind farms which increase the risks. [12]

1.1.2 Offshore wind turbines

The option of placing turbines offshore eliminates some of the disadvantages that onshore turbines experience. In 2016, the average distance to shore for an offshore wind farm built in that year was around 43.5 Kilometers [14]. For offshore wind farms that have an installed capacity of 400-500 [MW], the average distance to shore was around 70 kilometers [24]. A benefit for installed wind farms far from the coast is less visual and noise pollution affecting people [44]. Offshore turbines also get to experience wind that's been unaffected by natural/manmade structures. This means that the average velocity of wind offshore is faster and more consistent than that of onshore wind [7]. Because of this increase of consistency of higher velocity winds, offshore turbines generally generate electricity 2-3 longer than that of its onshore counterpart [7]. With this expansion to offshore, there are drawbacks. The construction costs are larger than that of an onshore construction[7]. Another drawback is that the considerations of waves must be taken into account which effects the design of the support structure.

Fixed Support Structures

When it comes to offshore wind turbines, the support structure keeps the wind turbine from touching the water and handles the loads of the waves. The most common support structure for offshore wind turbines are monopile foundations, reaching a number of 3720 units in 2017 [15]. Then with 315 units, the jacket support structure and with 283 units for gravity based structures [15]. Moving towards the year 2020, 74.8% of the global offshore wind foundation market while for jacket support structures totals at around 10.8% [38]. Support structures are chosen based on the soil conditions and the depth of the water of the area of interest. Fixed Support structures are generally limited by the water depth.

Floating

In deeper waters, there are many areas that provide fast and constant wind speeds that are too deep for fixed support structures [7]. Instead, floating structures are used. In addition for its advantage of being able to be placed in deeper waters, floating structures has no need for scour protection, and a reduction of noise during set up [6]. By eliminating the need for the support structure to be fixed to the ground, other considerations must be considered. The coupled dynamic motion of the Wind Turbine and floater, the excitation from the waves and the mooring system must now be included in the considerations for designing a floating Turbine. There are multiple different types of floating structures, but the 4 main types are the Spar-Buoy type,Tension-leg platform (TLP) type,Semi-submersible type (Column stabilised) and Pontoon-type (Barge-type)

1.2 LCOE

A big factor when determining if up-scaling is worth it is to consider the costs. When a turbine power rating increases consequently the mass, size and other parameters to increase. These increases in parameters cause the price of an individual turbine to become more expensive. Currently, the largest turbine available for the market is 11 MW with a 14-15 MW in prototype testing. Interestingly, even though the average turbine has increased, the levelized cost of energy (LCOE) has decreased by about 40% from 2014-2019 [31]. The LCOE can be described by the following equation. [50]:

$$LCOE = \frac{ICC \times FCR + O\&M}{AEP} \tag{1.1}$$

where the ICC is the Initial Capital Cost which covers the cost of material and instillation. FCR stands for the Fixed Charge Rate which is the percentage of the wind farms cost that is required per year to cover the minimal annual cost requirements, O&M is the operation and maintenance costs, and the AEP is the annual energy production. The method to calculate the LCOE is to take a wind farm that has a certain capacity and study the costs, then upscale the turbines but keep the capacity of the wind farm the same and again calculate the costs. By calculating the new ICC, the O&M costs and the AEP of the new wind farm, the LCOE can be found. Of course, this is easier said than done.

1.2.1 Effects of Turbine Up sizing for monopile based foundations

The goal of determining if up-scaling is economically feasible is by having a lower LCOE. To achieve this goal, Both the AEP must increase, and the O&M and ICC must be relatively low. Naturally, when increasing the turbines capacity, the AEP will increase, but the effects of the O&M and ICC needs to be determined.

By looking at different scenarios from [31], the effects of up-scaling the 6 MW monopile turbines in a 500 [MW] plant capacity can be seen.

Electrical Infrastructure

From going from 6 [MW] to 20 [MW] turbines, the cost of array cables are more than 50% cheaper [31]. This is because there are less turbines that need to be connected to the grid. However, this reduction of price begins to level off since the the spacing required by the turbines (7D) to reduce the wake increase with the increase of turbine rating [31].

Monopile costs

The trend for the electrical infrastructure is the similar for the capital costs for the monopile as it decreased by 13.7% from a 6 [MW] to a 20 [MW] turbine [31]. Since the monopile comprises a large part of the initial costs, this reduction for the monopile price contributes greatly to the overall reduced price.

Operations and maintenance's costs

When increasing the capacity of the turbines but keeping the overall wind farm capacity the same, the number of failures decrease since there are less turbines since failure scales with the number of assets as described in [31]. Since there is an inverses relation between the number of turbines and the failure rate, there are diminishing returns as the ratings increase.

Effects to LCOE

The results of the up-scaling showed that the levelized cost of energy reductions of over 23% is possible[31]. This study shows that up-sizing of monopile based foundation of wind farms is economically feasible and can be expected that future installations of wind farms would have an increased size of wind turbines.

1.2.2 Floating and the Effects of LCOE when upscaling

This trend is not just limited to monopile based foundations, but also applies to floating wind turbines based on the study of Yuka Kikuchi and Takeshi Ishihara 2019 [16]. The study looks at the LCOE for a 100 MW capacity farm for 2 [MW], 5 [MW] and 10 [MW] floating wind turbines. It is assumed that the annual O&M costs are the same. The results showed that there was a decrease in LCOE for larger wind floating turbines. Similar in the case for the monopiles, the reason for the decrease in the LCOE is the fact that less turbines are used. This makes the costs of installation, mooring lines and floaters decreases. The only price that increases is the wind turbine itself. The increase of the wind turbine price is offset by the decrease of prices mentioned earlier. This relation is summarized in the following figure can be seen in the following figure [50]:

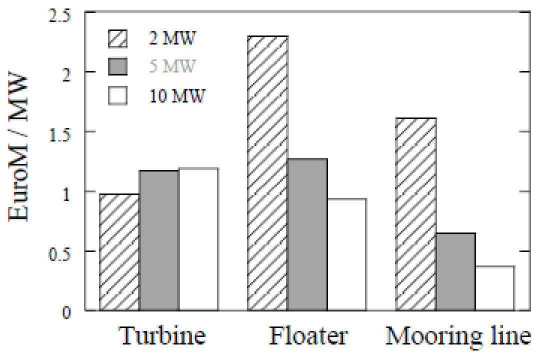

Figure 1.1: Up-scaling effects on cost

1.2.3 Up-scaling

WWhen the size of the Turbine increases, the support structure also must increase to accommodate the new turbine size. This is even more complicated for FOWTs as not only the supporting structure must be adjusted to fit the upscale turbine, the requirements for stability and flotation's must still be held. FOWTs have coupled motions from waves and frequency responses. These elements are why simple scaling of the power is not feasible and other methods must be explored.[12]

1.3 Uses for Hydrogen

To completely move away from oil and gas is more difficult in some industries compared to others. Electricity in itself is not enough for some applications, such as the steel or transportation industry.

1.3.1 Steel Industry

This type of industry is responsible for 9% of carbon dioxide emissions due to the need for coal [22]. Electricity does not meet the demands for the steel industry, but by using green hydrogen as a fuel source instead, the industry could largely decarbonize and overall lower the amount of carbon dioxide in the air. Using hydrogen in this sense is not new to industry and pilot programs are currently in progress [22]. Although the initial switch would cause an increase to the price of steel, this price change would likely decrease with decreasing costs of renewable electricity [22].

1.3.2 Transportation Industry

Not only can the steel energy lower its carbon dioxide emissions, but the transportation can also decrease theirs with the use of hydrogen. Hydrogen provides the best alternative for fossil fuels for heavy vehicles such as long-haul trucks because of the requirement for large energy storage and fast refuel rates. Theses heavy vehicles includes long haul trucks, buses, hybrid trains. There are cars now that can travel long distances by using hydrogen (Up to 604 km) [37]. For smaller sized vessels, hydrogen can be used as a fuel source, while for larger vessels, ammonia is the alternative. However, for aviation it is trickier. It is inevitable that fossil fuels will no longer be in production, either due to human interests to not use it or the world runs out of it. The question for aviation remains. For land-based transport, alternatives exists but for aviation it's still up in the air. Although hydrogen can be used for planes to burn in the engine, the fuselage needs to be much larger to compensate for the use of hydrogen [32] which would cause issues for transportation for long distances. One solution is in the use of ammonia but much more research and development are needed [23], but hydrogen could be a basis.

1.3.3 Storage

To be able to use hydrogen for a later period, it needs to be stored. There are a few main differences when storing hydrogen compared to storing natural gas: Hydrogen embrittlement and increased leakage at pipeline sections or links in valves due to small size of hydrogen molecules [34]. This means that the type of material the pipe needs to be to transport hydrogen must be resistant to embrittlement. The impact that hydrogen embrittlement has on pipes falls outside the scope of the thesis since the model used later in the thesis assumes the pipeline is meant for hydrogen transport with either low grade steel or plastic pipes. The two main storage methods of hydrogen is liquid or gas storage. For the storage of gas, there are two ways to do this. The first way would be to have fabricated tanks that would hold hydrogen between pressures of 350 - 700 [bars] for smaller storage vessels [25] while larger cylindrical storage devices can store hydrogen up to 100 [bars] [34]. The other method would use natural underground structures. These underground structures would generally be either aquifers or salt caverns. The most cost-effective way of storing hydrogen would be with the use of salt caverns. The second approach to storing hydrogen is in its liquid form. This means that hydrogen is cooled as a liquid and then stored. This method has an advantage as the density of hydrogen increases in its liquid state. The major drawback is that a lot of energy is needed to store hydrogen in this method [25].

1.4 Production of Hydrogen

Until recently, hydrogen production was mainly focused for petroleum refining and production of fertilizers. There was no real incentive for using hydrogen as a fuel source since the processes emits large amounts of CO2 from fossil carbohydrates so it would have been counter intuitive to use hydrogen as a storage device based on fossil fuel emissions when the goal is to have zero carbon emissions. Hydrogen production can be be classified as 3 different types: grey, blue and green hydrogen. Grey hydrogen is hydrogen production methods that use fossil fuels and gives carbon dioxide (CO_2) as a byproduct. Blue hydrogen also has CO_2 as a byproduct but up to 90% of emissions is stored and not released in into the atmosphere. Places of storage could be an empty gas field. [29] Lastly, green hydrogen is the production of hydrogen with no CO_2 emissions. There are multiple ways to get green hydrogen such as water thermolysis, or the thermochemical conversion of biomass[8], but for the focus of using electricity from wind energy, electrolysis is what will be used. With current breakthroughs in clean, renewable energy with the use wind turbines and electrolysis technology this sentiment has changed. Now there would be a shift to greener hydrogen production. With the production of green/low emission Hydrogen, another use for hydrogen to lower the reliance of fossil fuels would be the injection blend for natural Gas (up to 20%) [34]:

When it comes to using wind energy for electrolysis to produce hydrogen, there are multiple methods to accomplish this task. Historically, electrolysis has been done on land, but it can be done offshore. For an offshore wind farm the main question would be where the location for green hydrogen production is, either at the source (upstream) or onshore (downstream). Each location brings its fair share of advantages and disadvantages.

1.5 Offshore Hydrogen Production

In the case of offshore hydrogen production, the production is done upstream, where the farm is located at either a centralized location meaning central hub (similar to an offshore substation for wind farms), or a decentralized locations meaning at the individual turbine. when producing hydrogen offshore, only hydrogen is sent to the shore, no electricity.

1.5.1 Centralized Production

What centralized production means it that all the Hydrogen production is done in one centralized place. The wind farm produces electricity to the centralized hub for hydrogen production, and with the electricity converting desalinized water into hydrogen. With centralized hydrogen production there are many advantages and disadvantages. One main advantage is the amount of space for electrolyzers. With all the electrolyzers stored in one place it makes repairs easier. The disadvantage of this method is that its high risk to place all the electrolyzers together [34].

1.5.2 Individual Production

In this type of green hydrogen production, hydrogen is produced at the turbine. This means that each turbine is equipped with the proper equipment that is needed to produce hydrogen. Since hydrogen is produced at each turbine, no long distance power cables are needed [21] since the electrical infrastructure is replaced with a pipeline. Since production is done at the turbine level, the variability of power production would differ than the variably of power production for the farm as a whole. The reason why variability of power is effected when comparing an individual turbine to the wind farm as a whole is because of the spatial effect that are present in wind farms. This would possibly effect the performance of the electorlyzer operation and efficiency which would need to be taken into consideration.

1.6 Hybrid Onshore Hydrogen Production

To produce hydrogen onshore, a hybrid system is developed. The idea is that the wind farm produces electricity and transports it onshore and then a substation decides with either using the electricity to produce hydrogen or send the electricity straight to the grid. This gives flexibility to the power supply chain. If there is no need for electricity for the gird i.e., the price is very low or there is need for hydrogen, then the electricity can be used for hydrogen production.

1.7 Hydrogen infrastructure concepts for offshore wind

Using offshore wind turbines to convert wind energy to electricity, hydrogen can then be produced in different ways: upstream (at the offshore wind turbine (WTG)), at a more centralized location offshore or further downstream (onshore). Taking into account the surrounding energy infrastructure (e.g. offshore electrical grids and/or hydrogen networks), the following technical concepts for the production of green hydrogen using offshore wind power can be identified:

1. *Electrical transmission offshore, hydrogen production onshore:* Concept 1 builds on the existing concept of having all WTGs connected to the electrical grid. The produced electricity is transmitted from the wind farm to the shore and hydrogen is produced onshore

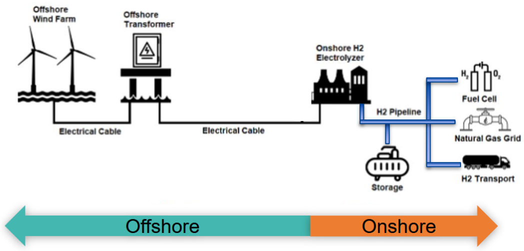

Figure 1.2: visual for onshore hydrogen production [34]

2. *Electrical distribution offshore, centralized hydrogen production offshore:* Hydrogen is produced offshore at a centralized location in the wind farm and the hydrogen is transported to shore. The offshore WTGs are connected only to a local offshore electrical grid to a central substation, where the hydrogen is produced. The substation may be connected to the onshore grid

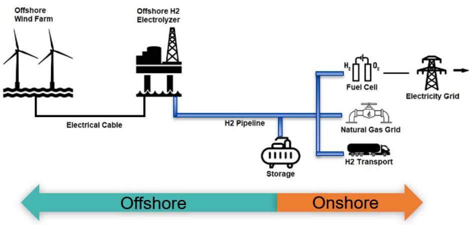

Figure 1.3: visual for centralized offshore hydrogen production [34]

3. *Individual WTG hydrogen production offshore, network-connected:* Each turbine is equipped with its own electrolyzer equipment and connected only to an offshore hydrogen pipe network. The network collects the hydrogen and transports the hydrogen to the shore, possibly using centralized pressure stations

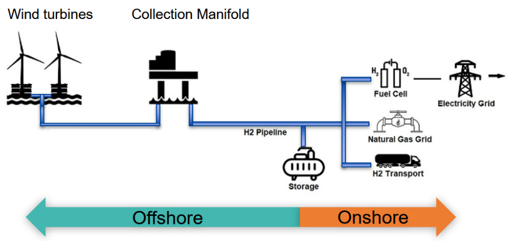

Figure 1.4: visual for individual hydrogen production [34]

4. *Individual WTG hydrogen production offshore, storage pickup:* As 3), but with local hydrogen storage on the WTG to allow for regular pickup of stored hydrogen using vessels. This option saves the investment in a hydrogen pipeline network offshore

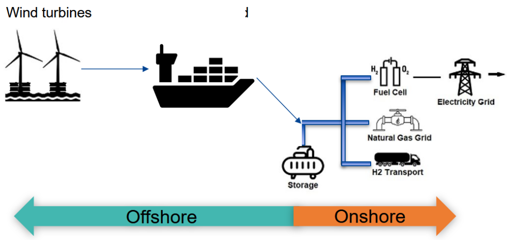

Figure 1.5: visual for individual storage hydrogen production [34]

1.8 Research Objective

The question arises, to what extent the above concepts are technically and economically optimal given the inherent variable nature of the wind, resulting in variable hydrogen production. For concepts 1 and (possibly to a lesser extent) concept 2, the variability can be reduced as the hydrogen facility is connected to the grid. In case concept 2 is not grid connected, only the short-term variations of wind power are reduced by spatial effects inside the offshore wind farm. For concepts 3 and 4, the hydrogen production will vary with the production of a single WTG. All concepts have different infrastructure investment costs and transmission losses. The objective of this research is to: "Analyze and compare different methods to produce hydrogen from offshore wind". The objective includes the development of a model to quantitatively compare the different technical concepts with a focus on technical efficiency/losses using offshore wind. Using this input, a preliminary cost benefit analysis will be performed to further analyze the differences of the hydrogen production methods. To reach this objective, the following questions will be answered:

- What are the typical and maximum variations in wind power output [MW] at the WTG and at the wind farm level?
- What effects do wind power variations have on hydrogen production for different hydrogen generation and transmission concepts?
- How can the different methods of hydrogen production be modelled?
- How much hydrogen is produced and available onshore for the different concepts?
- For the case of scenario 4, how large would the storage tanks need to be to accommodate for hydrogen production and regular vessel pickup.
- What is the economic impact for each concept and which concepts appear feasible?

1.9 Methodology

With a chosen wind farm layout, a model would be created that calculates the amount of hydrogen that is delivered onshore based on the wind data (time series of wind speeds at location). For this step, Matlab is used for model creation and running the simulation taking the wind time series as an input. The model will utilize a wake model to better simulate actual wind farm conditions. Using the model for onshore hydrogen production, the model will be altered to support hydrogen production for methods 2-4 using the same wind farm layout and wind. Steady state conditions would be used to calculate the amount of hydrogen produced for each method. For the case of centralized production, it would be assumed that there would be hydrogen produced at one point and then sent to shore where the pressure drops would be calculated and compressed based on pressure specifications on shore.

The system becomes more complex for method 3, individual hydrogen production. This is because each turbine produces hydrogen and injects the hydrogen into the pipeline that will be sent to shore. The wind farm piping would lead to a centralized point and then sent to shore. The goal of the dynamic model would be to calculate the pressure drops through the pipeline system and compensate for the pressure losses with the use of compressors. These compressors will ensure the hydrogen is pressured to the desired conditions at the shore. Each turbine would be modeled as an input for hydrogen, and then the shore would be modeled as the output. Using each model and the corresponding hydrogen that is produced, 1st order calculations can be made for the levelized cost of hydrogen based on approximate costs for all components of the wind farm. For method 4, a pipeline system is not needed since there are no pipes used to transfer hydrogen to shore. The storage for container sizes would need to be calculated based on the times for ship pickup. The size of the container for hydrogen storage needs to be large enough to ensure that there is no downtime of hydrogen production because of filled storage.

1.9.1 Overview of Model

To be able to compare the different methods of hydrogen productions, the only difference between the models would be the how energy is exported to the shore. For the first Scenario, it is assumed that hydrogen is produced on shore and all electricity is used to produce hydrogen. For the purposes of this model, scenario one is not considered to be a hybrid system meaning that it can only produce hydrogen not electricity. This makes the comparison of all scenarios simpler. For scenarios two and three, energy is exported to the shore in terms of hydrogen since electrolysis is used at the wind farm plant as opposed to onshore. This means that only hydrogen is exported to the shore. Another comparison to make is the aggregated effects of hydrogen production as scenario three is producing hydrogen at the turbine level and scenario two is producing hydrogen at the plant level. The biggest difference for scenario four would be fact there are no piping and rely on a ship transporting the hydrogen to shore.

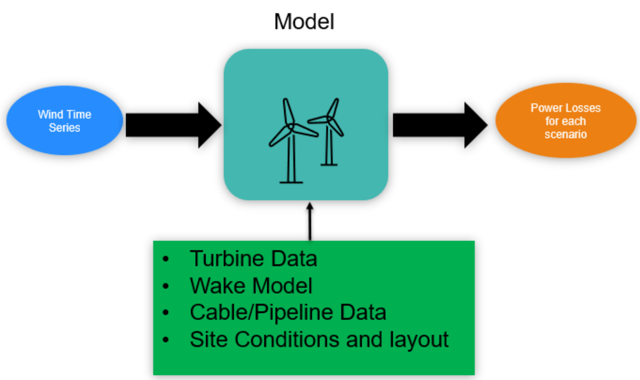

Figure 1.6: A simple visualization of the model

2 | Modeling wind, power and hydrogen production

In order to explore the 4 different methods of hydrogen production, a model must be created which must accurately represent what is seen in the real world and must also abide to it. The north sea was the selected location to create and simulate the model as there are are already wind farms present. As of 8-4-2021, there are 7 active wind farms that range from 17-752 [MW] in farm capacity, making a total of 2.45 [GW] [41]. The total offshore capacity will only increase in the future with increasing number of farms and up scaling of wind turbines. The way offshore wind turbines are organized into sets of turbine called strings. Due to the power capacity of different cables, there can only be a set number of turbines attached to a cable. These cables than lead to a centralized point in the farm and than would export all the power from the offshore wind farm to the shore using an export cable. These distances can range from 50 to 200 [km]. By using the thesis of M.V Sickler [28] as a guideline for cable layout, cable data and the individual turbine capacity as well as using the north sea as a reference a model can be created.

Wind turbine properties

The wind turbine that has been selected to be used in the model is the DTU 10-MW Reference Turbine. This Turbine has been selected since there has been published data on it courtesy of DTU (Denmark's Technical University). The size of 10 [MW] is used as it reflects the relative sizes of turbines in the north sea or that will be built. The most important turbine information that would be needed for the model would be the cut-in, rated and cut-out speed along with the diameter. The cut-in speed is the minimum wind speed required for the turbine to produce power. The Rated wind speed is the needed wind speeds to operated the turbine at rated power and for this case, it would be 10 [MW]. Lastly, the cut out speed of gives the maximum wind speeds the turbine can handle before it needs to shut down. In addition to these parameters, the power coefficient in relation to wind speeds is also given. The Power coefficient and the Power relation to wind speed is shown in figure 2.1.

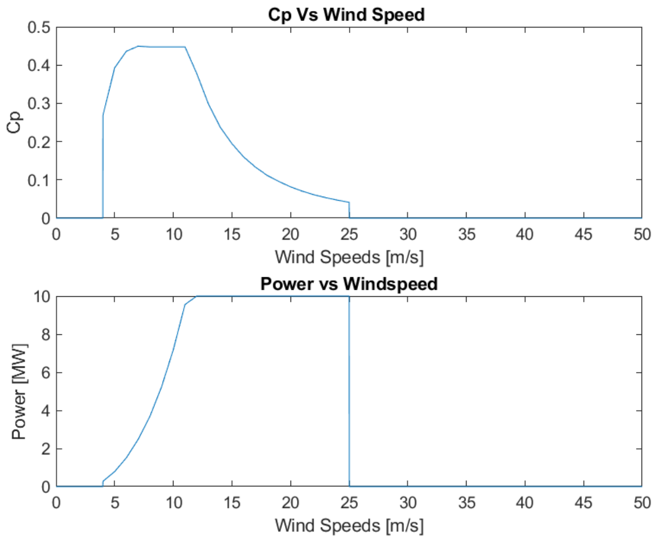

Figure 2.1: Power curve and Cp Curve

The formula used to calculate power is written as,

$$P = \frac{1}{2}\rho A v^3 Cp \tag{2.1}$$

where ρ is the density of air, v is the velocity, Cp is the power coefficient and A is the area of the turbine. Cp can be found by using figure 2.1. Essentially, the power coefficient of a wind to represent the overall efficiency of the turbine [54] and needs to be taken into account to use the power equation.

The spacing of a turbine is an important consideration when modeling a wind turbine string due to wake effects. For the purposes of this model, the turbine spacing is taken as 6 times the diameter and the spacing of the last turbine to the sub station is taken as 7 turbine diameters.

Inter Array Cables

In order to create a model, a limiting factor would need to used which would be the parameters of the cables used in the string. The cables that will be use to determine the string layout was also used in the thesis of M.V Sickler [28] and presented in table 2.1. Even though cables are only used in only two of the four scenarios, it will still be used as reference to create the strings for each scenario. This would make the comparison of each method easier and consistent.

Table 2.1: Cable Parameters from reference Thesis

	Type [mm^2]	**Ampacity [A]**	**Conductor resistance [Ω/km]**	**Phase operating Voltage [kV]**
Cable 1	400	424	.101	66
Cable 2	630	584	.063	66
Cable 3	800	750	.037	66

Ultimately, the cables are limited by the ampacity so there is a maximum amount of turbines that can be attached to the cable. This maximum can be calculated by the power equation for wires which is written as,

$$P_{max} = \sqrt{3} I V \cos\theta \tag{2.2}$$

where I is the current, V is the phase operating voltage, and $\cos\theta$ will be taken as .9. By using the ampacity that is shown in table 2.1 for I, the maximum power of that cable is calculated. For each of the cables, the maximum power is 43.4, 60.0 and 77.2 [MVA] respectively to the cable type. Since the turbines in the wind farm are the DTU 10 [MW], this means that cable 1 can handle a max of 4 turbines, cable 2 can handle 6 and lastly cable 3 can handle up to 7 turbines. Since the maximum number of turbines cable 3 can handle is 7, that means the total string capacity is 7 Turbines. The first 4 turbines in a strings would use cable 1, then for turbines number 5 and 6 would use cable two and finally, the last turbine would use cable three. With these limits in place, a string can be created which utilizes the 3 different types of cables and will be the template for all scenarios.

A simple illustration of the string layout that would be used for the model is shown in figure 2.2. Essentially each turbine is placed in a single line downstream of the previous turbines. The color of the line that connects each turbines shows the cable type as shown in Table 2.1. After turbine 5 in the string, the cable type must change to compensate the increased maximum power of the string. The same is true for turbine 7. The cable type changes to cable three, again to compensate for the increased in total string power. Lastly, at the substation, a last cable change is made. The reason for the cable change is that there is a increase of Phase Operating Voltage. A reason for this change is to limit the power losses due to cable resistances [9] (explanation on how to calculate the power losses through electrical cables will be described in the following chapter.) Hydrogen production will be done offshore. The spacing between the turbines, as mentioned earlier, would be 6 turbine diameters while the spacing between the last turbine and the substation is 7 turbine diameters. For the purposes of the model, wind will approach the string in only one direction, parallel with the string.

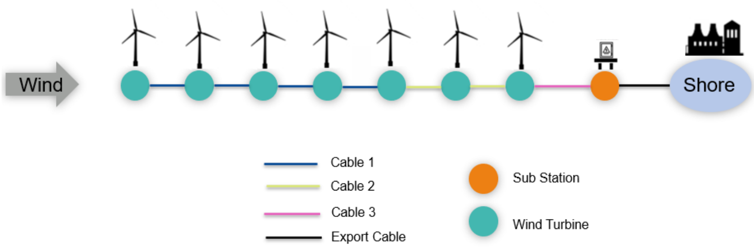

Figure 2.2: A Simple illustration of the string layout

Electrolyzer

Fundamentally, an electrolyzer uses electricity breaks down water to the base components, hydrogen and oxygen. This is where hydrogen gas is produced and extracted while the oxygen gas could also be stored or released back into the environment [26]. This reaction is visualized in the chemical equation written below:

$$2\,H_2O \xrightarrow{\text{electrolysis}} 2\,H_2 + O_2$$

The hydrogen gas that exits the electrolyzer can then be used for the desired purpose of either to be used immediately as an energy source or to be stored for transportation/later use. There are different types of electrolyzers that operate in different ways but all use a cathode, an anode and a membrane separating the two. The different types of electrolyzers are the following;

- Alkaline
- Proton Exchange Membrane (PEM)
- Solid Oxide Electrolyzers
- Anion exchange membrane (AEM)

Each type of electrolyzer comes with it shares of advantages and disadvantages, and vary in the age of technology. The electrolyzers all use DC electricity and must use pure/demineralized water

[34]. For the purposes of this thesis, only two types of electrolyzer are discussed in some detail, the Alkaline and PEM electrolyzer.

Alkaline

Of the different electrolyzer types, alkaline electrolyzers are one of the oldest in industry and the cheapest. The main principle of this type of electrolyzer is that it uses a electrolyte solution such as potassium hydroxide (KOH) or sodium hydroxide (NAOH) and water. [26] Hydrogen is then produced in a cell, where the cathode, anode and membrane are stored. The cells are placed in pattern that is called the cell stack which produce more hydrogen when the number of stacks increase. Current is then applied to the cell stack which cause hydroxide ions (OH-) to move through the electrolyte solution traveling from cathode to anode where hydrogen gas is produced on the cathode side and oxygen is then produced on the opposite side, where the anode is located. This can be visualized in Figure 2.3

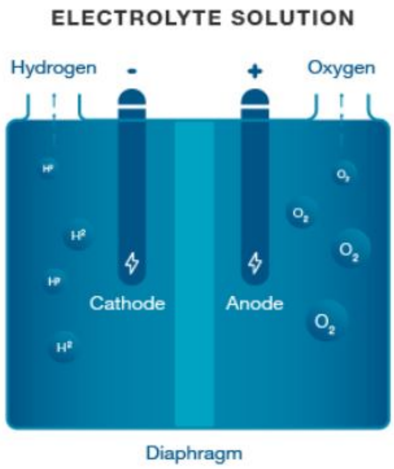

Figure 2.3: Alkaline Hydrogen Production [26]

The drawbacks of using alkaline electrolyzer is that it requires maintenance of the alkaline fluid, and has certain thresholds where it can not operate safely. The start up time is longer than compared to different types of electrolyzer which can be an issue for renewable energy sources that are not constant [34].

PEM

A Proton Exchange Membrane works with the use of a Proton Exchange Membrane that utilizes a solid polymer electrolyte [26]. When a current runs through a cell stack, the water is broken down into hydrogen and oxygen gas. The hydrogen protons pass through the proton exchange membrane to form hydrogen gas, again on the cathode side, where oxygen is produce on the anode side [26]. This can be seen in Figure 2.4

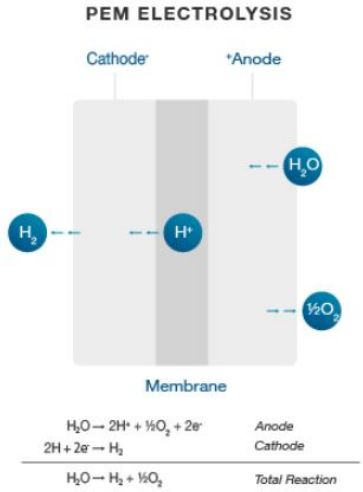

Figure 2.4: PEM Production [26]

This type of electrolyzer technology is more recent than Alkaline electrolyzers and comes with its fair share of advantage. One such example would be that it has a faster start up time compared to Alkaline electrolyzers. The purity of hydrogen is also increased and the operational ranges has increased. It can even produce more than its rated, up to (120 %). [33] [34]. It also has a higher output pressure, which could mean that less energy could be needed to compress hydrogen depending on design specifications. The main advantage that PEM electrolyzers have as compare to that of alkaline for the use of green hydrogen production is the start up time.

For the purposes for this model, only one type of electrolyzer would be selected to be used for each of the scenarios. The reason for this choice is because the consistency of the electrolzyers would make it easier to compare the different scenarios to each other. When producing hydrogen onshore, it would make sense to use alkaline electrolyzers since the main issue with using them would be the high maintenance. Alkaline electrolzyers offshore poses a much bigger issue since its harder to maintain, so for offshore purposes, a PEM electrolzyers is the better choice. Since 3 out of the 4 scenarios has hydrogen production offshore, this means that PEM electrolzyers are needed for those scenarios. Since consistency is important to be able to compare the different scenarios, the PEM electrolyzer will be used going forward.

2.1 Wake Model

To make the model a better Representative of the real world, a wake model was adopted. Since Wind turbines takes the wind from upstream, a wake is produced downstream of the turbine which results in lower wind speeds. As the flow continues downstream, the wake recovers back to free stream conditions. Because of these wake effects, turbine spacing is important and the reason of the chosen distances from earlier. For this model, the chosen wake model would be the NO Jensen Wake Model.

2.1.1 NO Jensen Wake Model

By neglecting the near fields right behind the wind turbine since periodic and deterministic swirling that makes contributions to wake effects, its possible to treat the wake downstream of the wind turbine as a turbulent wake [1]. A relation can be made using the dimensions of the rotor diameter, (radius r) of the wind turbine with respect to the distance down stream denoted as x. By balancing the momentum from figure 2.6, the following equation is found,

$$\pi r_0^2 v_0 + \pi(r^2 - r_0^2)u = \pi r^2 v \tag{2.3}$$

where v_0 is the velocity right behind the rotor, u is the free stream velocity, v is the distance velocity in the downstream direction of distance x. r_0 represents the diameter of the turbine that creates the wake. By solving equation 2.3 for v and assuming a linear wake in relation to r, and the velocity right behind the wake is $\frac{1}{3}u$ according to classical theory gives the following equation [1],

$$v = u\left\{1 - \frac{2}{3}\left(\frac{r_O}{r_O + \alpha x}\right)^2\right\} \tag{2.4}$$

where α represents the wake entrainment constant, also known as the wake decay coefficient [40]. The wake decay coefficient describes the expansion of the wake behind the rotor. By modifying this value, the wake behind the rotor either becomes narrow or wide. The value for wake decay coefficient which has been derived from surface roughness [42]. One method of calculating the coefficient comes from turbine intensity, but that varies depending on the initial velocity. For the purposes of this thesis, α is taken as .075 as N.O Jensen performs most accurately for onshore cases [42]. With the entrainment constant, the rotor radius of the turbine producing the wake and the distance downstream of the turbine, the resulting velocity deficit can be calculated.

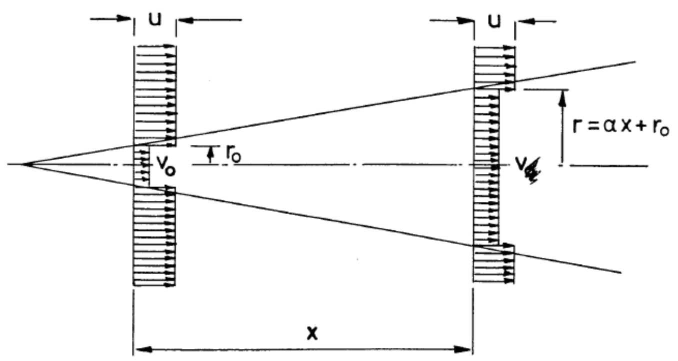

Figure 2.5: Schematic wake model with definition of symbols used in the text [1]

By taking an example of the DTU 10MW turbine with a rotor radius of 89 meters and taking α as .075, the following graph can be plotted that shows the recovery of the wind speed in relation to turbine diameters spacing where the free stream velocity is 14 m/s,

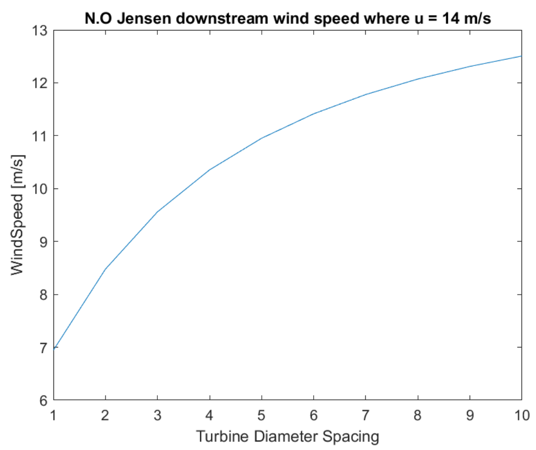

Figure 2.6: Wind speed recovery in terms of turbine diameter spacing.

It comes to no surprise that the bigger the distance, x, the more the wake recovers to the free stream velocity. This is why turbine spacing in wind farms are important, as it allows for wake recovery so when a turbine is downstream of another turbine, the second turbine would meet a higher wind velocity.

Since wind farms contain more than 1 wind turbine, this means that there will be cases where there are multiple turbines that can create wakes and interact with turbines downstream. In this case, the relation in Equation 2.3 can be used for cases of multiple wake interactions [1]. The velocity of the wind speed that the turbine downstream experiences of a wake produced by the previous turbine can be found using Equation 2.4, where the distance is the spacing between the turbines. To find the velocity right in front of the third turbine in a wake, a momentum balance of Equation 2.3 is used where the velocity directly behind the second turbine would $\frac{1}{3}v_1$ and the resulting Equation would be,

$$r_0^2(\frac{1}{3}v_1) + (r^2 - r_0^2)v_1 = r^2 v_2 \tag{2.5}$$

where v_2 is the wind speed right before the third turbine in a row and r is the radius of the wake from the second turbine at turbine 3. By making the assumption of that $\bar{v_1} = u$, and solving Equation 2.5 for v_2 is approximately,

$$\frac{v_2}{u} = 1 - (1 - \frac{1}{3}\frac{v_1}{u})(\frac{r_0}{r_0 + \alpha x_0})^2 \tag{2.6}$$

by letting constant, k, represent the following expression, $(\frac{r_0}{r_0+\alpha x_0})^2$ and denoting the relation of $Y_N = v_N/u$ where v_N is the wind speed that the Nth turbine in a wake meets, a general expression can be calculated as,

$$y_n = y_{n-1} - 2\left(\frac{k}{3}\right)^N \tag{2.7}$$

Since it was calculated earlier by using the cable data in Table 2.1, the maximum amount of wind turbines in a string, and using the spacing mentioned earlier, it is possible to see what the wind speeds that each turbine in a string experiences and is plotted in Figure 2.7. A wake visualization of a string is plotted in Figure 2.8 where the different colors represents the different wakes that each turbine produces.

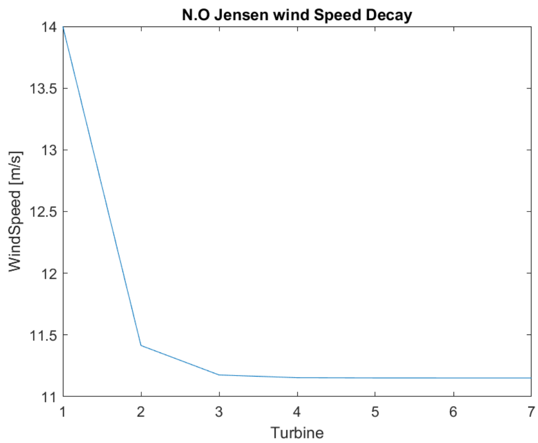

Figure 2.7: The wind speed decay based on number of turbines in a string with the initial velocity of 14 m/s

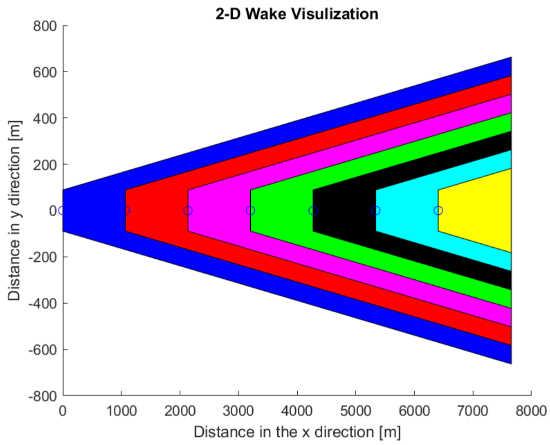

Figure 2.8: A visualization of wakes produced be each turbine in a string where each colour represents a turbine's wake.

An interesting observation in Figure 2.7 is that after a certain amount of turbines, it appears that the wind speed deficit does increase and instead appears to level out. This is of course due to the general equation that, when N increases, y_n stabilises. In the case for the string, the biggest velocity deficits can be seen from turbines 1 to 2 and 2 to 3. After turbine 3, the changes in velocity become very slow. Since the rated wind speeds for a DTU 10MW reference turbine is 11.4 m/s it can be seen from the graph that turbine 3-7 produces less power than turbines 1 and 2 since the wind speeds that those turbines experiences are less than the rated wind speeds. Without modeling these wake effects, and assuming each turbine experiences the same wind speeds, a overestimation of power production is made. The lower the initial velocity is, the the greater this decrease in power production becomes. Of course, when dealing with wind speeds greater than rated so that even with wake effects taken into account, each turbine produce their rated power wakes it might appear that wakes are not important however they still play a role when it comes to wind speed time delays.

2.1.2 Time Delay

Considering the size of the 10 MW turbine, and the spacing between each turbine in a string and based on Figure 2.8, the total distance from the first turbine to the last turbine is 6408 meters. That means that if a constant wind speed of 14 m/s where to travel from the first turbine to the next turbine uninterrupted, it would take about 457 seconds or 7 and a half minutes to reach the final turbine in the string. Considering the fact that wakes cause a decrease in wind speed, the time it would take for wind to travel the entire sting would increase even more. Some way of incorporating this idea needs to be implemented into the model to better make it reflect a real world scenario.

In the thesis of M.P.C Bontekonig, which looked at the reduced wake effect during curtailment [13] proposed a way to calculate the time delay based on the turbine spacing and the wind speed behind the turbine. That formula was implemented by post-processing and with existing data. For the purposes of this model, a simplification would be made that would be able to approximate the time delay. By taking the average of the incoming wind speeds, and then applying the N.0 Jensen Wake Theory, a time delay can be estimated for how long it would take for a given wind speed to travel from the start to the end of the string. This time delay is written in Equation 2.8

$$t_{delay} = \frac{\Delta x}{\bar{u}} \tag{2.8}$$

where Δx is the spacing between the turbine and $\bar{u}$ is the average velocity with the wake in consideration and can be calculated as,

$$\bar{u} = \bar{v} * Y_n \tag{2.9}$$

where $\bar{v}$ is the average free stream velocity, and Y_n is calculated from Equation 2.7. This approach to calculate the time delay is discrete and depends on the resolution of the incoming wind speed time series. This means that if the wind speeds are given in a time series that has a resolution of seconds, so will the time delay. Another note to make on the accuracy of this approach to calculate the time delay, is that smaller the time interval of to average for the wind speeds, the more accurate the time delays become. In reality, to get a more accurate model to calculate the time delays would be difficult to implement since that would require to fully model the dynamic behavior in wind and would be outside the scope of this thesis. The way the time delay is calculated in Equation 2.8 should be accurate enough to represent real world conditions.

Resolution and simulation lengths

The resolution of the model is chosen to be in seconds to reflect . Since the input time series has a resolution of seconds, this means that the model resolution must also be in seconds. The wind speed time series is shown in Figure 2.9. This wind speed time series was taken from measurements from the north sea and should reflect the fluctuations of typical wind speeds for offshore winds at the height of the hub of the turbine. The mean wind speed of the 1-hour long simulation is 10.14 [m/s]. The question still remains on how to accurately account for the time delay. Since the resolution of the model is in seconds, the time delay will also be measured in seconds. In order to get a more accurate measurement of the time delay and based on Equation 2.8, the smaller the average interval (in terms of minutes), the more accurate the time delay becomes.

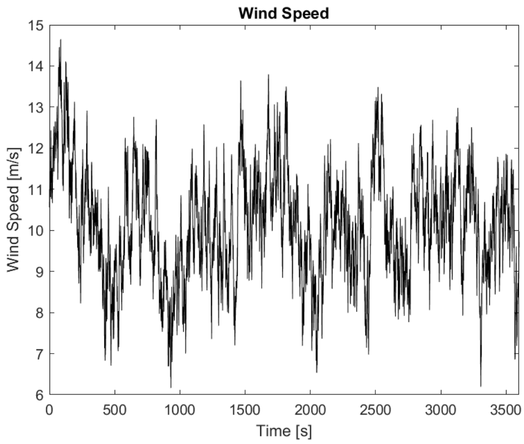

Figure 2.9: The time series that will be taken as an input to the model.

Since it is shown in Figure 2.9 that the time span of the wind speed time series is an hour, there are multiple options to reduce the average interval. By just taking the average of the wind speeds in an hour interval, the time delay looses accuracy. However, by breaking the intervals in smaller but equal portions, such as 4, 15 minute averages, the interval is made more tight and thus giving a better accuracy for the time delay. By making the intervals smaller, there is an issue that occurs which will be explained in the following section.

Model Power Output

It is assumed that at the start of the simulation, all turbines are not operational. The simulation starts where the first turbine in the string meets the beginning of the input time series, and the time delay is calculated for when the following turbines would meet the wind and start up. It is assumed that the startup of the turbine is instant. For the purposes of the model, the transient would need to be discarded since that information is not useful. As an example, based on Figure 2.9, by using the full hour interval to calculate the time delay, the total time it would take for the wind to go from the beginning of the string to the end would take about around 13 minutes. This means the

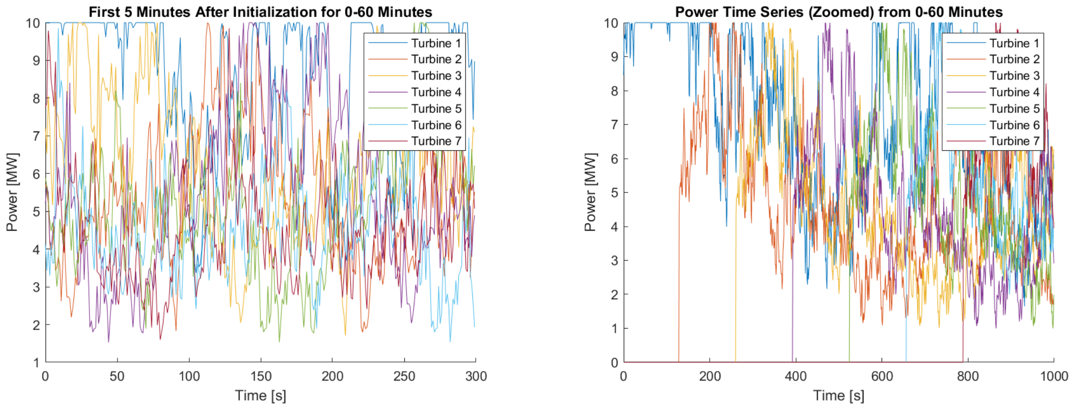

(a) First 5 minutes after the initialization period

(b) Hour long Power time series zoomed

initialization of the simulation ends at about the 13 minute mark, and thus limiting the amount of data points available to use. By dividing the hour long time series into smaller portions, the time delay will differ for each portion since the wind speeds are not constant. By splitting the time series into smaller, equal portions, there would be different time delays based on the different averages. If four, 15 minute averages were taken, that means that there will be 4 simulations to account for each 15 minute average. That also means that there are 4 initialization since each new simulation would reset all the turbines in the string. The trade off for making the time delay more accurate would mean that there are a limited number of data points available to be used since the transient would be ignored.

An example is plotted in Figure 2.10a - 2.10b by taking taking only one average (60 minutes) to calculate the time delay and the power output of each turbine is calculated based on the wind speeds. Different average periods and different simulated wind speeds has been plotted in Appendix A. Since an average interval of an hour is taken and the individual power is looked at for each turbine, presenting the entire time series would be chaotic and not very helpful, instead the first 5 minutes of the time series is presented and a look at the initialization period of the simulation. The initialization period is presented in Figure 2.10b. The transient/initialization period represents the time when each turbine starts. It can be seen that all turbines are operational at about 800 seconds which corresponds with the time delay estimated earlier. The information after the transient is what is important, meaning the time between 0 and 800 seconds is to be discarded.

That is where the issue of creating smaller time segments come into play. Taking 6, 10 minute averages to calculate the time delay is a problem since it takes about 800 seconds (about 13 and a half minutes), that is longer than the 10 minute average used for the time delay. In that case, the transient is not completed in those 10 minutes meaning the simulation is not possible. Different averages will now be used to run the simulation by taking 30, 20 and 15 minute averages. These Figures will be shown in Appendix A. The main point is to show that lowering the average intervals decreases the amount of data points due to truncating the transient.

Aggregation of wind variations

One of the question that this thesis tries to solve is the variation that comes with wind and the effects it has on power generation on the WTG level to farm level. With the model created so far, this question can be answered. By looking at the resulting power output from each turbine, it can be shown what the effects of power variations on the wind turbine level and the string level. The total string power is calculated based on the power output of each turbine in the Power time series. For the 60 min average, the Total sting Power Series is shown in Figure with the transient removed.

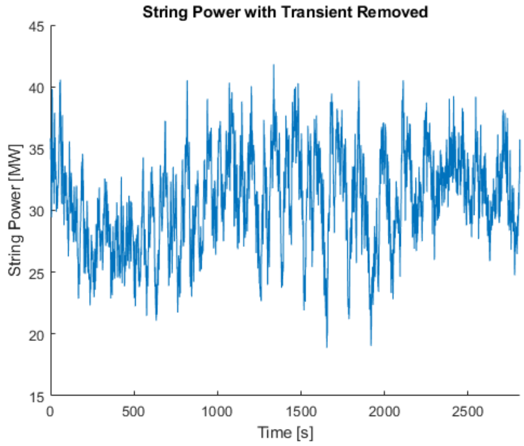

Figure 2.11: 60 min power time series with the transient removed

The variance can be calculated by taking the power difference at each time step ($P_t - P_{t-1}$). The difference in power is than separated and sorted in decreasing order and normalized [5]. This results in a power variability curve. By taking 15 min averages, the power variation of the first 15 minutes was plotted in Figure 2.12. Due to the fact that the initialization period is removed, there is limited amount data points available. Due to the limited amount of data points, the graph becomes jagged and the variability is more extreme. . However, a clear trend is noticed. To get a better understanding of the variance a 60 min average is taken instead since there will be more data points available. This means that the time delay is less accurate, but for the purposes of calculating the variance that is not that important. The variance of a 60 min average is plotted in Figure 2.13

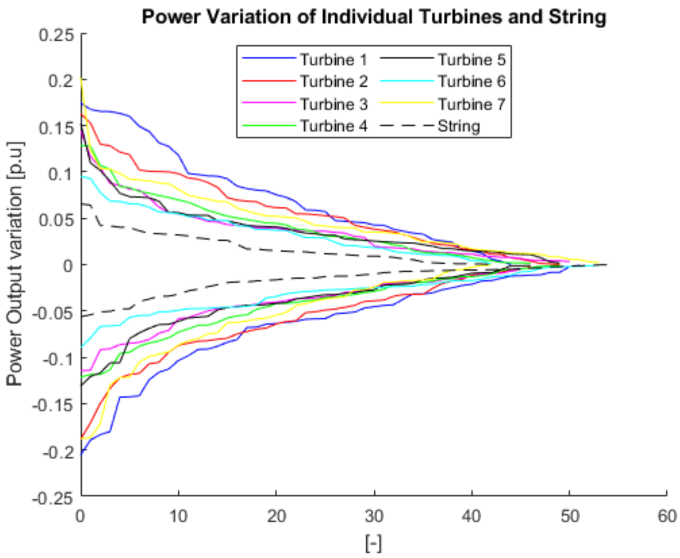

Figure 2.12: Variation of Power of the string vs individual turbines (First 15 min average)

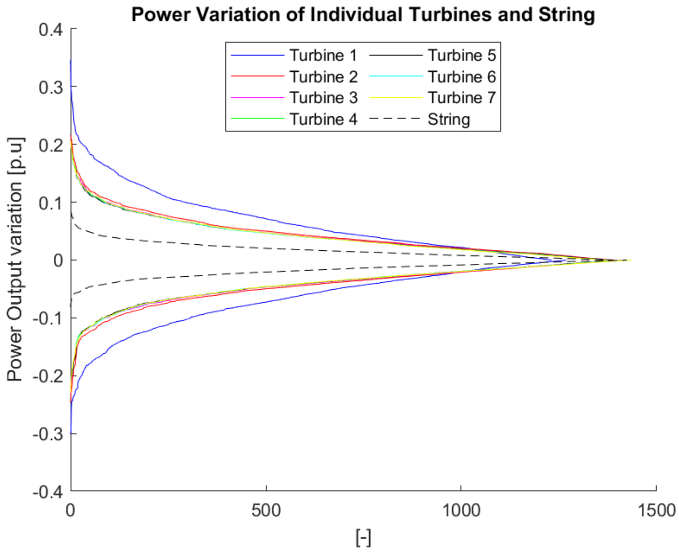

Figure 2.13: Variation of Power of the string vs individual turbines 1-hour average

It can be seen that the normalized variance on the string level is actually lower than the variance on the individual turbine level. This can be explained because of spatial/wake effects. Even though the power variation is higher on the string level (the total power of a string is 7 times higher than of 1 turbine), the normalized variance is lower. Since electrolyzers favor steady state conditions and the impact of efficiency decreases with larger fluctuations of power [4], lowering the normalized variation would have be beneficial. By looking at the Wind Power Equation 2.1, it can be seen that the higher the wind velocity, the larger the Power variation. This is because of cubic nature of wind speeds in the wind power equation. Looking where the variability in power is the highest, the wind speeds are just below rated. This is because after rated wind speeds, the power is constant and as long as the changes in wind speeds does not decrease lower than rated power the variance is zero. But by looking at the Power Curve of the 10 [MW] wind turbine, wind speeds just below rated gives the highest variance.

3 Modeling of Offshore Hydrogen Production

With the Modeling of string is complete, now it is time to include the modeling of offshore hydrogen. Scenarios 2 and 3 involves transporting hydrogen at the cite of production to the shore by using pipelines. The modeling of these pipelines must be taken into account in order to give a fair comparison of offshore and onshore hydrogen production. The task of modeling the effects of hydrogen being transported by a pipeline can be completed by looking at the oil and natural gas industry. Since hydrogen is produced and shipped as a gas, by specifically looking at the natural gas industry, a method can be created for modeling hydrogen transportation in pipelines using the same method for modeling natural gas.

3.1 Modeling A hydrogen Pipeline

Generally, a simulation of natural gas pipelines is a computationally intensive process, especially if a high accuracy is needed due to complexity that comes with these simulated networks [10]. A well known method of modeling the flow of gas through a pipeline comes from the principles of conservation of mass, momentum, and energy [10] [2] to a cylinder of a infinitesimal length. The resulting equations is composed of differential and algebraic equations of gas properties and internal energy. A natural gas pipeline system is composed of more than just the pipe itself. Compressor and regulation stations and control valves are included in pipelines and must also be taken into account in the model. Once this model is created, there could be many parameters that are important to be analyzed. These parameters could be the gas pressure along the pipeline, or even the flow rate (mass [kg/s] or volumetric [M^3/s]) of the gas.

In a simple linear pipeline system, where there are no loops and branches, the most common parameter to find in that type of system would be to find the pressure of the gas over multiple points in the pipeline. In a more complex pipeline where branches or loops are present, it would be necessary to determine the flow rate as a function of pressure at the nodes in the system. Because of the complex and general description of the equations to create a mathematical solution, there is no analytical solution. To counteract that, simplifications are added to the model which could include, isothermal regime, and negligible inertial terms [10]. The processes of simplification creates expressions directly relating pressure and flow. These implementation are used in many of today's commercial simulations and are used recent works in pipeline design [10].

Pipeline operations are by definition a transient processes, the use of steady-state models are commonly used to not only design pipelines but also estimate the flow. These steady state models are usually used for optimizers and marketing tools [10]. For the purposes of simplifying the model, none pipe elements such as compressors are not included in the mathematical model but included later since the main point of the model is to analyse the gas flow.

3.1.1 Equations of State

Gas flowing in a pipeline can be described by a one-dimensional flow [2]. Essentially what that means is, that the gas flow is only moving in one spacial direction. The basic equations that describe the flow in a pipeline, which have been mentioned earlier, equation of motion (or momentum), an equation of continuity, equation of energy and state equation [2] [10]. These equations can be derived from looking at a control volume for a small segment of the pipeline, which is shown in Figure 3.1.

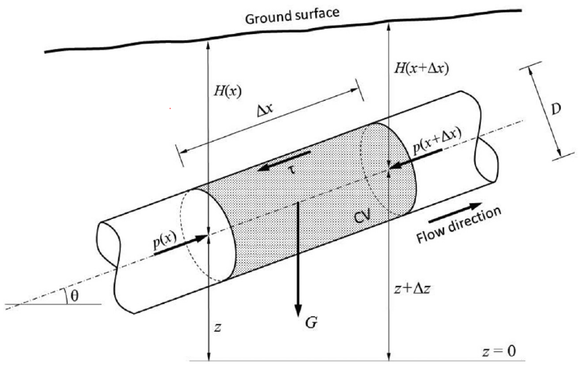

Figure 3.1: Control volume (CV) in a gas pipe [10]

It is important to note that it is assumed that the pipe is straight with a constant diameter of D. The pipe is buried at a depth of D with a coordinate system in the x direction. The control volume has a length of Δx and the forces acting on the are due to the shear stress, τ, gas pressure and the gravitational force. Since the length of the pipeline is usually significantly greater than the diameter of the pipeline, it is assumed to be one-dimensional. The pipeline diameter also does not change in time.

Conservation of mass: continuity equation

The continuity equation is written in the full state as,

$$-\frac{\partial(\rho w)}{\partial x} = \frac{\partial \rho}{\partial t} \tag{3.1}$$

where ρ is the density of the gas, w is the velocity of the gas $\frac{\partial \rho}{\partial t}$ represents the change in density with respect to time. It is usual to have the equation in terms of mass flow, which is written as $M = \rho w A$ where A is the cross sectional area, and substituting that expression into the equation, the following equation is found.

$$-\frac{1}{A}\frac{\partial(M)}{\partial x} = \frac{\partial \rho}{\partial t}. \tag{3.2}$$

Since it was mentioned that the diameter of the pipeline is constant in both time and space, that also means the area is constant. This is why the area can be taken out of the partial derivative of the mass flow with respect to x. As mentioned before, modeling in steady state is used often. Steady state means that there is not time dependency as it is constant in time and the mass flow does not change. Finally the steady state expression can be written as,

$$\begin{aligned} &-\frac{1}{A}\frac{\partial(M)}{\partial x} = 0 \\ &M = c \\ &\rho w A = c \end{aligned} \tag{3.3}$$

where c is a constant value determined by a predetermined value for the mass flow rate.

Newton's second law of motion: momentum equation

By applying a basic form of the momentum equation to the CV, the following expression is found [2].

$$\frac{\partial p}{\partial x} - \frac{2f\rho w^2}{D} - g\rho\sin\alpha = \frac{\partial(\rho w)}{\partial t} + \frac{\partial\left(\rho w^2\right)}{\partial x} \tag{3.4}$$

where f is the Fanning friction coefficient, g is the gravitational force per unit mass and α is the angle between the horizon the the x direction. The terms in the equations represent the inertia, hydraulic friction force and the gravitational forces. The shear stress is included from the CV in Figure 3.1 and can be written in multiple ways, either as $\frac{\rho w^2}{2}\frac{\lambda}{D}$ or $\frac{2f\rho w^2}{D}$. The only difference between these two expressions is that λ is the Darcy's friction factor. By looking closer at the expressions is that the Darcy friction factor is 4 times larger than the Fanning friction factor.

Again, by making the equation comply to steady state conditions, the Equation 3.4 can be rewritten as,

$$\frac{\partial p}{\partial x} - \frac{2f\rho w^2}{D} - g\rho\sin\alpha = \rho w\frac{\partial w}{\partial x} \tag{3.5}$$

Conservation of energy

The basic form of the energy equation can be written as [2],

$$\begin{aligned} q\rho A\ \mathrm{d}x =& \frac{\partial}{\partial t}\left[(\rho A\ \mathrm{d}x)\left(c_v T + \frac{w^2}{2} + gz\right)\right] \\ &+ \frac{\partial}{\partial x}\left[(\rho w A\ \mathrm{d}x)\left(c_v T + \frac{p}{\rho} + \frac{w^2}{2} + gz\right)\right] \end{aligned} \tag{3.6}$$

where q is the heat addition per unit mass per unit time, T is the gas temperature, and c_v is the specific heat at the constant volume. The next step is to rewrite the equation for steady state conditions. This means that the term,

$$\frac{\partial}{\partial t}\left[(\rho A\ \mathrm{d}x)\left(u + \frac{w^2}{2}\right)\right] = 0 \tag{3.7}$$

gets cancelled since there is no difference in time because of the definition of steady state. According to Equation 3.6, temperature is a function of the length of the pipe. This can be calculated using the heat balance equation, written as,

$$c_p M \mathrm{d}T = -k_L\left(T_{\text{soil}} - T\right)\mathrm{d}x \tag{3.8}$$

where c_p is the specific heat at constant pressure, [J/kgK], M is the mass flow [kg/s] and k_L is the heat transfer coefficient [W/mk] and T is the temperature of gas [k] and T_{soil} is the temperature of soil. By solving Equation 3.8, the following expression can be found to calculate the temperature along a pipeline [2],

$$T(x) = T_{soil} + \left(T(0) - T_{soil}\right)\mathrm{e}^{-\beta x} \tag{3.9}$$

where $\beta = kl/(c_p M)$.

State equation

The state equation relates the density, pressure and temperature of the gas to each other and is widely used in the natural gas industry and written as,

$$\frac{p}{\rho} = Z(p,T)RT \tag{3.10}$$

where Z is the impressibility factor, which itself is a function of pressure and temperature and R the specific gas [J/kg K].

3.1.2 Applying the Equations

In the gas industry, the following equation can be used to calculate the pressure of the gas along the pipeline [2].

$$p(x) = \sqrt{(P(0)^2) - KM^2} \tag{3.11}$$

where $p(0)$ is the initial pressure and k is defined as,

$$K = \frac{ZR}{A^2}\left[\frac{4f}{D}\left(T_{\text{soil}}\ x + \frac{T(0) - T_{\text{soil}}}{\beta} - \frac{T(0) - T_{\text{soil}}}{\beta}\mathrm{e}^{-\beta x}\right) - 2(T(0) - T(x))\right] \tag{3.12}$$

where, where x is the spatial coordinate. By using the example problem in [2], the temperature can be defined throughout the pipe using Equation 3.9 and is shown in Figure 3.2

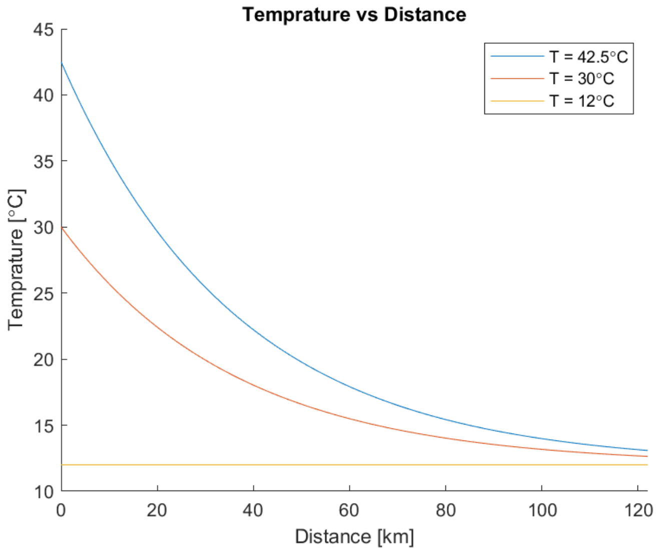

Figure 3.2: Temperature of gas along the pipe in the example problem

Figure 3.2 gives three different cases. Two Non-isothermal conditions where the starting temperatures are 30^o C and 42.5^o C. The last example is isothermal, meaning that the temperature of gas is constant throughout the pipe, and the starting temperature is the ambient soil temperature. As it can be seen from the figure, the temperature converges to the temperature of the soil. Equation 3.12 can be written to reflect isothermal conditions as,

$$K = \frac{ZR}{A^2}\left[\frac{4f}{D}\left(T_{\text{soil}}\ x\right)\right] \tag{3.13}$$

The example that was solved in [2] shown that for steady state conditions, the pressure changes over the full distance compared to isothermal and non-isothermal is relatively low. From now on, only isothermal conditions is looked at.

Alternative method of calculating pressure

As the above equations was given by the natural gas industry, and was not derive, another method would be preferably used. The above method is still useful to verify if the derived equation is correct. To start, the assumption of isothermal and steady state is applied. By assuming isothermal conditions, Equation 3.6 become redudant and can be neglected. This reduces the equations to be used to just 3.4 and 3.3. Further, from equation 3.3 the following relation can be made,

$$\frac{du}{dx} = -\frac{u}{\rho}\frac{d\rho}{dx} \tag{3.14}$$

where u is the velocity and then,

$$\frac{du}{dx} = -\frac{u}{\rho}\frac{1}{RTZ}\frac{dp}{dx} \tag{3.15}$$

from the state Equation 3.10 RTZ is found. An important thing to note is that $\sqrt{RTZ}$ is the velocity of sound in the gas stream, which is usually constant. Finally, by implementing these definitions back into the Momentum Equation 3.4, the following expression is written,

$$\frac{dp}{dx} = -\frac{RTZ}{RTZ - u^2}\left(\frac{\rho u^2}{2}\frac{\lambda}{D} - g\rho\frac{dz}{dx}\right) \tag{3.16}$$

To keep things more consistent with the natural gas industry equation, the following assumptions are made; Since the limit for fluid speed in a pipe is up to 20 [m/s], the expression $\frac{RTZ}{RTZ-u^2}$ can be set equal to 1 because the speed of sound is significantly higher than the fluid velocity making it a good approximation. The next assumption is to assume the pipe is not on an incline, making $\frac{dz}{dx} = 0$. Finally, Equation 3.16 can be written as,

$$\frac{dp}{dx} = -\left(\frac{\rho u^2}{2}\frac{\lambda}{D}\right) \tag{3.17}$$

This expression shows the relationship between the derivative (the slope) of pressure in terms of x. To get a finite result from this expression finite differences is taken,

$$\frac{dp}{dx} = \frac{p_{i+1} + p_i}{\Delta x} + O(\Delta x) \tag{3.18}$$

where $O(\Delta x)$ denotes the truncation error (From the truncated Taylor series [3]) and Δx represents the small incremented distance. By implementing this substitution for derivative of pressure back into Equation 3.17, and solving for p_{i+1} the following expression is found,

$$p_{i+1} = -\rho_i u_i^2 \Delta x \frac{\lambda}{2D} + p_i \tag{3.19}$$

It is important to know that ρ_i and u_i^2 is the density and velocity at point i since those properties are related to each other and dependent of the state equation. In order to solve this equation, some initial conditions must be determined. The initial pressure and temperature must be defined along with the mass flow rate. Two final details are needed in order to solve for pressure and that is to calculate the compressibility factor and the Darcy Friction Factor.

3.1.3 The Friction Factor

The properties of a pipe are the following, d the diameter, L the length of the pipe, ϵ the roughness of the pipe. The relative roughness can be calculated as the following equation [45]:

$$r_{rel} = \frac{\epsilon}{d} \tag{3.20}$$

where r_{rel} is the relative roughness. The relative roughness will be used to calculate the friction factor.

Reynolds Number

The ryenolds number is a dimensionless number used to describe if the flow is laminar or turbulent. With the finding the density and the viscosity of the gas , the Reynolds number can be calculated with the following equation [45],

$$Re = \frac{\rho V d}{\mu} = \frac{4\dot{m}}{\mu\pi d} \tag{3.21}$$

where $\dot{m}$ is the mass flow rate of hydrogen, d is the diameter and μ is the dynamic viscosity. By using the mass flow rate determined earlier and the computed Reynolds number, the friction factor can be computed using the Moody Chart. Another way to calculate the friction number would be through the use of the colebrook-White Equation,

$$1/\sqrt{f} = 1.14 - 2\log_{10}\left(\frac{e}{D} + \frac{9.35}{\mathrm{Re}\sqrt{f}}\right), \ \mathrm{Re} \ > 4000 \tag{3.22}$$

The Moody diagram was used in an era where personal computers was a thing of the future, and solving this equation was very difficult. Now, it can easily be calculated, thus making the calculations more streamlined. The Moody Diagram can be still be used to check if the friction calculations are correct. It is important to note that calculating the friction factor needs to be calculated for each point in the pipeline. However, if the flow is steady-state and isothermal, than the friction factor is constant throughout the pipe.

3.1.4 Calculating the Compressible Factor

The compressibity factor of a natural gas depends of the temperature and pressure. The method outlined by the natural gas industry uses GERG 88 to solve for the compressibity factor based on the composition of the natural gas. Hydrogen is assumed as the only gas to be transported through the pipeline. By using this assumption, the compressible factor can be easily be interpreted from Figure 3.3. The range of importance to calculating the pressures in the pipeline is in the range of 0-100 [bars]. The compressible factors are similar in that range for different temperatures.

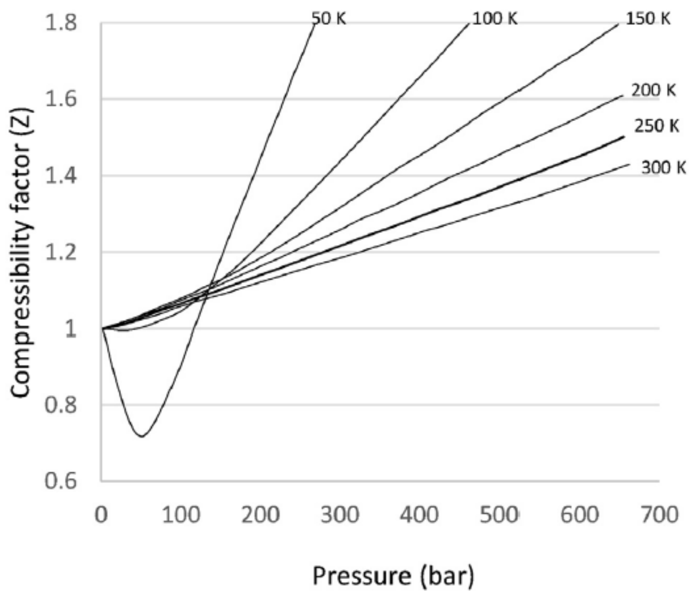

Figure 3.3: Hydrogen Compressibity factor [30]

3.1.5 Validating the Derived Equation

Inorder to check if the derived pressure equation by taking the finite difference is valid to use, it should be compared to what is used in industry. By changing the gas to hydrogen instead of natural gas, the following parameters are defined in Table 3.1

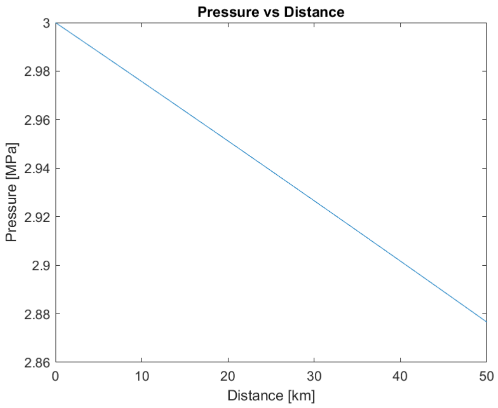

(a) Using the derived equation

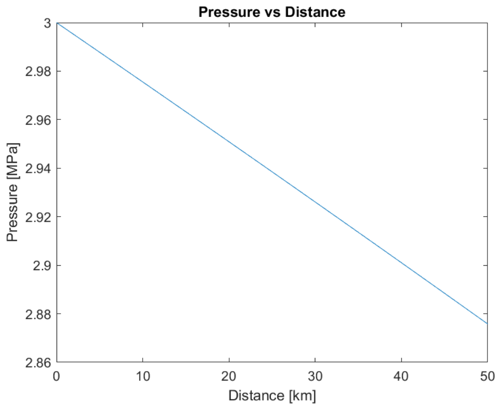

(b) Method using the natural gas industry equation

Table 3.1: Initial Conditions and parameters to find the Pressure drops for steady-state isothermal conditions.

Parameter	**Value**	**Units**
Mass Flow	0.3889	[Kg/s]
R	4029	[J/kgK]
Viscocity	$.85 * 10^{-5}$	[Ns/m^2]
Pipe Length	50	[km]
Pipe Diameter	.2	[m]
Pipe Rougness	0.03	[mm]
Temperature	12	[C]
Inital Pressure	30	[bar]

Theses parameters appear to be arbitrary but will be explained later. By keeping the parameters constant for both models is the main important point as the purpose is to check the validity of Equation 3.19. The results are plotted in Figure 3.4a-3.4b. It can be shown that the pressure decrease in relation for both methods are similar. There is only a very small difference. This can be explained by the truncation error. Equation 3.19 has been validated to be used further on.

3.2 Updating the Model to Include Pipelines

When implementing pipelines to the model, the determining factor for the parameters is the properties of the PEM electrolyzer as that will determine the initial pressure and the flow rate of hydrogen. According to [33], the electrical efficiency of an electrolyzer explains how much energy in terms of kwh to produce a kilogram of hydrogen. For example, if a PEM electrolzyer has an electrical efficiency of 50 kwh/kg H_2, that means if a power plant of 50 [kW] runs at constant power for an hour, 1 kilogram of hydrogen is produced. For the purposes on selecting the properties of an electrolyzer, only data taken from 2020 and not the target for 2050. For the Purposes of this thesis, the utilities (pumps and desalination) of running the electrolzyer is included in the electrical efficiency.

3.2.1 Fully Defining the Model

Since it was earlier chosen that the electrolyzer that should be a PEM electrolzyer, the properties of 2020 ideal PEM electrolyers are written in Table 3.2,

Table 3.2: PEM main electrolzyer Properties

Paramater	**Value**	**Unit**
Load Range	5%-120%	[-]
Electrical efficiency	50	[kWh/Kg H_2]
Production Pressure	30	[bar]
Stack Size	1	[MW]
Cold Start	20	[min]

Only a few more details are needed in order to fully define the model. One important factor would be pipe distance from farm location to shore. Wind farms in the north sea can range in distance 18-100 km. For the purpose of this model, an appropriate distance from the wind farm to the shore would be 50 km. This would reflect current and future wind farms in the north sea. Also, it is assumed that the pipes are buried under the sea floor, making the soil temperature an important value as this model assumes isothermal conditions. With these last points, the model has been fully defined and pipes can now be added to the model.

3.3 Modeling Scenario Two: Centralized Offshore Hydrogen Production

Scenario one and scenario two only differ in one regard, hydrogen is produced at the farm level offshore and transported by a pipeline to the shore. This means that the PEM electryolzers is are located on a single platform. For the purposes of this model, that platform would be the same platform as the substation for export cables. The cables that connect the individual turbines are still present in Scenario two. Now comes the question on how to model the pressures of the pipeline with wind production. Since it is an iterative process to calculate the pressure along the pipeline, it would first be advantages to look at constant cases, instead of first looking at the intermittence of wind. Since the string has 7 turbines that are rated at 10 [MW], that means the string capacity is 70 [MW]. An since wind intermittence is not the focus at the moment, it would be interesting to see what the pressure profiles of the string at a range of capacity i.e 5% string capacity to 100% string capacity. Since all the parameters of the model have been defined, this is now possible.

As for scenario 1, a simple illustration is shown in Figure 3.5 that represents the string used to model scenario 2. By simply looking at the model, it is clear that the string looks very similar. From turbines 1-7 to the substation, the layout is the same as for scenario 1. The change comes at the substation itself. Hydrogen is produced at the a centralized place, the substation. This means no electricity is sent to the shore but instead hydrogen is exported. Hydrogen is transported to the shore. The export cable gets replaced by an export pipeline. This pipeline should support the flow of hydrogen at max string power. No other aspects of the sting changes besides the export/substation.

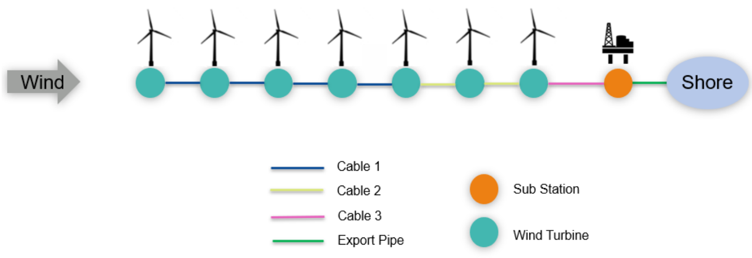

Figure 3.5: A simple illustration of the string layout for scenario 2

As from Equation 3.19, the mass flow measured in [kg/s] needs to be determined. Getting the mass flow rate is fairly simple since the electrical efficiency of the electrolyzer is given. Since the

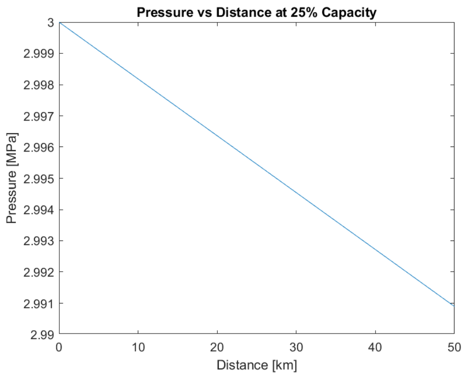

(a) Pressure Plot for 25% string capacity

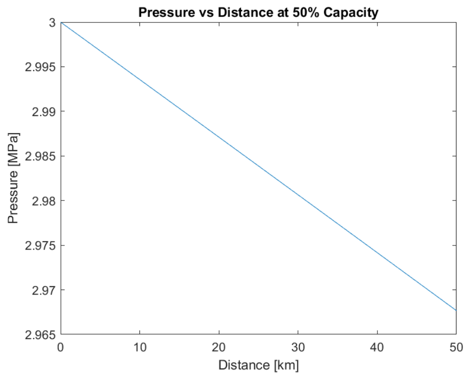

(b) Pressure Plot for 50% string capacity

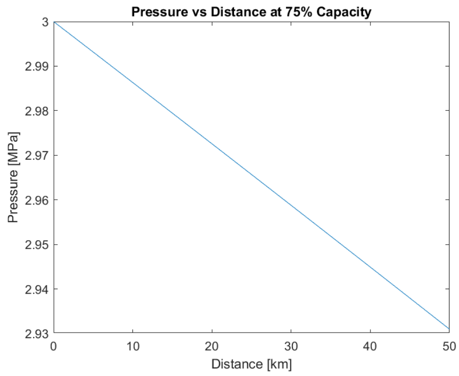

(c) Pressure Plot for 75% string capacity

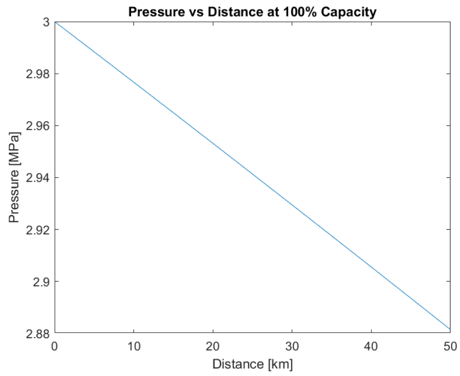

(d) Pressure Plot for 100% string capacity

electrical efficiency gives how much energy [kWh] is needed to produce a kg of H_2, by Up-scaling the PEM to be the same rated size as the Turbine, a simple formula can be used to determine the kg of hydrogen produced,

$$M_{H_2} = \frac{E_u}{E_e} \tag{3.23}$$

where M_{H_2} is the mass of hydrogen in kg, E_u is the energy that the electrolyzer uses and E_e is the electrical efficiency of the electrolyzer. Now, this is the total mass of the kg produced per hour, by converting it to seconds instead of an hour would give us the flow rate in terms kg per seconds. With the mass flow rate known, the pressure drops can now be calculated and are presented in Figure 3.6a- 3.6d. Since there are a total of 20 graphs to describe the pressure changes in the pipeline for the different string capacities, only 100% and 50% string capacity are shown since there is a clear trend that the lower the string capacity, the lower the pressure drop is from the start to the end of the export pipeline.

When dealing with string capacity lower than 25%, it is seen that that the pressure difference from the start of the pipe to the end of the pipe is quite small. The two big factors that determine how large the pressure difference is the pipe diameter and the flow rate. The diameter of the pipeline was chosen to be .2 meters. The mass flow rate in Figure 3.6a- 3.6d only decreased by a factor of 4, and by doing so made the pressure drop at 25% capacity practically negligible compared to 100% capacity. The next step would be implementing this to a change in wind speeds.

Since the input data of the model is a time series that gives the wind speeds at turbine 1, that fluctuates, the question comes of how to implement the pressure drops in this case. Since the pressure drops were found for string capacity of 5% to 100% has been calculated, this can be used in the model. In order to calculate these pressure ranges, it is an iterative process since every discrete point in the pipeline must have the pressure properties calculated. Since the time series has 3600 of data points to use, and to calculate the pressure for each of those points makes the process very computationally expensive. To alleviate this issue, its the time averages that become more important. By running the model based on what the average interval (15,20,30 or 60 min), an average power can be calculated. Since the pressure drops for various capacities of the strings have already been calculated, the average pressure drops over the average interval can be interpolated. The results from implementing pipelines to the model will be talked about in the following chapter.

3.4 Modeling Scenario three: Individual Offshore Hydrogen Production

Similar to scenario two, scenario three also has an export pipeline. The main difference is that in scenario three, there are no internal cables. These cables are replaced by a pipeline that connects each turbine together. Since hydrogen is produced at the turbine level, hydrogen is exported from the first turbine of the string to the last turbine of the string and hydrogen is then exported to the shore. This scenario can be broken down in two parts, the internal hydrogen transportation and external hydrogen exportation. External hydrogen exportation can be modeled the same way as for scenario two, but for internal transportation it gets a little trickier. The string power can only be a single value at a time, and thus can be interpolated at any time. The problem comes at the turbine level. Since there there is a time delay that has been included in the model and wake effects, there are times that all turbines in the strings produce different power levels. Since each turbine is connected in the string, the pipe pressure after turbine two is reliant on the hydrogen produced after turbine one since they share the same pipe. This goes on until the last turbine in the string, where turbine seven is dependent on amount of hydrogen produced from turbines 1-6. If a key were to made in the same way for export, then there would be to many graphs and the computational time for process would be far to great.

A work around would be to assume as if there would be a unique pipe for every turbine. This way, the power of the previous turbines can be included. What this means is that for the first turbine in the string produces hydrogen based on the same capacity range used earlier and than the pressure drops until the next turbine is stored. The following turbine (Turbine two) would produce hydrogen as if it had the total power of turbine 1 and two. The same capacity range is used and then the pressure drop until turbine three is measured and stored. This process is then repeated until the final turbine in the string. The pressure drops for the string can be calculated through interpolation, similar to scenario 2. For the string, the internal pipeline diameter of .1 meters was chosen.

A simple illustration of the string for scenario 3 is presented in the Figure 3.7. As the theme goes, the string layout looks similar to scenario 2. The difference now comes from the fact that each turbine is equipped with electrolyzer equipment and the internal cables that connected the turbines to each other is replaced with an internal pipeline. The role of the substation also changes. The substation now is used to collect and pressurize the hydrogen to be sent to the shore. No hydrogen production is done at the centralized location.

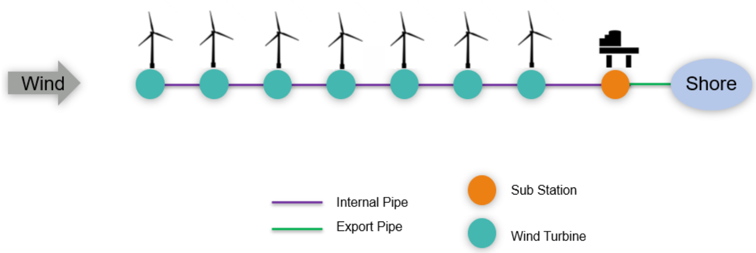

Figure 3.7: A simple illustration of the string layout for scenario 3

3.5 Power Losses

The last thing that needs to be determined in order to compare the different processes to each other is to determine the losses from each scenario. Whether it is electricity through a cable or a fluid traveling in a pipe, there are losses that need to be taken into account. The losses need to be calculated in different ways based on what form of transportation is needed. The following sub sections goes over the methods used estimate for the losses. These losses are then used to compare each scenario.

3.6 Electrical cable Loss Calculations

The losses of and electrical cable is determined by the current and the Resistance of that cable. The equation for Power loss is written as:

$$P_{loss} = 3I^2R \tag{3.24}$$

Where R is the Resistance and I is the current and varies with the amount of power produced by the WTGs ($P = VI$), assuming a constant voltage. Since it is assumed that the configuration of all the strings are the same, the losses in power for just one string need to be calculated. To do so, The current through each cable needs to be calculated since the cables do not reach their maximum rated amperage. This is quite easy to do by using equation Equation 2.2, where all the properties are know except I. By solving for the current, the power loss is easy to calculate since the distances are known. Lastly, by multiplying the losses for one string by 11, since that's the total amount of strings in the wind farm, the total losses can be calculated. For calculating the export cable, the properties of the cable would be different. It would be assumed that the export cables have the following parameters [39]:

Table 3.3: Cable Parameters for Export

	Type [mm^2]	**Ampacity [A]**	**Conductor resistance [Ω/km]**	**Phase operating Voltage [kV]**
Export Cable	2000	-	.015	220

For calculating the Power losses due to export, the same steps are taken. The total power is calculated at the substation, and then is used to find the current. After the current is calculated, the power loss calculations are simple to calculate as the resistance is provided in Table 3.3.

3.6.1 Compressor Power Calculations

The power losses that is from transportation of fluids through a pipeline is measured by the amount of power it takes to recover the pressure change through a compressor. These losses can vary greatly depending on the design parameters. For the purpose of this thesis, it is assumed that the hydrogen needs to be pressurized to a certain level. The equation for the power to adiabatic compress a fluid from the inlet pressure to outlet pressure is written as [46]:

$$P = \frac{\gamma Q_1 P_1}{\gamma - 1}\left[\left(\frac{P_2}{P_1}\right)^{\frac{\gamma-1}{\gamma}} - 1\right] \tag{3.25}$$

where Q is the volumetric flow rate , P_1 is the inlet pressure, P_2 is the outlet pressure, γ is the ratio of specific heat at constant pressure and the specific heat at constant value. For this case study, γ was taken as 1.4. Since this process is considered adiabatic, it is assumed that the compressor has a 70% efficiency as that resembles compressors in the real world. The following chapter will go over results based on the wind speed time series highlighted in chapter 2.

4 | String Results

Since now that the model has been fully defined, it is now possible to model scenarios 1-3, but before reviewing the results for the string based on the wind speed time series in Figure 2.9 preliminary results can be found in the form of the losses for cables and pipelines based on the capacitance established in the previous chapter. The power losses based on the string capacity has been plotted in Figure 4.1 and an interesting trend can already be seen. It can be seen that the losses for cables are larger than pipelines. The difference can be noticed even more for the power losses from inside the string. These values are based on string capacity, and shows that the higher the string capacity, the larger the losses become for both cases. The determining trend comes from the power loss equations. By looking at the compressor equation, what dictates the power losses would be the pressure ratio between the target pressure and the actual pressure. Since hydrogen is produced at the electrolyzer at 30 bars, that would be the target pressure to reach with the compressor.

Scenario one produces hydrogen at the same pressure as hydrogen produced offshore, by compressing the hydrogen that arrives to shore back to 30 bars, essentially compensating the pressure drop that occurs when transporting hydrogen through a pipeline gives a good benchmark for comparison of the scenario one and two. The same can be done for the internal pipeline, where the power losses comes from compressing the gas before export. This also gives a good benchmark for comparison of all three scenarios.

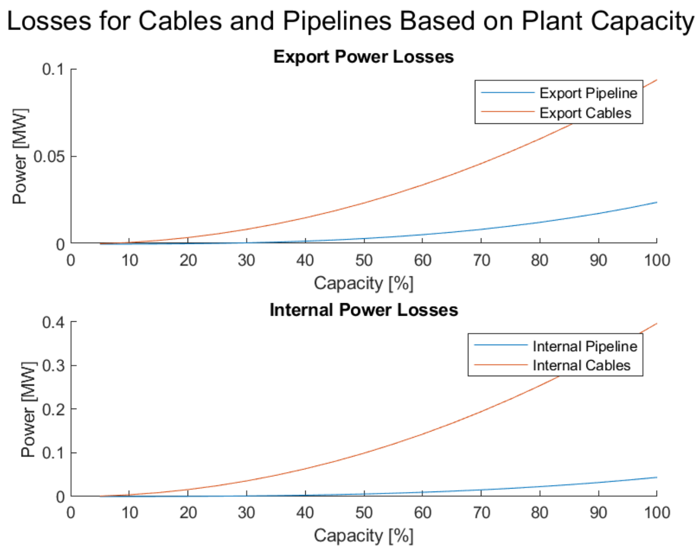

Figure 4.1: The losses for both cables and pipeline based on the total string capacity

With these Capacity losses established, its now possible to fully implement the pipelines into the full model. By looking at the averages based over the desired interval, for Figure 4.2a-4.2b, 15 minute intervals were used. For the 1 hour long time series, there will be 4, 15 minute averages of the power that will be used to calculate the pressure changes and the resulting power losses. As

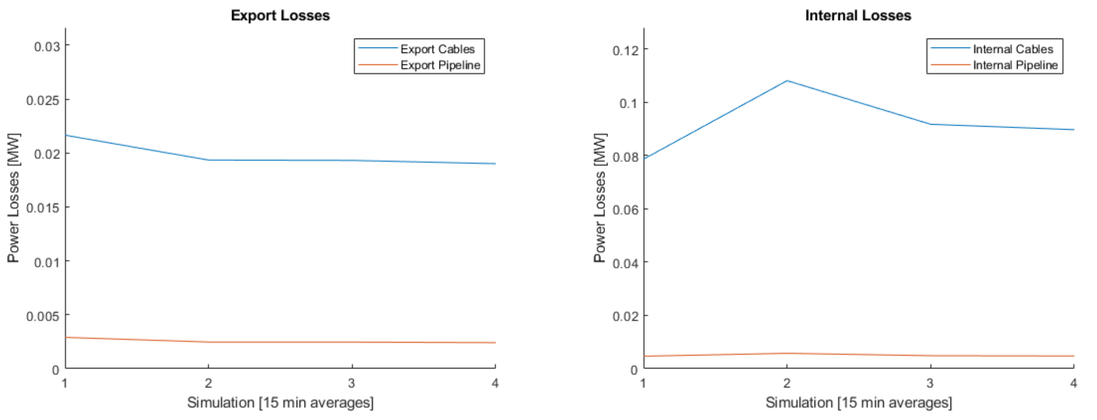

(a) External Power Losses for 15 Min Averages

(b) internal Power Losses for 15 min averages

it comes to no surprise, it can be seen that the losses from cables are higher than the losses from pipelines. Already, there is some evidence that supports the idea for producing hydrogen offshore due to the lower losses.

So far, only the individual parts has been shown. By combining the power losses for each scenario, Figure 4.3a shows the power losses for each scenario. The scenario with the lowest power loss is scenario 3. Scenario 3 is individual hydrogen production. There are no cables present in this scenario and that explains why the power losses are the lowest. By looking back at the capacity graph for power losses, cables are significantly higher which is especially true when looking at capacitance range 30-60%. The average string capacity for the simulation was around 44-48% further establishing the differences in power losses for cables and pipes. Based on the magnitude of both graphs, internal cables provide the most power losses compared to export cables. This explains the little difference from scenario's one and two since both those scenarios include internal cables and why the shape of the graphs follow the same shape as the internal cable power losses.

The results above have been plotted in terms the total power loss [MW] as opposed to a percentage of the total power of the string and the corresponding string capacity. Figure 4.1 represents the losses in terms of the percentage of the total string power. By presenting the results as a percentage, it makes it easier to see the overall losses of each scenario.

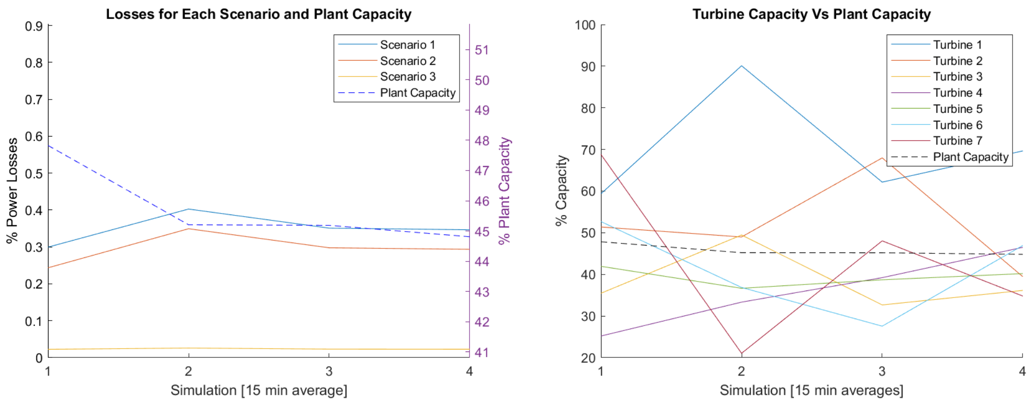

(a) Capacity of farm to losses

(b) Capacity of farm to turbine

Figure 4.3: Capacity of the plant and individual turbines for an increased wind speed

When looking at the string capacity, the percentage of power available to the max power string can reach (70 [MW]), it is shown that the losses seem to increase when string capacity decreases. Intuitively, it should be the opposite when the capacity of the string increases, the transportation losses increase and vice versa. That would also correspond with the trend shown in Figure 4.3a. The reason for this trend seen in Figure 4.3b comes from the individual turbines. When comparing the string capacity and the individual turbines capacity, Figure 4.3b ,the individual turbines vary quite significantly. The difference is capacity comes from both the time delay and the wake effects. Some turbines increase in capacity while others decrease in capacity. So, by simply looking at the capacity losses at Figure 4.1 can be a bit misleading as those losses corresponds to every turbine in the string to produce at that capacity. Based on the model, that is rarely the case. No turbines for the simulation operate at the same capacity. Since there are 3 different cables used in the string, that means the effect of losses differs based on the capacity from turbine to turbine. So even though the mean string capacity decreases, the overall internal losses might increase depending on the individual turbine capacity.

These results are for a single string. Normally offshore wind farms are composed of multiple strings and if the model would better represent real world conditions. The following chapter will go into detail on how to upscale this model to better reflect an actual wind farm. It would be important to see the effects of pressure drops and resulting power losses for increasing the capacity of the model.

5 | Upscaling the Model

As of 08-04-2021, the total capacity of active Dutch offshore wind farms range from 108 to 752 MW. Currently the string capacity of the current model is only 70 MW. It is predicted that Wind farms will only increase in size [41]. The up scaling of the current model should somehow reflect the sizes that can/will be seen in the north sea. For this purposes, the farm capacity of the model should be around the size of the largest offshore wind farm from the above range.

There are multiple ways to increase the capacity of wind farm model. The fist way would be to increase the rated power of the wind turbine. The second way would be to increase the number of turbines in a string. The issue with both of these approaches means that the string layout would no longer abide by the limiting properties of the selected cables and would mean new cable would need to be implemented. A way to increase the wind farm model without the need for new internal cables would be to simply add strings. The string layout doesn't change. There are still 7 turbines in a string with turbines rated at 10MW. By adding strings separated in a way so wakes don't overlap, the total capacity of the model increases but the string itself does not need to change. This is a simple method to increase the model capacity. Since it was determined that the new model size should be about 750 MW, by adding ten more strings to the model, a model capacity of 770 MW can be found.

5.1 Model Changes

5.1.1 Scenario One

Scenario one is not effected much by the increase in plant capacity. The only thing that needs to be done is to redo the calculations to represent the new wind farm capacity since the string layout is unaffected. Since the strings do not interact with each other and only connect to a central substation, the biggest impact for calculating the losses comes from export. It is assumed that the export cable can handle the increased plant capacity. The reason why this increase in capacity effects the exporting cable as opposed to internal cables comes from the power loss in cables Equation 3.24. Since the power losses for the internal cables increase linearly (strictly based on the amount of strings), the exporting cable losses increase based on the square of the current that runs through the cable.

5.1.2 Scenario Two

By increasing the number of strings, the calculations for the losses for exporting hydrogen through a pipeline changes the most. This is because at the original pressure and pipeline diameter is not good and would produce invalid results based on the given equations. This means that at the rated power the model is now, the pipeline diameter and initial pressure is not valid and these two properties must change to compensate for the increased rated power of the farm.

New Chosen export Diameter

Inspiration is looked at [27]. This paper looks at hydrogen potential in the north sea and produced an example of a 1 GW wind farm, and the chosen diameter for that example was .25 meters. In that paper they also compress the gas before export. By using these details, it is now possible to update the model by increasing the diameter to .25 meters. Simply changing the pipe diameter won't be enough. The initial pressure must also be increased, and this process is a bit more of a challenge.

Calculating new initial pressure

Ultimately, the goal of this thesis is to be able to compare the different methods of hydrogen production to each other. When the model was just a string by compressing hydrogen back to the initial pressure, this was a good measure for a benchmark to compare the the scenarios to each other since the initial pressure is the same pressure hydrogen is produce. However, when it comes to the increased model size, the initial pressure is not enough to transport the hydrogen to the shore, even with the increased export diameter size. This means that after hydrogen is produced from the electrolyzer, a compression must be applied to the hydrogen in order to ensure it arrives to the shore. To be able to compare the different scenarios to each other, the new initial pressure needs to be carefully selected that ensures that the end pressure would be the same pressure as the production pressure of the PEM electrolyzer. By compressing the gas from the hydrogen production pressure, 30 [bar] to an initial pressure that ensures the pressure at the end of the pipe is 30 [bar], the new power losses can be calculated. The same approach of calculating the plant capacity range and the corresponding pressure drops can be taken.

The method used to calculate the initial pressure is an iterative process. By making small incremental increases to the initial pressure, eventually an initial pressure is selected to ensure the end pressure is 30 [bar]. The process of calculating a new initial pressure needs to be done for every capacity level for the farm, i.e 100%, 95% to 5%. This is because the effect of the mass flow rate significantly effects the pressure drop in a pipe. The initial pressure for the model at 100% capacity (56 [bar]) is significantly higher than at 50% capacity (approximately 40 [bar]). If only the initial pressure for 100% capacity is chosen, the power losses to compensate the pressure would be significantly higher than it should. Once the new pressure drops are calculated with the new initial pressures, it can be applied to scenario 2.

A flowchart is shown in Figure 5.1 that outlines the algorithm used to find the new initial pressure and the resulting compressor power needed to compress hydrogen to the initial pressure to ensure that hydrogen at the shore is 30 [bars] so a comparison can be made for each of the scenarios. The searching algorithm used to find the initial pressures so that the pressure at the end of the pipeline is roughly 30 [bars] is similar to a binary search algorithm. This algorithm can be used because it exploits the relation between initial pressure and the pressure at the endpoints. When initial pressure increases, the pressure at the endpoint increase. That means for every unique value of initial pressure, there is a unique value for the end pressure. A key fact that needs to be considered is the consequence of having to small of an initial pressure causes the results to be invalid since the pressure drop equations will not hold up. This condition needs to be checked before continuing the search algorithm. Essentially the algorithm works by choosing a maximum and minimum values. Than the average between those two point is calculated and the pressure drop in the pipeline is calculated. If the pressure is less than 30 [bars] at the end of the pipe, then the new minimum pressure becomes the average pressure. If the pressure is higher then 30 [bars] at the endpoint, the new maximum value becomes average pressure. This way, the algorithm keeps searching the intervals until it finds the appropriate initial pressure. Constraints have to be put in place to specify an acceptable range to end the search. If a strict 30 [bars] is needed to end the program, the algorithm would possible run indefinitely since it can never find the exact 30 [bars]. The tolerance for finding an acceptable range for the end pressure was within $1 \cdot 10^4$ of 3 [Mpa], or simply 30 [bar] $\pm$ .1 [bar]. By going any lower than this value, the algorithm is more accurate but the time to run the algorithm increases and the differences in accuracy is small and has little effect to the overall losses.

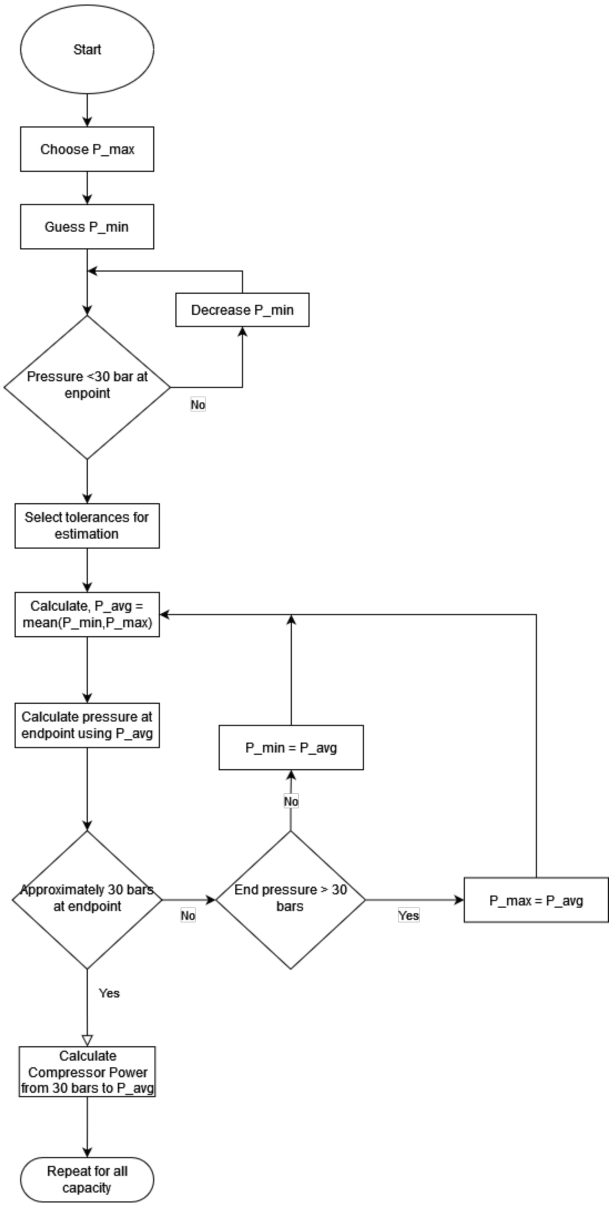

Figure 5.1: Flow chart to calculate the new initial pressure and corresponding compressor power

5.1.3 Scenario Three

Similar to scenario one, to update scenario three to compensate for the increased model capacity, the process is simple. Again, this is due to the fact that the strings them self are not changed, they are simply added to the model. This means that the effects of the power losses also increase linearly based on the number of strings. Again, its really the export of hydrogen that is significantly effected by an increase of the model capacity. The same method used for scenario two would be used.

6 Farm Results

After up scaling the single string model to a 770 [MW] farm, the same simulation can be applied. By doing so, the losses for each scenario can be seen in Figures 6.1-6.2b. As mentioned earlier, the power losses from export are now more dominant than the power losses from the internals of the wind farm. Again, that is because of the effects from up scaling. The power losses of the internal pipeline are significantly smaller than the power losses for internal cables. The power loss for internal cables is less than the power losses for the export cables. This difference in power plays a role on the trends for the comparison of power losses for all scenarios. The trend of the losses for the 770 [MW] farm is very similar to Figure 6.2, the sing string model, but the difference between the losses for scenarios 2 and 3 is lower. The peak for the 770 [MW] farm is also less dominant than when the model was a single string. The power losses percentage wise has also increased when compared to the single string model. By adding more stings, the percentage of losses also increase, however the scenarios that use a pipeline has a lower percentage of losses compared to scenario 1.

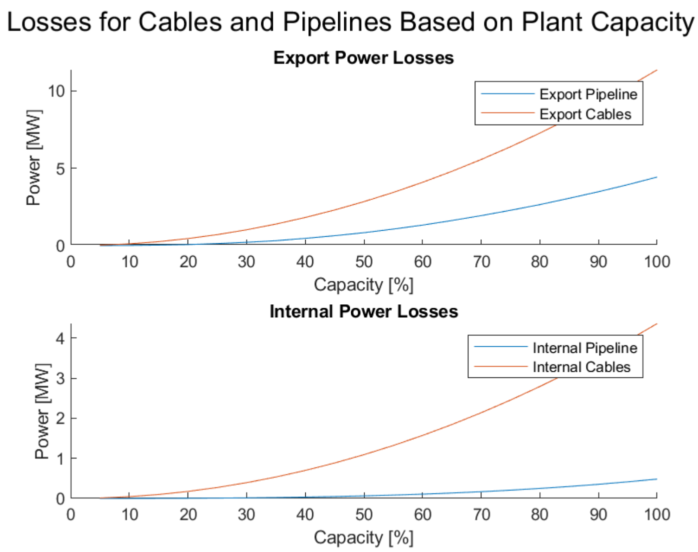

Figure 6.1: Capacity Losses for the up-scaled wind farm

Figure 6.1 shows that the losses for the export pipeline is 4.42 MW when the wind farm is at 100% capacity, or at full load. The power losses of the export cable when the wind farm is at full load is 11.3 MW. The electrical losses are about 2.6 times higher than the losses of exporting hydrogen through a pipeline. At full load, the electrical losses are 1.46% of the total power produced while the export losses are only 0.57 % of the full load. When the wind farm operating capacity decreases to about 50%, the difference in power loss is smaller, and the benefits of exporting hydrogen through a pipeline is smaller. For the internal pipeline, the losses are small and for wind farm ranges of 5% to 35%, using a pipeline gives the smallest benefit.

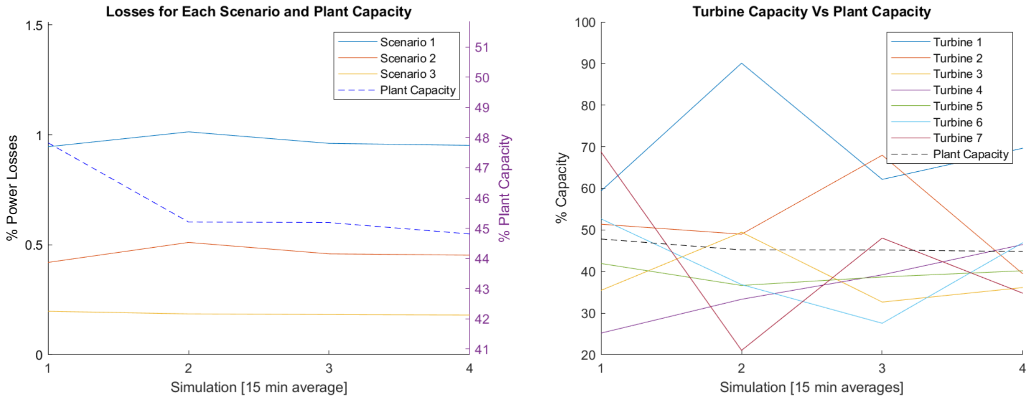

(a) Capacity of farm compared to losses

(b) capacity of farm vs turbine

Figure 6.2: Capacity of the Plant and turbine vs the losses

6.1 Sensitivity Analysis

Since the original parameter values used is a bit arbitrary, it would be important to analyze the effects if one of those parameters where to change. For this reason, a sensitivity analysis has been implemented to determine which parameter would positively or negatively effect the losses for each of the scenarios. The following list describes the parameters that will be modified, while keeping all other parameters the same, and the outcomes will be plotted in figures.

- Increase export diameter
- Increase distance to shore i.e the export cable/pipeline length
- look at the effects of changing the wake entrainment constant i.e wake decay coefficient, α
- Changing the roughness of the pipes (.03 [mm]) to see how much of an effect the friction factor plays a role on the power losses
- Decrease the efficiency of Electrolyer/Hydrolyzer
- Increase the simulation wind speeds to see the how it effects the farm/turbine capacity and the corresponding losses
- Up-scale the model further

6.1.1 Increased Diameter

Figures 6.3a-6.3b represents a change of the export diameter from the original .25 [m] to .35[m]. This change in diameter causes a significant decrease of the overall power losses when it comes to export. The diameter of the pipe plays a large role on the pressure drops and the corresponding power of the compressor needed to overcome that pressure drop. By increasing the diameter to .35 [m], the power losses of exporting hydrogen in a pipeline is even lower than the power losses for internal cables. This increase in export diameter further lengthens the gap between scenario 2 and scenario 3. Since this change just effects the export diameters and not the internal pipeline, the difference between scenario 2 and 3 do not differ.

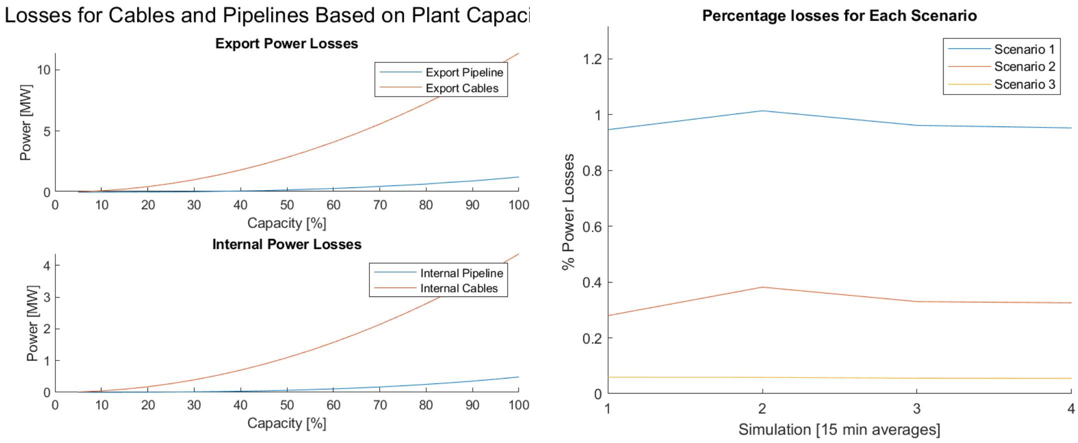

(a) Capacity Losses

(b) Power Losses

Figure 6.3: Increasing the export pipe diameter to .35 [m]

Figure 6.3a shows that at full load, the electrical losses is the same as Figure 6.1 but the losses of exporting hydrogen through a pipe is calculated to be 1.24 [MW] or about 0.16% of the total power. For scenario 2, at full load, the largest influence on the losses would be the internal cables. Looking at scenario 3 at full load, the total losses would be 0.21 %. This value is significantly lower than the losses of scenario 1, 2.03%, almost 10 times lower. Since changing the diameter only effects the pipeline, this comes at a price since the larger a pipe is, the more expensive that pipeline becomes.

6.1.2 Increased Shore Distance

Figures 6.4a-6.4b represents an increase distance that the farm is from the shore. The shore distance increased from 50 to 100 [km]. This has no effect on the strings but just the export. It shows that the power losses from the cables are higher than the power losses from just 50 [km] while the power losses of the pipe only increases slightly. The reason why there is not a big difference for export pipelines is because compressor power relies on two main details. The volumetric flow rate and the inlet/outlet pressure ratio. Since the pressure ratio hasn't increased that much and the increase of pressure has little effect on the volumetric flow rate. This means that even though the pressure drops increase and thus the initial pressure increases, overall the power losses do not increase significantly at least not in the same way export cables increase. If the distances becomes too large, the pressure needed to transport the hydrogen would be large and a change in diameter is recommended.

Looking at the full load losses in Figures 6.4a, the power losses for exporting hydrogen is 6.60 [MW] (0.85% of the full load), while export electrical losses is 22.3 [MW] (2.9% of the full load). By increasing the length of the exporting pipeline/cable, the total losses for each scenarios increased, but favors the use of a pipeline.

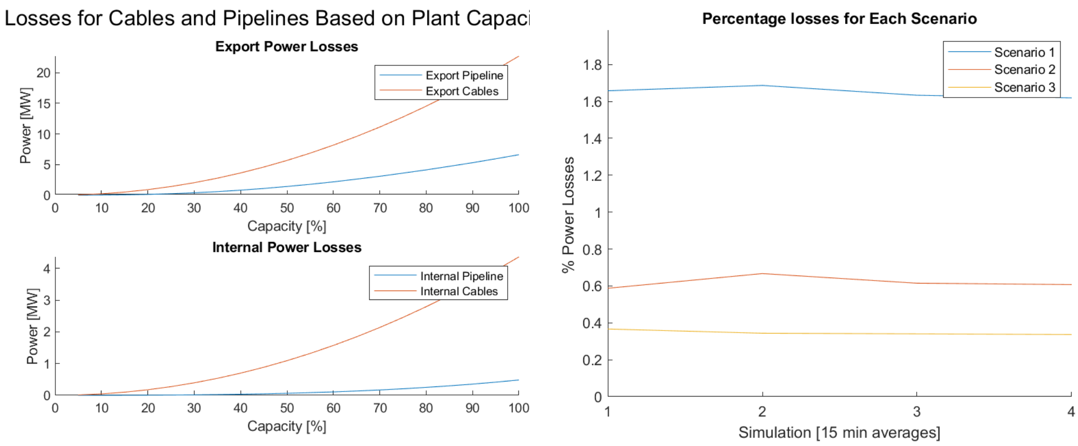

(a) Capacity Losses (b) Power Losses

Figure 6.4: Increasing the Distance to shore to 100 [km]

6.1.3 The Wake Entrainment Constant Effect on the Simulation

By changing the wake decay coefficient either widens or narrows the wake behind the rotor which in return causes a deficit to the wind speed. How much the defecate is depends on the wake shape. The effect on the wake can be seen in Figure 6.5, where the solid colored lined represents the wake when $\alpha = .1$ and the dashed line represents when $\alpha = .065$ By increasing the wake decay coefficient, the resulting wake becomes wider and the resulting wind deficit decreases. This means that the wind velocity that the following turbines in the string meets would be higher, and result in a higher power output. For the purposes of the model, by increasing the wake decay coefficient, the resulting capacity of the farm would increase, as can be seen in figure 6.6a. The average capacity of the farm has increased by about 5%, which in return also increases the power losses for each scenario, which would favor the use of pipelines. The shape for average plant capacity is also different, this is due to the initialization of the simulation. Since the average wind speed is higher, the time it takes for wind to travel down the string has decreased, which causes a smaller initialization period.

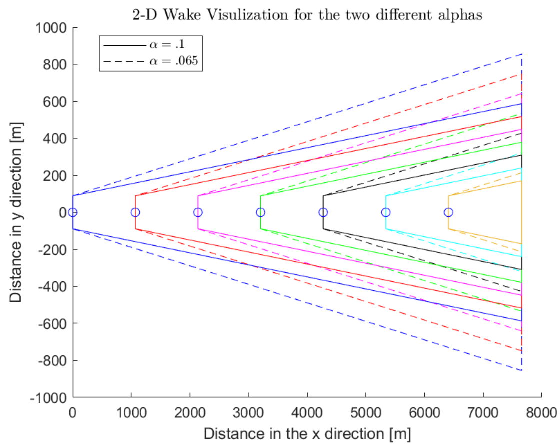

Figure 6.5: A visualization of the wakes for the two different α values

By decreasing the wake decay coefficient, the average wind speeds decrease due to a narrower wake. This causes the plant capacity to decrease and the resulting losses to lower. The initialization period is also longer from the lower wind speeds and resulting in a different Plant capacity shape.

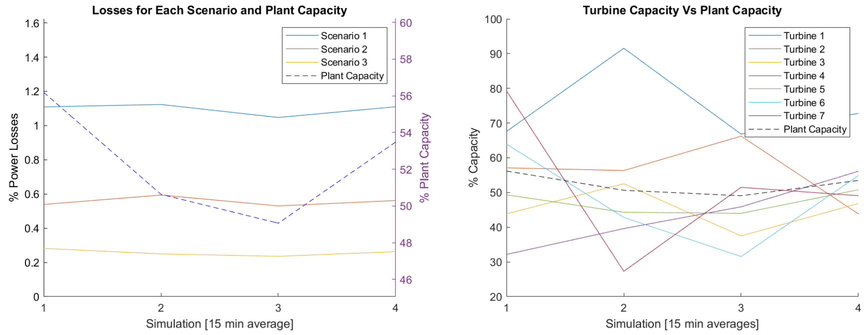

(a) Capacity of farm compared to losses (b) capacity of farm vs turbine

Figure 6.6: Capacity of the plant and individual turbines for $\alpha = .1$

Changing the wake decay coefficient does not affect the capacity losses themselves, it just effects the individual turbines, and the power they generate at a time step due to the fluctuations in wind speeds. Ultimately it makes the model produce more or less power and that is how it effects the transportation losses. For a larger powers, the losses in power from cables and pipelines becomes more prominent.

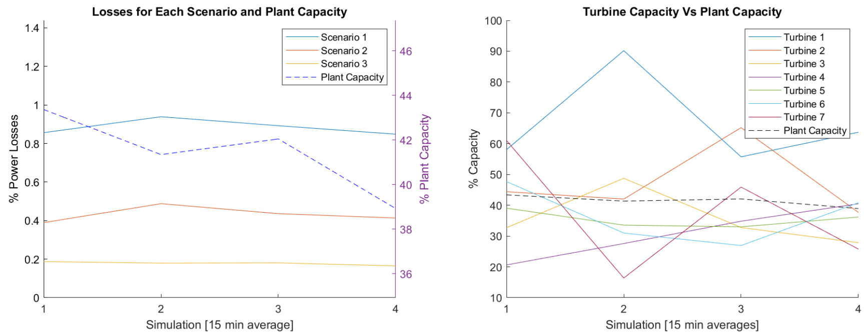

(a) Capacity of farm compared to losses (b) capacity of farm vs turbine

Figure 6.7: Capacity of the plant and individual turbines for $\alpha = .065$

6.1.4 Increasing the surface roughness of the pipe

When calculating the losses for a fluid in a pipe, the friction factor is part of that calculation. The friction factor of a pipeline is determined by the Reynolds number, and the ratio the of the roughness of the pipe and the pipe diameter (relative roughness), as shown in Equation 3.22. Increasing the diameter earlier decreased both the Reynolds number and relative roughness. But by changing just the relative roughness or the roughness of the pipe, the friction factor also changes. The surface roughness of the pipe is affected by multiple factors such as pipe material, fatigue or corrosion. By increasing or decreasing the surface roughness the model can to an extent simulate the above factors. Figure 6.8 represent the following corresponding losses. By increasing the surface roughness, the frictional pressure drops through a pipe increases, and the resulting power needed to compensate for the pressure drops increase, and as expected, the opposite occurs when decreasing the surface roughness. For a increase of pipe roughness, at full load, the compressor needs 5.04 [MW] of power, or 0.66% of the total load. The total power the compressor needs for the internals also increase to 0.54 [MW], this however is a very small change. By decreasing the pipe roughness, the compressor power needed at full load is 4.04 [MW], about a 1 [MW] difference.

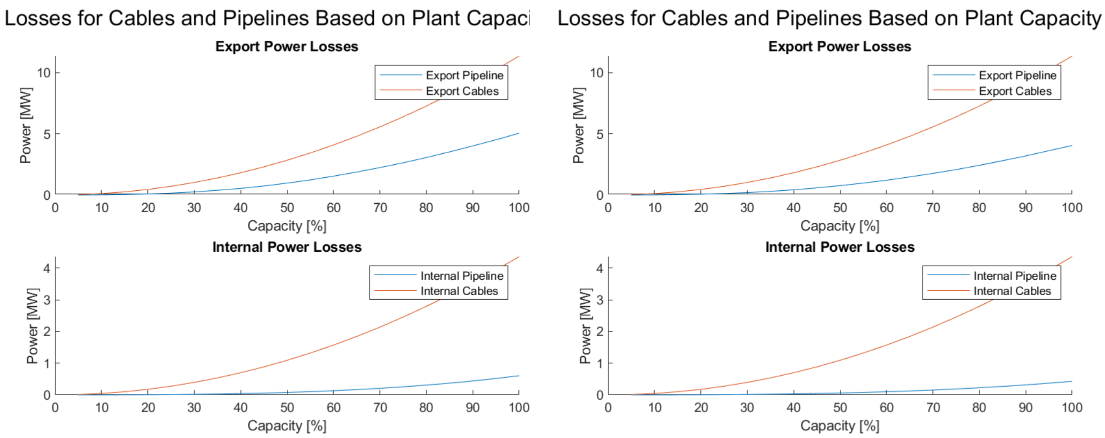

(a) $\epsilon = .1$ [mm] (b) $\epsilon = .01$ [mm]

Figure 6.8: Comparison of Capacity losses for when $\epsilon = .1$ and $\epsilon = .01$[mm]

By disregarding corrosion/fatigue effects on the surface roughness of the pipeline, the main determining factor would be material of the pipeline material. Depending on the material, the surface roughness can range from .26-.0015 [mm] [45]. There would be multiple factors involved when determining the pipeline material such as strength, available diameter sizes or the strength of the pipeline.

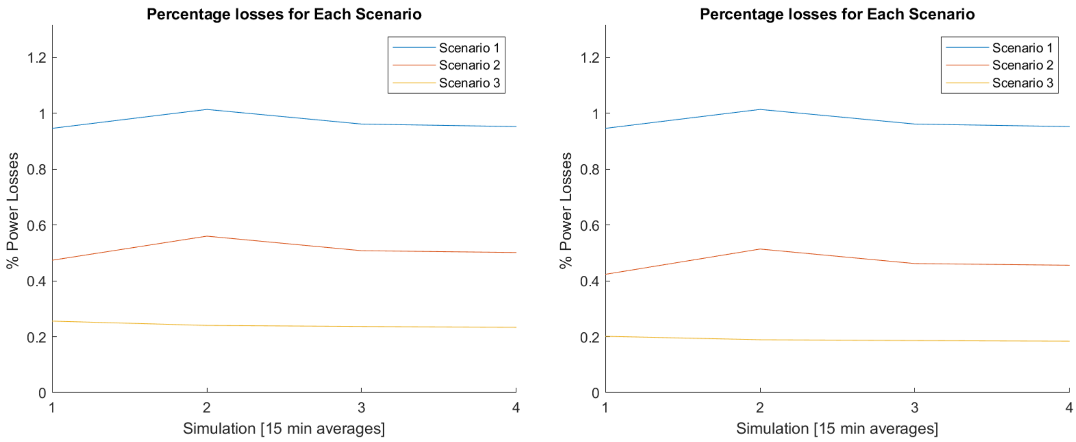

(a) $\epsilon = .1$ [mm] (b) $\epsilon = .01$ [mm]

Figure 6.9: Comparison of Scenario losses for when $\epsilon = .1$ and $\epsilon = .01$[mm]

6.1.5 Effect of Decreasing electrolyzer efficiency

Figures6.10a-6.10b represents a decrease of electrolyzer efficiency to 52 instead of 50 [kWh/kg H_2]. This change effects only the losses of a pipeline. By decreasing the efficiency of the electrolyzer, more energy is needed to produce a kilogram of hydrogen. Since the plant capacity stays the same, overall, less hydrogen is produced. Since less hydrogen is produced, the flow rate [kg/s] of the hydrogen traveling through the pipeline also decreases and the resulting pressure drop decreases. This means the compressor needs less power to compensate theses losses (4.04 [MW] at full load). This causes the transportation losses of hydrogen through a pipeline to decrease which favors the pipeline. However, this means less hydrogen is produced which could have financial impacts.

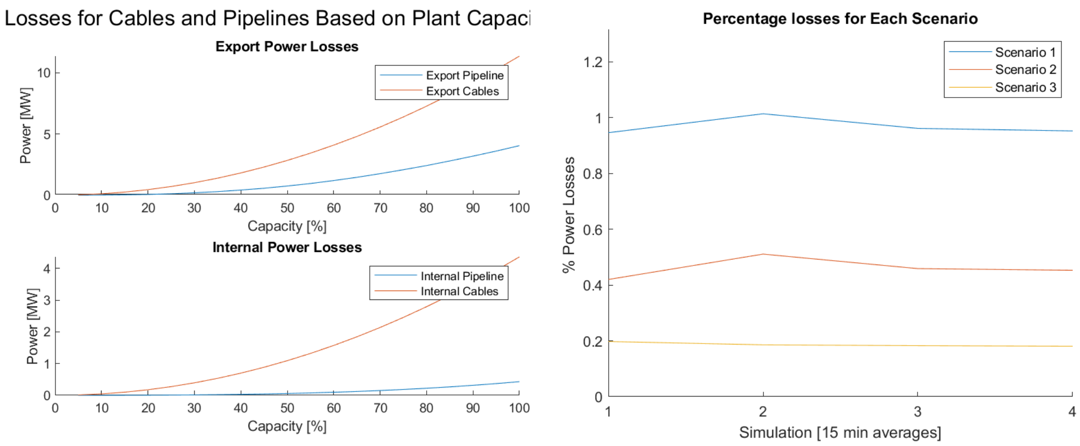

(a) Capacity Losses (b) Power Losses

Figure 6.10: Decreasing the electrical efficiency to 52 [kWh/kg H_2]

6.1.6 Increasing the simulated wind speed

Lastly it would be interesting to see the effects of an increase wind speed of the simulation and the effects that has on the losses. This is shown in Figure 6.11a. The losses increase, due to increase farm power production but the difference between scenarios 2 and 3 increase. Again, this is due to the role that internal cables have and that difference has been increased because of the faster wind speeds that produce higher power. Similar for the case of increasing the wake decay coefficient, the pant capacity graph has a similar shape. This is because the increased wind speeds lower the initialization period of the simulation. By increasing the wind speeds, the farm operates closer to the full load limit and shows the model would favor the use of a pipeline from just the power losses.

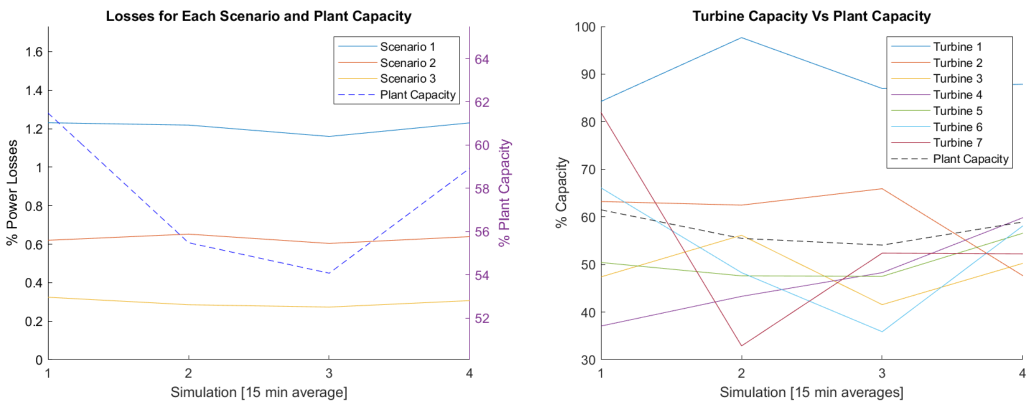

(a) Capacity of farm to losses (b) Capacity of farm to turbine

Figure 6.11: Capacity of the plant and individual turbines for an increased wind speed

6.2 Further Up scaling Effects on losses

The last part of the sensitivity analysis would be the effects of further up-scaling. By implementing the same method that was used to up-scale a single string, to a wind farm that had 11 strings. This new plant would have a total power of 1050 [MW] and would have 15 strings. By increasing the capacity can see how well the pipeline can handle this increase in production. Opposite to when decreasing the electolzyer efficiency, the increase in power means that an increase of hydrogen production will take place. This causes an increase in flow rate and consequently cause a greater pressure drop. The compressor must compensate for the increased pressure drop. At full load, the compressor requires 8.60 [MW] (.81 % of the total losses) of power, while the cable losses is 21.0 [MW] (2.0% of the total losses). When compared to the 770 [MW] plant at full load, the export pipeline losses were 0.57 % of the total power and while export cable losses were 1.47% of the total power. The difference in percentages for the 1050 [MW] farm is higher, meaning that further up-scaling favors the pipeline.

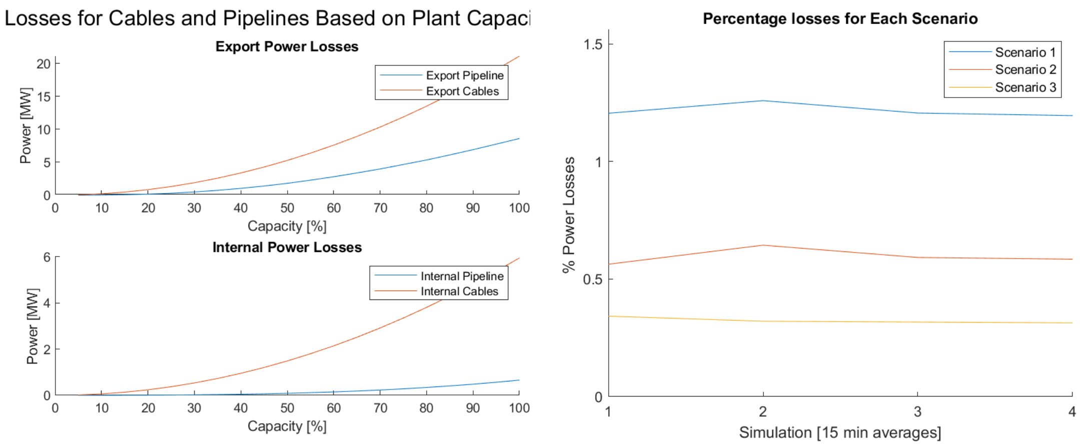

(a) Capacity Losses (b) Power Losses

Figure 6.12: Increasing the number of strings to 15, having a plant size of 1050 [MW]

6.3 Losses Effect on overall amount of hydrogen produced.

Currently, only power losses have been looked at for each scenario has been analyzed. What should be compared also is the amount of hydrogen produced for each scenario to really see the impact of these losses on the amount of hydrogen produced. In Figure 6.13 gives a visualization on for getting the different amount of hydrogen that is either produced at the shore or is transported from the wind farm to the shore. The diagram is broken down for each scenario and color coded based on the type of losses for corresponding to each of the different scenarios.

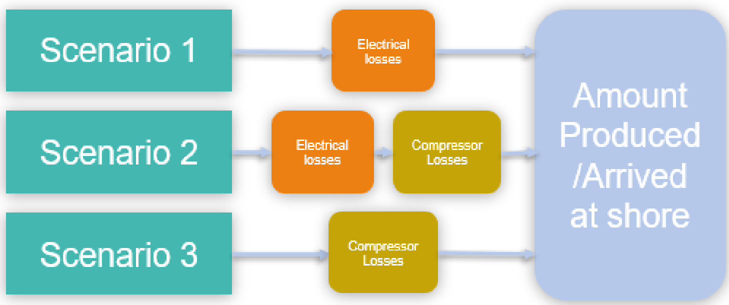

Figure 6.13: The methodology to get the compare the losses

An example of comparing the different amount of hydrogen produced for each of the scenarios is shown in Figure 6.14 where it is assumed that the wind farm is operating at full power, 770 [MW]. The losses are split into internal and external losses. The power losses are then subtracted from the initial amount leaving the Net Power for hydrogen conversion. For scenario 1, the power losses comes from the cables themselves and the measured power at the shore would be the initial power subtracted by the power losses coming from the cables. However for scenarios 2 and 3, measuring the true power losses is a bit different. Again, the power losses for pipelines comes from the power needed to compress the hydrogen with the use of compressors. The only power source that can be used to power the compressors would be the power from the wind turbines since there is no other external power. This essentially means that power needs to be taken away from the plant to be used to power the compressor. Since the plant power is less to provide the power needed for compression, the amount of hydrogen being produced is also less. This creates an iterative problem that needs to be solved to find the perfect ratio between the power for the compressor and the hydrogen produced. However, by looking at the maximum power needed to compress the hydrogen at full load and taking the power away from the plant and spread evenly to each turbine i.e instead of each turbine producing 10 [MW], they would produced 9.9434 [MW] and then calculating the pressure losses and the power needed to compress the hydrogen with less power, it is observed that the new power needed is very close (within .2 [MW]) to the original amount. The biggest discrepancies actually comes from the tolerances of the search algorithm as it might slightly over pressurize the hydrogen based on the difference in plant power. With this in mind and the small effects in compressor power, the losses are simply subtracted from the total amount, the same way it has been done for scenario 1. By subtracting the net hydrogen of scenario 1 with scenarios 2 and 3, it is shown how much more net power scenarios 2 and 3 have compared to scenario 1 for hydrogen production.

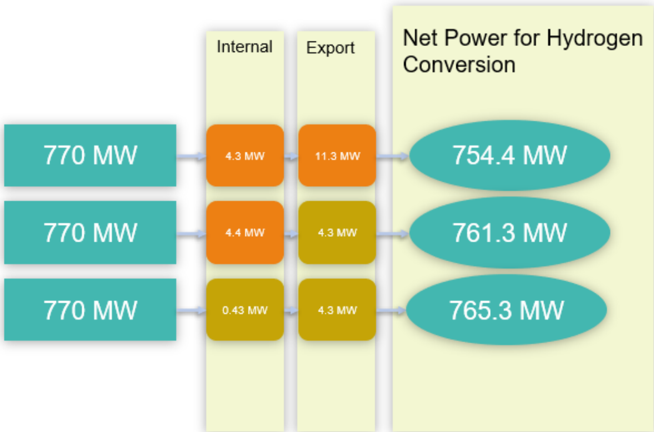

Figure 6.14: Full Load Loss example

7 Cost Comparisons and Considerations

From the results of farm model, it was shown that the least amount of losses comes from individual offshore hydrogen production (Scenario 3) while centralized hydrogen production losses is in between Scenario 1 and Scenario 3. This does not necessarily mean that Scenario 3 should be the DeFacto choice for hydrogen production using offshore wind. There is another important consideration to take into account, capital expenditure. Capital expenditure, also known as CapEx, is the money that is used to purchase, upgrade and/or extension the life of an assets[51]. This means that an alternative method of the production of goods might be more efficient in terms produced quantity, but if the Capex is too high, it would make that alternative method not worth it for investors. This is why Capex should be considered when comparing the different methods of hydrogen production to give a fair assessment.

7.1 Typical equipment needed for electrolysis

Unfortunately, the production of green hydrogen by the means of wind energy is more complex than simply installing an electrolyzer on a wind turbine or at an offshore electrical substation. There needs to be many systems in place to ensure the continual production of hydrogen. Since water is the main ingredient for the production of hydrogen, there needs to be a continuous source of water to the system. Since the electrolyzer requires water that has no impurities, a filtering process is needed. Not only a constant source of water is needed to ensure constant production of hydrogen, a constant source of power is also needed [21] [34]. As the name applies, wind power can only produce electricity when winds of sufficient speeds are present. In order to prevent the shutoff of the electrolyzer, the use of an alternate source of power should be included. Lastly, a means of transportation of hydrogen is needed for the hydrogen to either be used as power or stored.

7.1.1 Sea water pump

Depending on where the water comes from to be used in an electrolyzer, different means of supplying the water is needed. If hydrogen were to be produced offshore, the obvious choice would be to use sea water. The use of water pumps are necessary for either cases, decentralized or centralized hydrogen production. The sea water pumps inlet must be at proper locations to limit the intake of flora life. It should also be placed in an area to limit the brine intake as much as possible [21]. The optimal location is something that must be further studied and depends on the location of the wind farm.

7.1.2 Desalination

Again, depending on where green hydrogen is produced a desalination process is needed. For the case of production offshore, the uses of desalination is necessary to meet the specifications of hydrogen production. However it might be the case for onshore production, pure water is already available. The main concept of the desalination unit is to remove salt and impurities to create a constant flow of pure water. The purity of water is important to avoid maintenance repairs and downtime [21]. Desalination units is not a new concept and has been used in the oil and gas industry.

7.1.3 AC to DC Rectifiers

The electrolyzer that will be used to produce green hydrogen needs a constant stream of DC power. Since a wind turbine produces alternating current, there needs to be a converter in place to ensure the electrolyzer gets the correct specifications [21]. However, the green hydrogen DC power may be connected to the DC-AC converter side on the WTG.

7.1.4 Export Compression and appropriate pipeline

A pipeline system must be in place for the transportation of hydrogen, either long distances or to a centralized collective place for ship pick up. For cases of long distance export, a use of a compressor must be used to overcome the pressure drops that occurs when a fluid moves through a pipe [45]. These pressure drops can come from the roughness of the pipe, the length the fluid must travel in the pipeline and the diameter of the pipe. Export compressors are used in the fields of oil and gas to transport natural gas from offshore to the shore [21].

In the case for floating wind turbines, the dynamics of motion must be taken into account and that would require a flexible pipeline to accommodate for the motions of the turbine. If a rigid structure would be used, the pipeline system is sure to fail. The use of flexible risers are also used in the oil and gas industry although the dynamics of offshore wind turbines either bottom fixed or floating are quite different.[21].

Lastly, when transporting hydrogen, there is a potential for hydrogen embrittlement. Hydrogen embrittlement has been studied for years and is the risk of degradation of metals due to the presence of hydrogen [20]. Essentially, hydrogen is absorbed in the material making it more prone to fatigue damage [20]. By the use of different type of materials, such as low strength stainless and carbon steels have been used to transport hydrogen [21].

7.1.5 External Power Source

To ensure the constant production of hydrogen, an alternative power source must be considered. Multiple external power sources are considered, the main being solar PVs. This use of intermittent source of power is to ensure that the electrolyzer is able to retain power when there is not enough wind power available. For green hydrogen production on shore, then the grid could supply the power in case of low wind speeds. For offshore purposes, it appears illogical to supply external power from the grid onshore considering large distances. The use of solar Pvs or potentially even hydrogen fuel cells can be used during periods of low wind speeds. The use of Diesel generators are not considered because that produces carbon dioxide. One consideration could be a ship on standby to provide power but that could be relatively expensive.

7.1.6 Different Costs of Electrolyzers

All types of electrolyzers are not the same and fluctuates in price. Outlined in the report of "Green Hydrogen Cost Reduction" by IREA [33], the prices of a PEM and Alkaline electrolyzer are different. As mentioned earlier, Alkaline electrolyzer is cheaper than the PEM counterpart. For a 10 MW system, the cost of a PEM is 700-1400 USD/kW while the costs for an alkaline electrolyzer is 500-1000 USD/kW [33]. These prices don't include the costs of maintenance. Another important note when analyzing the costs is the lifetime of the electrolyzer. For a PEM or Alkaline electrolyzer, it is 50,000-80,000 and 60,000 hours respectively. The target life span of a wind farm is 20 years, which is roughly 175200 hours. Because of this, if the farm were to be operational for the full lifetime, the electrolyzer stacks must be replaced. This would increase the capital costs and effect the total pricing compared to the different electrolyzers.

7.1.7 Offshore Hydrogen Production Costs

For this scenario, the main difference for hydrogen production would be the pipeline that transports the hydrogen to the shore. It also includes a compressor that exports the hydrogen to the shore. These are capital costs that need to be incorporated to be able to determine if the scenario is feasible. The biggest capital costs are listed below,

- Pipe
- Compressor/Valves
- Ac to DC rectifiers
- Modifications to support structures

Since an electrolyzer needs the aforementioned equipment, this also means the support structure that houses the electrolyzer unit must also be able to support this additional equipment. This is more evident for individual hydrogen production since each support structure needs to not only support the wind turbine but also support the necessary equipment needed for hydrogen production.

Estimate costs for a lifetime

The prices for pipes are shown in Figure 7.1 as well as the cost for the export cable used in the model.

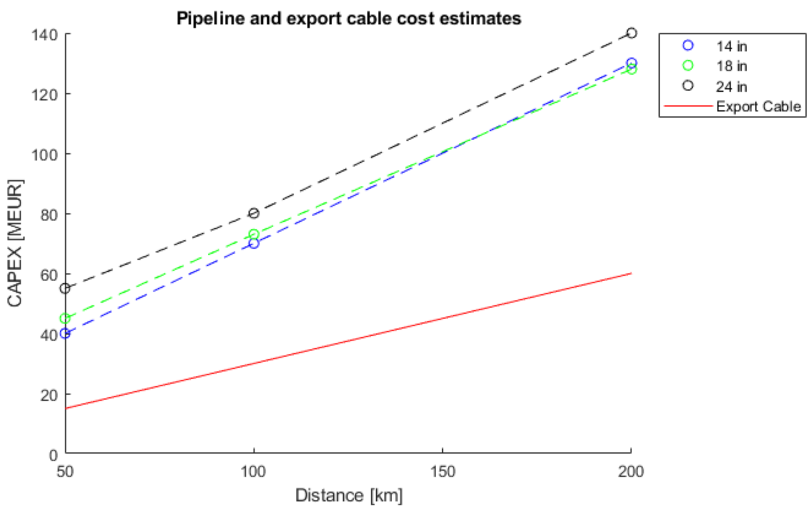

Figure 7.1: Prices for Pipes and cables

The prices listed above are specifically the costs of export. For costs of internal pipeline is estimated using the trends in prices using the figure shown above. The costs for the internal cables in the string that scenarios 1 and 2 use are shown in Table 7.1 [28]. The table shows the approximate price of installation per meter. Table 7.2 shows the overall price and the total lengths of the different strings used in the model. These prices can be used to further analyze the costs between the different scenarios, specifically the CAPEX.

Table 7.1: Cable and pricing

	[EUR/m]
Cable 1	145-160
Cable 2	165-180
Cable 3	240-255
Export Cable	300

Table 7.2: The total lengths and the total costs for cables inside the string

	Total Length [km]	Total Cost [MEUR]
Cable 1	47.0	6.81-7.52
Cable 2	35.2	5.81-6.34
Cable 3	13.7	3.29-3.50

The last step is to estimate the costs of the pipeline in the string for scenario 2 and scenario 3. The model used a diameter of .1 [m] for the internal pipeline while the external pipeline used .25 [m] , and by using Figure 7.1 as a reference, a function can be estimated to predict the prices for a .1 [m] diameter by looking at different total lengths. A best fit line was created for 50,100 and 200 [km] distances and presented in Appendix C. It is shown that from the previous tables and figures that the installation costs of cables is cheaper than the installation costs of pipes.

7.1.8 Cost of Compression and pipelines for scenarios 2 and 3

The capital costs of compression can be estimated to be 2000 EUR/kW [27]. By using this estimation, the capital costs of compression calculated for scenarios 2 and 3 would be based on the maximum power compressor needs to use i.e when the capacity of the plant is at 100% power. Even though it is rare for a wind farm to be be at max load for an extended amount of time, for the purposes of determining the costs for compression, the max compressor power is used when the farm is at max load. The total costs for compression is shown in Table 7.3 for each of the scenarios and the costs for the 50 [km] long .25 [m] export pipeline and .1 [m] internal pipeline shown in Table 7.4. The costs for the internal pipeline and the external pipeline is estimated to cost more, even though the diameter and the cost per meter is smaller. This is due to the fact that the internal pipeline is much larger than the export pipeline (50 [km]) for the model.

Table 7.3: The Cost of compression

	Total Compressor Power [MW]	Compressor Capital Costs [MEUR]
Scenario 2	4.4	8.84
Scenario 3	4.8	9.72

Table 7.4: The costs of pipelines

	Pipeline Costs [MEUR]
Export	25.7
Internal	37.9

7.2 Preliminary cost benefit analysis

The expected life time for an offshore wind farm is 20 to 25 years [36]. During the lifetime, it is expected for the payback of the wind farm to exceed the capital costs for construction, otherwise the farm would be considered a loss in investment. This concept must also be somewhat explored when looking at different methods of offshore hydrogen production. It is shown that the losses using pipelines is lower than the losses of electrical cables, but it has also been shown that costs for installing pipelines is more expensive than the costs of cable installation. Since the thesis specifically looks at the wind farm and the losses of transportation, what happens to the hydrogen after it gets transported/produced at the shore is outside the scope. This means that for the model, only scenarios 2 and 3 has the use of a compressor, specifically offshore compression. This then adds to the total costs to scenarios 2 and 3 as compared to the cost of scenario 1. Essentially, to make scenarios 2 and 3 more profitable is lower losses to compensate for the increased capital costs.

7.2.1 Assumptions for calculating the cost benefit analysis

A different method will be used for the preliminary cost benefit analysis each scenario. Instead of looking at 15 min averaged based on incoming 1 hour time series of wind data, a capacity factor would be introduced. A capacity factor is the net ratio of electricity generated, unit-less, for the time considered to the maximum amount of power possibly generated during the same period [53]. A capacity factor of 55% was used [48]. Since the losses based on the capacity of the wind farms has already been calculated in the model, the losses for each scenario is found by simply looking at internal and external losses for 55% capacity. The next step is to determine the differences for capital costs for each model. Since the difference of payback is relative for each model, it is important to determine what parameters are the same for each model and what differs. It is assumed the following is the same for each scenario:

1. The costs for desalination and water pumps.
2. The costs for electrolyzers and all other supporting equipment.
3. The costs for support structures for each scenario.
4. The cost of maintenance

It is also assumed that the wind farm would be newly constructed, so no scenario would use existing structures such a pipeline to reduce the capital costs. The only difference in costs for each scenario comes down to compressor and pipeline/cable costs. This way, its only the transportation of hydrogen is looked at. An assumption of 20 years is also taken into account. The estimated energy that the farm produced in its 20 year lifetime is calculated by the following equation where P is the plant power, C_f is the capacity factor, h_{20y} is the number of hours in 20 years.

$$E_{life} = P \cdot C_f \cdot h_{20y} \tag{7.1}$$

However, since the goal is to calculate the relative cost benefit for each scenario not the overall payback for each scenario, a modified approach is taken by looking specifically at the losses. Each scenario produces losses and in return means that less hydrogen is produced. Scenario 1 having the highest losses while scenario 3 has the lowest amount. By looking at difference in the amount of hydrogen produced as the payback and subtracting different capital costs for scenario 2 and 3 an estimate can be made if scenario 2 or 3 produce more income relative to scenario 1. The process is shown in the following equations where H_{total} is the amount in kg for the total amount of hydrogen lost due to losses, H_{loss} is the amount of hydrogen lost per hour based on the plant the the specified capacity factor,

$$H_{total} = H_{loss} \cdot h_{20y} \tag{7.2}$$

The total hydrogen lost is calculated for each scenario and then to find the relative hydrogen produced for scenarios 2 and 3 to scenario 1 is calculated as where H_S is the total losses of hydrogen in kg for scenario 2 or 3, H_1 is the total amount of losses in hydrogen in kg for scenario 1.

$$H_{net} = H_S - H_1 \tag{7.3}$$

H_{net} is how much more hydrogen is the lifetime for scenario 2 or 3. This value can than be used to determine the payback. By assuming a fixed price for hydrogen and the prices for export/internal pipeline and cables each the relative costs for each scenario can be calculated. A fixed price of 4 EUR per kg of hydrogen is assumed. The relative costs of pipelines is calculated by subtracting the pipeline costs for each scenario with the cables. Table 7.5 shows the relative payback for each scenario compared to scenario 1. It can be seen with the current assumptions that the relative payback from scenario 2 is higher then scenario 3. This is mainly due to the costs of internal pipelines and the losses at the capacity factor chosen. Since the internal losses of cables and pipelines do not scale linearly, the effects of losses are better shown when increasing the capacity factor of the wind farm. Its important to note that the cost of maintains for each is not applied to the model.

Table 7.5: The relative payback for a lifetime for each scenario

	Pipeline Costs [MEUR]
Scenario 2	13.65
Scenario 3	3.93

7.3 Economic Sensitivity study

To get a better idea behind the economics for the different scenarios, a sensitivity study is developed to determine which factors impacts the difference of lifetime payback for each scenario by using the parameters established above as the baseline. The following parameters will be changed, distance to shore, export pipe diameter, price of hydrogen and the capacity factor of the wind farm. Not only is the goal of this sensitivity study to determine the effects that different parameters have on the payback differences, but also see what the parameters must be so that scenario 3 has a higher cost benefit compared to scenario 2. Since scenario 3 has the highest capital costs for transportation since there are only pipelines used for the transportation of hydrogen, it would be interesting to see what parameters need to change (If there is one) so that the cost benefit for scenario 3 is higher than scenario 2.

Based on the sensitivity study that looked at losses completed earlier, the first parameter for the economic sensitivity study that would change would be to look at increasing the diameter size. The model used a diameter of 0.25 [m] and a line of best fit was used to estimate the capital costs of the 50 [km] pipeline. By increasing the diameter size to .35 [m], the costs for that sized pipeline based on the distance has already been established in Figure 6.3a. By using this new parameter to the model, it is shown in Table 7.6 that the cost benefit is even higher compared to the baseline even though the capital costs increased for the increased diameter. It seems that the losses through the pipeline decrease significantly enough to compensate the increased capital costs for the increase in pipeline diameter. The difference between scenarios 2 and 3 do not change since both are equally affected by the export diameter.

Another important factor when determining both the losses and the capital costs would be the distance of the wind farm to the shore. By changing the distance from 50 [km] to 200 [km], a table comparing the different diameter sizes to the different differences and the cost benefit for scenario 2 is presented in Table 7.6. The Scenario 3 is not looked at since the export diameter and distance to the shore effects scenarios 2 and 3 equally. It is important to note that in Table 7.6 that for the .25 [m] pipeline, distances of 150 and 200 [km] could not be solved for as the pressure required passed the limit set for the model.

Table 7.6: The cost benefit for scenario 2 in MEUR.

Diameter [m]				Distance [km]
	50	100	150	200
0.25	13.65	44.48	-	-
0.35	17.17	55.42	74.43	103.73
0.46	16.4	49.93	84.83	118.45
0.6	7.606	45.01	74.06	110.68

From Table 7.6, it can be shown that increasing the diameter size of the pipeline can increase the cost benefit depending on the distance the wind farm is to the shore. For the 50 [km] case, having a diameter of .35 [m] would give the highest cost benefit as going any higher would result in a lower cost benefit. For all export diameters for the 770 [MW] offshore farm, the payback difference increases when the distance to the shore increases. Even though the initial capital costs are higher, the losses are significantly less than compared to the losses through a cable which in return compensates for the capital costs. The main point is that the longer distances favor pipelines as the losses are lower compared to losses through a cable.

As the cost benefit has been looked at for scenario 2, scenario 3 is yet to be analyzed. The reason why scenario 3 has a lower cost benefit compared to scenario 2 is because the difference in internal losses is not enough to compensate the increased costs of the internal pipelines. Table 7.7 gives a set of parameters to change so that the cost benefit between for scenario 3 is about equal or a little higher than scenario 2. This gives a good indication of what conditions the model must have to determine that scenario 3 has a higher cost benefit based on the transportation losses. The first parameter to change would be the capital costs for the internal pipeline. By having the pipeline about 75% of the original price, scenario 3 would have about the same cost benefit as scenario 2. Another parameter to change would be the capacity factor of the wind farm. By simply increasing the capacity factor to 60%, scenario 3 has a slightly higher cost benefit. This comes from the effects of increasing losses of cables compared to the losses of the internal pipeline. The last factor to look at would be by looking at the costs for a kilogram of hydrogen. By increasing the cost by 1 euro, already there is a higher cost benefit. Ultimately, the model is quite sensitive to these changes, especially when it comes to hydrogen costs and the capacity factor.

Table 7.7: Parameter and the change needed to make scenario 3 have a higher cost benefit than scenario 2

Parameter	Base Case	New Case	Unit
Internal Pipeline Costs	37.9	28.4	[MEUR]
Capacity Factor	55	60	[%]
Hydrogen Costs	4	5	[Eur/kg H2]

The last aspect of the sensitivity analysis would be the effects of up scaling, essentially having the wind farm to increase in capacity. Since the strings themselves are limited by the cable type, by increasing the number of stings would increase the wind farm. The cost benefit for both scenarios is presented in Table for different plant sizes, 12,14,16,20 strings which correspond to 840,980,1120 and 1400 MW. By increasing the capacity of the wind farm this way both scenarios 2 and 3 are affected as the internal and external losses differ. Since the wind farm is being upscaled, the export pipeline will have a diameter of .35 [m] and the distance to shore is 50 [km] but all other parameters will be kept the same. The cost benefit is displayed in Table 7.8. Upscaling the farm in this method, cost benefit favors scenario 2 more than it does scenario 3. Again, this comes from relationship of internal losses to the capital costs of internal pipelines.

Table 7.8: Up scaling Effect on the difference of payback for each scenario

Plant Capacity [MW]	840	980	1120	1400
Scenerio 2 [MEUR]	24.9	41.6	61	105.454
Scenario 3 [MEUR]	13.9	29.4	48.7	93

Overall, the cost benefit is sensitive to many different parameters and of course depending on the value of the parameter itself either scenario 2 or 3 has a higher cost benefit. The results of the sensitivity analysis shows that offshore hydrogen production, specifically centralized offshore hydrogen production is favored when it comes to increasing distances to shore and up scaling while for the case of individual offshore hydrogen production, the capacity factor or the price of hydrogen is key when it comes to having either a higher or lower cost benefit than centralized offshore hydrogen production.

8 | Scenario 4: Offshore Hydrogen Storage

A keen eye would have noticed that Scenario 4 has not been talked about. This is because a different approach is taken to model the individual production and storage offshore of hydrogen. Scenario 4 is more of a logistics problem than the other scenarios. This is because the size of the tanks that hydrogen will be stored in would determine the time for ship pickups. For the purposes of this scenario, hydrogen is stored as a gas, since storing hydrogen as a liquid is extremely difficult to do offshore due to the very low temperatures required for that. There are multiple methods when it comes to storing hydrogen. Hydrogen can be stored in pipes, spherical or cylindrical vessels. Since the maximum pressure for spherical storage container is 20 [bar], this type of storage vessel will not be an option. Instead the more traditional type of storage, cylindrical storage would is chosen. These containers can be pressurized up to 100 [bar].

8.1 Calculating Storage Vessel Dimensions

As mentioned, to find the correct size of the storage vessel, it depends on how long the wait time is for ship pickup. Ideally, it would be large enough to to be able to store all hydrogen that has been produced. If the container were to small, then any extra hydrogen that could have been produced would be wasted. This is what makes this scenario a logistics problem and why Scenario 4 is mentioned last. The approach to try to model this scenario would be different. The rated turbine size and electrolyzer size would be the same as the previous scenarios. The time chosen in between ship pickups is the most important factor and thus chosen first. A series of different wait time of can be selected to create an in depth study. Since it assumed a constant stream of power is used for hydrogen production, this value needs to be determined. With these different parameters chosen, the dimensions of the storage can than be calculated with the use of this following equation,

$$V = h \cdot \pi \cdot r^2 \tag{8.1}$$

Since volume of the cylinder is dependent on both the radius and height, by fixing the radius to different values, the heights can then be calculated. The volume is dependent on the density of hydrogen. The density is depended on the pressure and temperature. These are all the considerations needed to be taken into account to create an in depth study on the storage vessel dimensions.

The chosen wait time for ship pickup is 1,3,7 and 14 days. By choosing this range for ship pickups, it can give a general idea for the dimensions needed for hydrogen storage. The next thing needed to establish would be to calculate the hydrogen output for a 10 MW electrolzer. For the purposes of scenario 4, a capacity factor of 55% is selected [48]. The capacity factor is an estimate of the percentage of power that can be extracted due to the variability of wind. For this scenario, a capacity factor of 55% means that a 10 MW wind turbine would on average produce 5.5 MW. The flow rate of hydrogen is now calculated as [kg/h]. The mass is not used directly to calculate the volume of the storage vessel, the volume of the gas is what is needed. Mass and volume is related by the density of the hydrogen. The density is calculated the same way as from scenario 2-3 by the state equation. The chosen temperature for scenario four is different, Since hydrogen is not being transported with buried pipes. For this case, 20°C was chosen. The volumetric flow rate is calculate as,

$$V_{H_2} = \frac{24 \cdot M_{H_2}}{\rho} \tag{8.2}$$

Where M_{H_2} is the mass flow rate [kg/h] of hydrogen exiting the PEM electrolyzer with the capacity factor included. ρ is the density of hydrogen based on the state equation. V_{H_2} is the volumetric flow rate [m^3/day]. Multiplying V_{H_2} by the amount of days between pickups would give the total volume of the gas. This volume is then used in Equation 8.1.

8.2 Results

The results are presented in the form of tables. Table 8.1 are the parameters for each Data set. Data set 1 represents normal allowable conditions of pressure for cylindrical storage vessels while data sets 2 and 3 represents conditions if the allowable pressures were allowed to increase. The main factor that determines the volumetric flow rate of hydrogen is the density. Density increase greatly with pressure increases as can be seen from the tables. Tables 8.2- 8.4 gives the results for the height of the volumetric cylinder for the fixed radius. Lastly, Table 8.5 represents the total mass of the produced hydrogen. The produced mass is the same for each data set, the difference comes from the volume of the gas which is largely based on pressure.

Table 8.1: Different Data sets to use to calculate the volume of the storage containers.

	Data Set 1	Data Set 2	Data Set 3	Units
Temperature	20	20	20	Celcius
Pressure	100	400	750	[bar]
Density	7.8	26.211	40.602	[kg/m^3]
Volumetric Flow	338.5	100.72	65.02	[m^3/day]

Table 8.2: Results for heights using Data Set 1

Cylinder Heights for Data Set 1						
	Radius [m]					
	3	4	5	6	7	Units
1 Day Pickup	11.97	6.73	4.31	3.00	2.20	[m]
3 Day Pickup	35.91	20.20	12.93	8.98	6.60	[m]
7 Day Pickup	83.80	47.13	30.17	20.94	15.39	[m]
14 Day Pickup	167.58	94.27	60.33	41.90	30.78	[m]

Table 8.3: Results for heights using Data Set 2

Cylinder Heights for Data Set 2						
	Radius [m]					
	3	4	5	6	7	Units
1 Day Pickup	3.56	2.00	1.28	0.89	0.65	[m]
3 Day Pickup	10.69	6.01	3.85	2.67	1.96	[m]
7 Day Pickup	24.95	14.03	8.98	6.23	4.58	[m]
14 Day Pickup	49.87	28.05	17.95	12.47	9.16	[m]

Table 8.4: Results for heights using Data Set 3

Cylinder Heights for Data Set 3						
	Radius [m]					
	3	4	5	6	7	Units
1 Day Pickup	2.30	1.29	0.83	0.57	0.42	[m]
3 Day Pickup	6.90	3.88	2.48	1.72	1.27	[m]
7 Day Pickup	16.09	9.05	5.80	4.02	2.96	[m]
14 Day Pickup	32.20	18.11	11.59	8.05	5.91	[m]

Table 8.5: Mass for each pickup time.

	Mass [kg]
1 Day Pickup	2640
3 Day Pickup	7920
7 Day Pickup	18480
14 Day Pickup	36960

A use of a compressor is needed in order to be able to store hydrogen in the storage vessel. The wind turbine would be used to power the compressor assuming no external power sources are used. The power the compressor would use would be small compared to the power of the wind turbine. The equation for the compressor relies on the volumetric flow rate and the pressure ratio. The larger the compression ratio, the larger the power is needed to compress that gas to the desired pressure. The trade-off for compressing to higher pressures to decrease the storage vessel size would be that the compressor would require more power. For data set 1, the power the compressor would need at full load would only be 0.31 % of the total power. When increasing the pressure to data set 3, the power that would be needed for the compressor at full load would be 1.13 % of the total power. As shown in Chapter 4 and 5, the compressor power would fluctuate based on how much power is available for the wind turbine to produce. If the used of compressors was Incorporated, the dimensions of the storage vessels would be smaller. However, for data set 1, the difference would be very small. It would be more noticeable for data sets 2-3 as the compressor needs more power.

9 | Conclusion

The different production methods of green hydrogen were analyzed in this thesis (scenario 1: on shore hydrogen production using offshore wind, scenario 2: Centralized offshore hydrogen production, scenario 3: Individual offshore hydrogen production and scenario 4: Individual storage offshore hydrogen production) and then a model was created looking at the feasibility for each production method. The offshore scenarios were compared to the base case (scenario 1). By keeping the scenarios as similar as possible to be able to compare the results, a conclusion was formed. By comparing the power losses from compressing and electrical cables, it is noted that the losses transported through a pipe with the chosen diameters are smaller than that of using electrical cables. Ultimately what matters is not necessarily the losses itself, but the amount of hydrogen produced with the power losses in consideration. It was shown that for the offshore individual hydrogen production, this method becomes the most efficient in terms of the amount of hydrogen produced. The second most efficient scenario is centralized production.

Besides the transportation losses from individual and centralized offshore hydrogen production, the effects of the variability that wind has on the power production should also be studied. It was shown that the normalized variation of power was smaller for the string level than for the individual turbine level. That means that if hydrogen productions suffers from the variability of power, clustering several wind turbines electrically with one electrolyzer should be considered.

Based on the sensitivity analysis, it could be seen that the model that incorporated pipelines is flexible so that the changes of the parameters does not significantly increases the losses relative to cable losses. The parameters that were analyzed in the sensitivity study was the diameter size, distance to shore, the wake decay coefficient, the roughness of the pipe, efficiency of electrolyzer, increased simulated wind speeds and further up-scaling of the model. It was seen that increasing the distance to the shore, the export losses for the pipeline did not increase significantly while electrical losses doubled. By further increase of the diameter, the losses would lower. The model was most sensitive to changes to the diameter, distance to shore and any effect that changed the wind speeds that the turbines in the model would experience. Increasing the friction factor or lowering the efficiency of the electrolyzer did affect the losses, however this was minor compared to the other parameters, therefore not as sensitive.

The preliminary cost benefit analysis was performed and further supported the use of pipelines for offshore hydrogen production. By comparing the costs of pipelines/electrical cables and the resulting effect they have on the losses in the model, it was shown that the export of hydrogen for centralized offshore hydrogen production was more economically beneficial by assuming a fixed price for hydrogen over the lifetime. An economic sensitivity study was researched to analyze the effects of changing the parameters of the model has on the preliminary cost benefit analysis. It was shown that increasing the distance to the shore or increasing the diameter was beneficial since the losses were significantly lower. When compared to centralized offshore hydrogen, individual hydrogen production is not as beneficial even though the losses are lower. By either increasing the fixed cost of hydrogen for the model or decreasing the costs of the internal pipeline would make individual production of hydrogen more beneficial.

A capacity factor of .55 was used to determine both the dimensions of the cylindrical storage containers and the preliminary cost benefit analysis. In reality, there could be times where the turbine produces at rated for an extended period of time (e.g. several days in succession). Excess hydrogen produced during those periods would be wasted. Although, the initial costs might be cheaper for this scenario since it excludes the costs for a pipeline system, ships are expensive, especially if modification need to be made to be able to harvest the hydrogen. Ship pickup is found to be unfeasible since the amount of storage on every WTG and the frequency of ship pickups must be very large. For the preliminary cost benefit analysis, the capacity factor plays a significant role. By increasing the capacity factor from .55 to .60, it was shown that it would be more beneficial to have individual offshore hydrogen production. The reason the capacity factor plays a large role is that the losses does not scale linearly and the difference in losses for cables and pipelines increase more dramatically the larger the capacity factor.

The method of calculating the losses for individual storage was not explored as the scenario differs to much from the other 3 to form a valid comparison. Unlike in scenario 1-3, where it was assumed that all hydrogen produced would be immediately sent away and there was no period where hydrogen was not able to be transported, so measuring the losses for individual storage would not just be the compressor power needed for the storage of hydrogen, but also the energy ships would need to pick up the hydrogen. This makes scenario 4 a logistics problem and would be difficult to compare in the same way as scenarios 1-3 were.

9.1 Limitations of Thesis and Recommendations

The following limitation and recommendations are established to further continue the research of the thesis and the effects that the assumptions have on the results.

The wind farm was designed based on the spacing of the turbines and the limiting factors of the cables. It was assumed that all turbines in the string were in line and the wind direction was parallel with the turbines to capture the wake effects during the simulation. The wind speed time series with a length of one hour and a resolution of seconds was generated and applied to the model. The model then split the time series into 15-minute sections to calculate the time delay based on the chosen wake model. This caused the model to run 4 simulations and resulted 4 corresponding power series where the initialization period has been removed. It was also assumed that the turbine could change its power production at the same rate the wind speed changes. This is not the case since the turbine's hub and blades have mass meaning it takes time to reach the new power that the wind speed is at. This means that the variance in power is less prominent and the difference between the string variance and individual turbine variance is smaller however the variance on the string level will still be lower.

To calculate the losses for each scenario, the average power was taken for each simulation and the corresponding losses was calculated as a steady-state condition. This was done because the equations to calculate the pressure drop in a pipeline assumes steady-state. The model does not account for abrupt or steady changes in hydrogen production which could affect the pressure drop and compressor performance. Another assumption for simplified calculations was to assume isothermal conditions. Since the pipes would be placed in soil, there would be heat transfer interactions from the pipe/soil and the change in temperature would also affect the pressure drop of the pipeline. Another simplification for the calculations concerning pipe friction losses was that there were no inclines, bends or junction losses. Since the sea floor increase in elevation the closer it reaches the shore, the fluid traveling in the pipeline must overcome the force of gravity and would increase the pressure drop. The effect from the difference of elevation was neglected since the model dealt with a distance to the shore of over 50 [km].

Finally, the calculations of the losses for centralized and individual offshore hydrogen production were simplified. The losses were calculated in the same manner as the electrical losses. Normally, this would not be the case since the compressor will take away power from the farm to compress the hydrogen meaning that less power would be available for hydrogen production. Since it was found that the losses were already small that even taking this account does not affect the results by a significant amount. If this were considered, the losses for pipelines would be even smaller with less hydrogen produced.

If the thesis were to continue, it would be recommended to go further in-depth with the transportation losses of pipelines by making the model non-isothermal. If even more complex calculations are desired, the model could also include the effects of elevation and appropriate junctions/bends which would give accurate pressure drop calculations and the resulting compressor power could be calculated more in depth. A more in-depth economic analysis could then take place using the new loss calculations and be able to determine the levelized cost of hydrogen for each scenario by taking the entire model into account (costs of support structures, electrolyzes, desalination units, ect.), not just the transportation of hydrogen. By estimating the total capital costs for each scenario, the LCoH could then be established and can determine which scenario would lead to the lowest LCoH. It would then be possible to see how different factors would impact the LCoH and which production method would be most desirable

A | Continued simulation of model for wind data

Different average intervals are displayed in FiguresA.1-A.6. For the 15 and 20 minute intervals, the initialization period has been removed and and the time series for each turbine has been displayed. When dealing with intervals greater 20 minutes, only a segment of the power series has been displayed, the first 5 minutes after the transient. This was done to make the figure easy to understand.

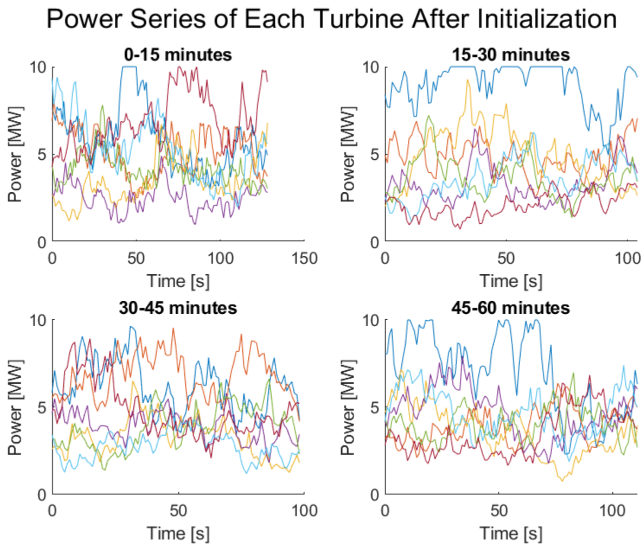

Figure A.1: 15 minute simulations time series for individual turbines

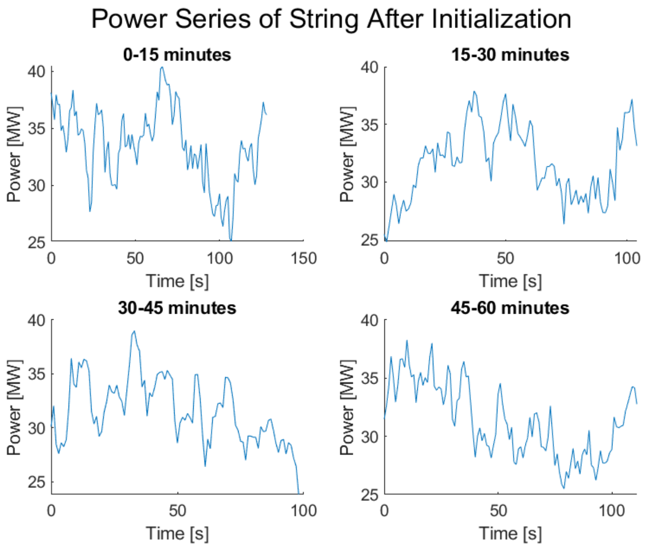

Figure A.2: 15 minute simulations time series for the string

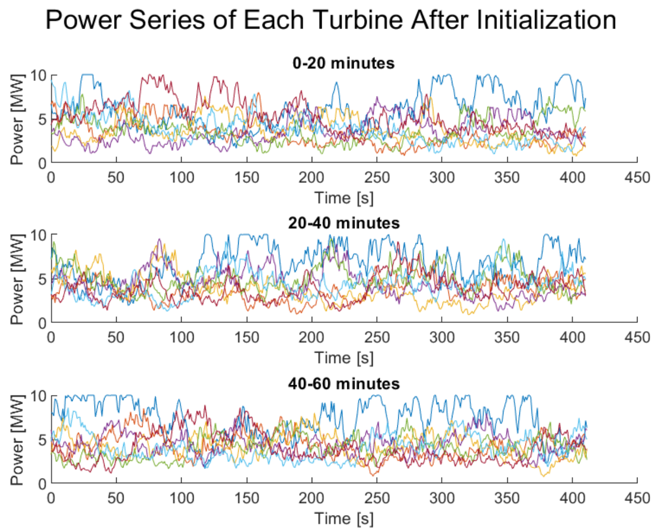

Figure A.3: 20 minute simulations time series for individual turbines

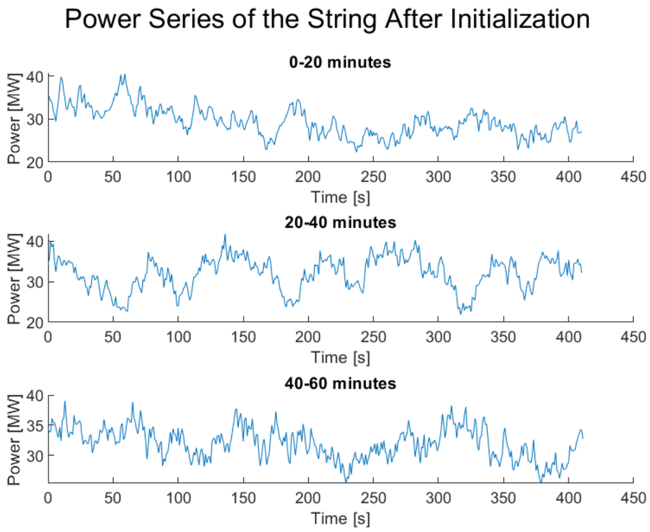

Figure A.4: 20 minute simulations time series for the string

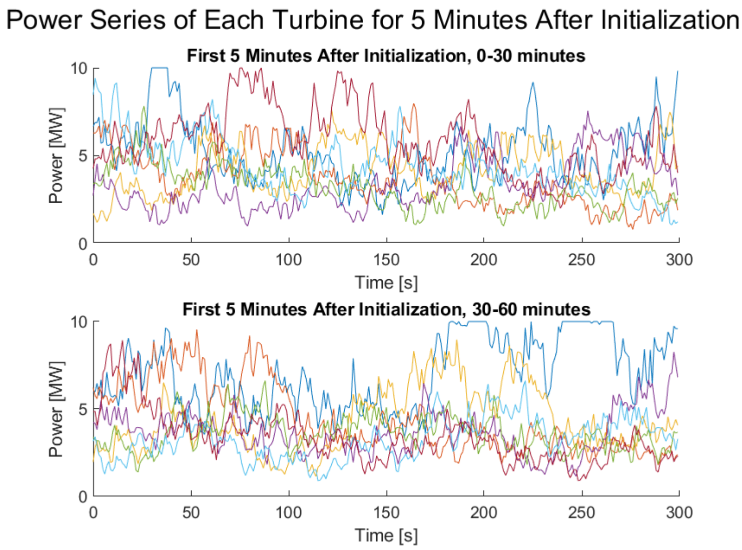

Figure A.5: First 5 minutes after the transient period for individual turbines

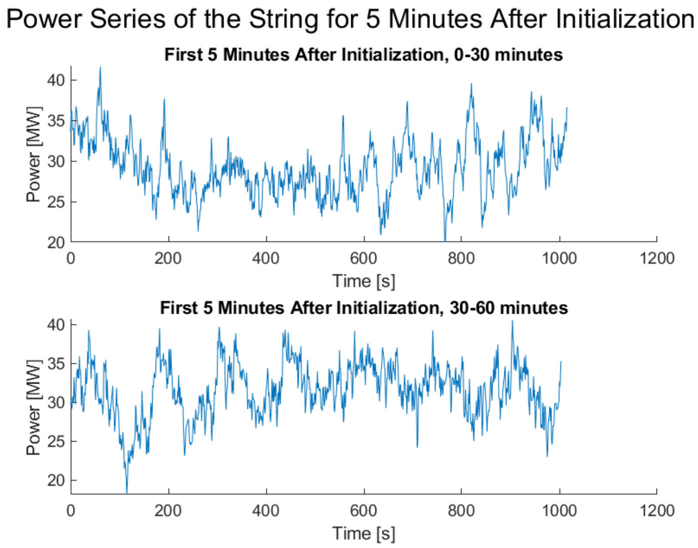

Figure A.6: First 5 minutes after the initialization period for the string

In Figure A.7a-A.7b, two different wind speeds are simulated that have different mean wind speeds. Figure A.7a has a mean wind speed of 11.3 [m/s], which is slightly below the rated wind speeds. This was chosen to see the effects of the wakes has on the following turbines in the string. Since the average wind speed is rated, the first turbine should produce at rated most of the time, but the other wind turbines should not operate at rated for most of the time like turbine one does since the average wind speed is about rated wind speeds.

By looking at the 15-minute averages, Figure A.8 shows that turbine two operates at rated as predicted while other turbines in the row does not operate at rated for most of the time. When wind speeds of 14-15 [m/s] is measured at turbine the first turbine of the string, only then will all other turbines in the string produce at rated, which happens only a few times in the wind speed time series. Due to the decrease in wind speeds, the initialization period is longer and there is less data points available for the power time series which can be evident by looking at the x-axis in Figures A.8- Figures A.10.

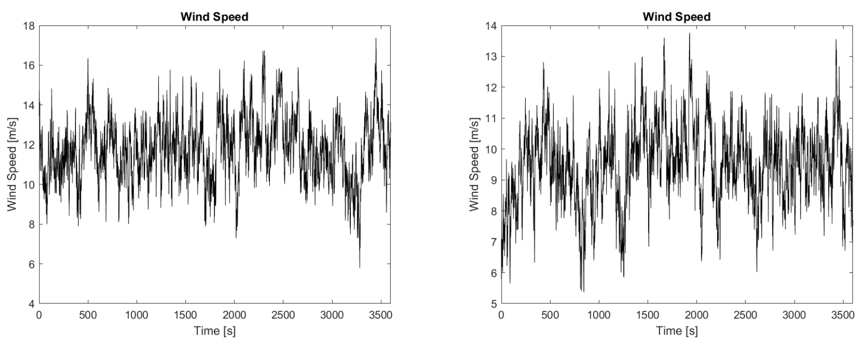

(a) 11.3 [m/s] mean wind speed

(b) 9.5 [m/s] mean wind speed

Figure A.7: Different Simulated Wind Speeds

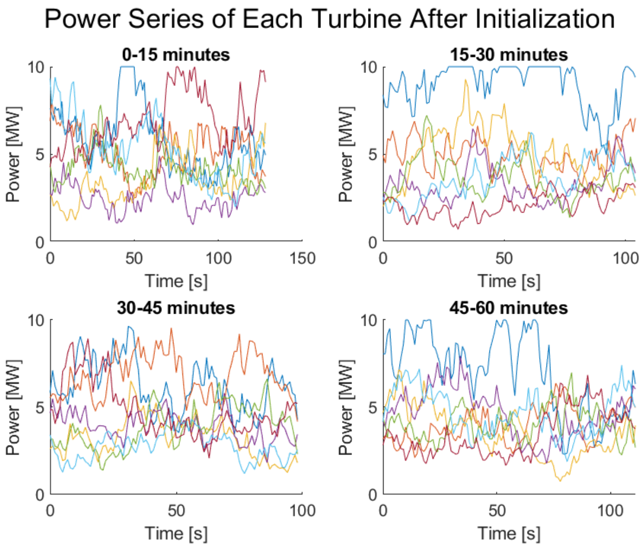

Figure A.8: 15 minute simulations time series for individual turbines, 11.3 [m/s] mean wind speed

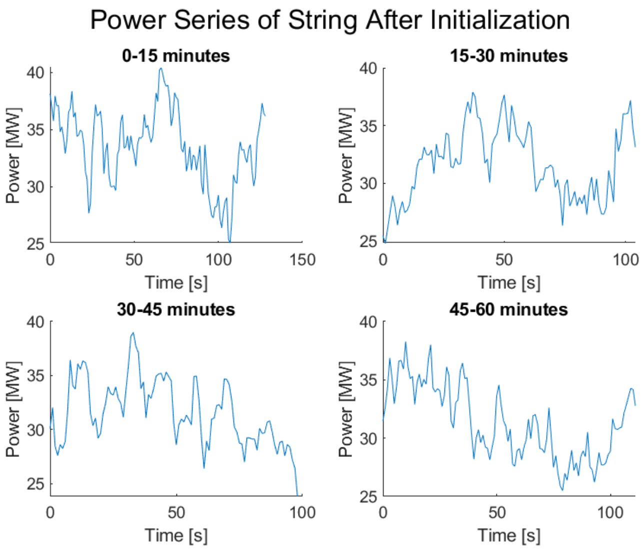

Figure A.9: 15 minute simulations time series for the string, 11.3 [m/s] mean wind speed

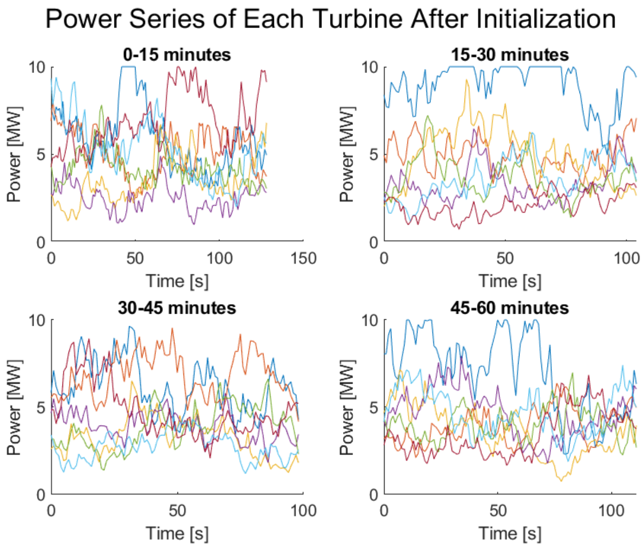

Figure A.10: 15 minute simulations time series for individual turbines, 9.5 [m/s] mean wind speed

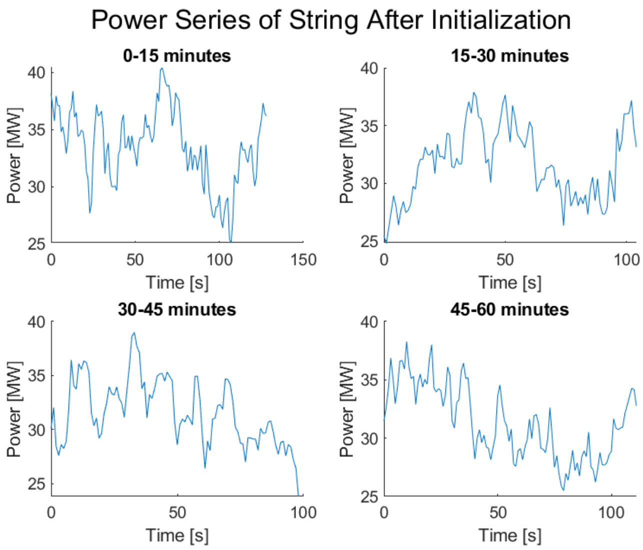

Figure A.11: 15 minute simulations time series for the string, 9.5[m/s] mean wind speed

By looking at the power variation for the string level and the individual turbine levels, as seen in Figures A.12a- A.12b the trend is similar what was shown in chapter 2, with one key difference. The variation of turbine one differs in trend from all other turbines and the string. The variance in power is calculated by taking the difference in power from two sequential time steps. Since turbine one spends most of the time at rated power, the variation in power is zero since the turbine can't provide more power than it is rated. For wind speeds slightly below rated, the power fluctuations are high due to the power equation for wind turbines, Equation 2.1. This means the variation in power is high, but the amount of data points for the high-power variations is smaller when compared to the string and other turbines in the row. But for both wind different wind speed simulations, the trend remains that the normalized power variations is smaller for a string then for individual turbines.

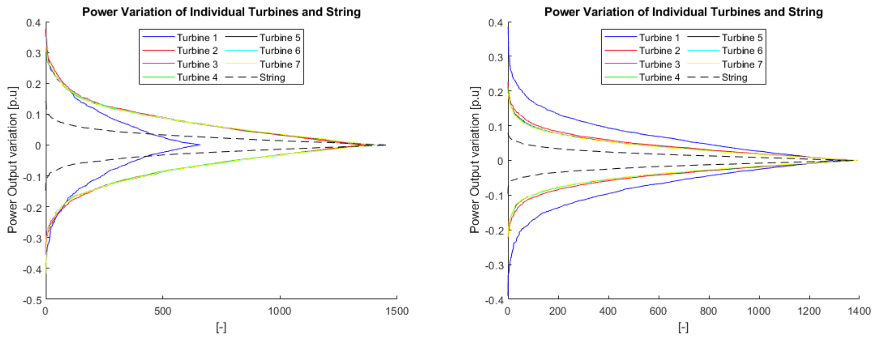

(a) 11.3 [m/s] mean wind speed (b) 9.5 [m/s] mean wind speed

Figure A.12: Different 1-hour Simulated Power Variations

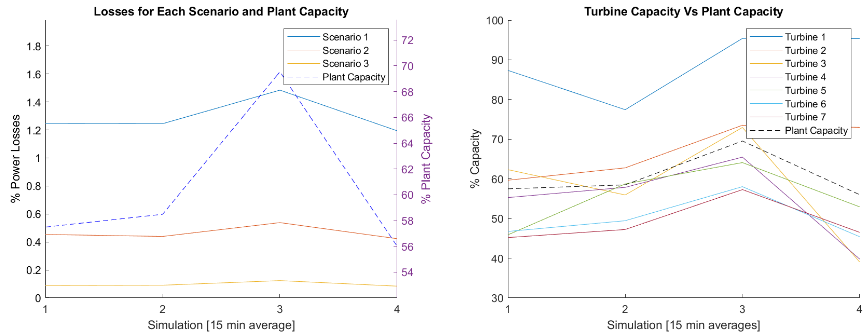

(a) Capacity of farm compared to losses (b) capacity of farm vs turbine

Figure A.13: Capacity of the plant and individual turbines for 11.3 [m/s] wind speed average

By looking at the Figures A.13-A.14, the losses are higher for the higher wind speeds as the relation goes. When looking at the relationship that the plant capacity has compared to the power losses is the same for Figure A.13a except for the beginning. The string capacity increases the and losses slightly decreases. By looking at the plant capacity and the individual turbines, not all turbines increase in power which explains the difference in the trend. For looking at the lower wind speed simulation Figure A.14a, the difference is more noticeable for the individual turbines which contributes to the different trend of plant capacity and losses.

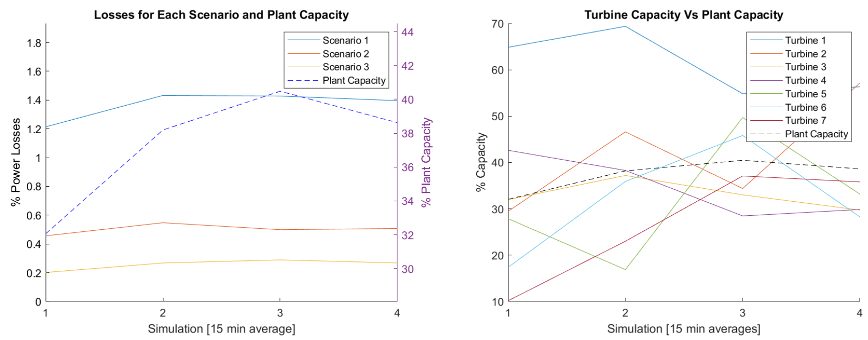

(a) Capacity of farm compared to losses (b) capacity of farm vs turbine

Figure A.14: Capacity of the plant and individual turbines for 9.5 [m/s] wind speed average

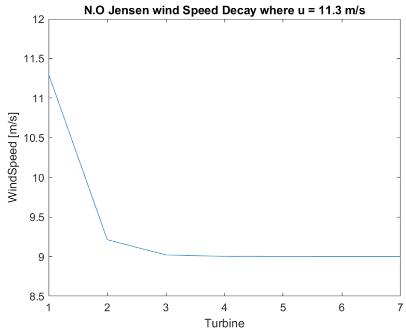

(a) Wind speeds that each turbine meets

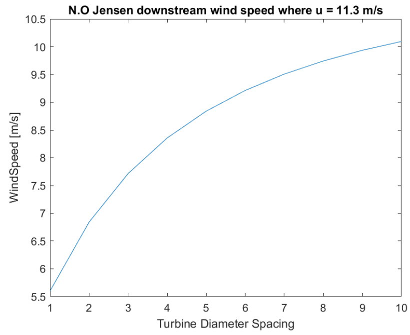

(b) Down Stream wind speeds for varying turbine spacing

Figure A.15: wake effects for constant free stream velocity for u = 11.3 [m/s]

The last aspect to look at for the different simulated wind speeds would be the effect the wake has on the wind speeds that the different turbines in the strings would meet. The trend for the two different mean wind speeds are the same and gives an idea on how much the wind speeds where to decrease in velocity. As shown in chapter 2, the effects that multiple wake effects have on the different turbines in the string diminish after turbine 3.

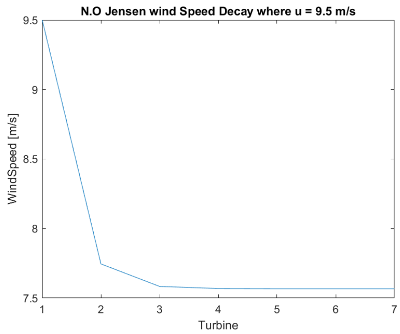

(a) Wind speeds that each turbine meets

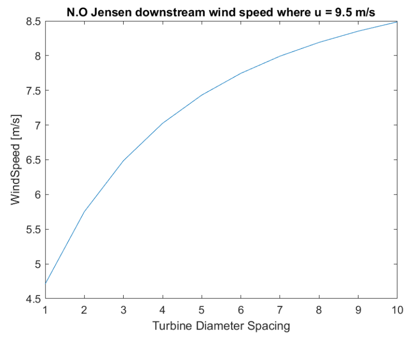

(b) Down Stream wind speeds for varying turbine spacing

Figure A.16: wake effects for constant free stream velocity for u = 9.5 [m/s]

B | Desalination and Pump Considerations

The electrolysis process requires the use of water. Water is broken down into the base parts of hydrogen and oxygen. The hydrogen is then exported to the desired location while the oxygen is either released or captured. Scenarios 2 and 3 produces hydrogen offshore and would have access to an unlimited amount of water, however this comes at a price. Since the electrolysis process specifically requires pure water, meaning that the water should not contain any impurities such as salt or other minerals, this means that water in the ocean must be treated first before the production of hydrogen can be accomplished. For this process, desalination units can be utilized. The issue that comes up with using desalination is that it is both costly in price and energy consumption and furthermore a demineralizer is needed to ensure that the water is pure. In addition to the mentioned units, a water pump is also needed to be able to pump the water from the ocean into the desalination unit. This process also costs power [17].

The main contributed to the energy consumption of a desalination unit comes from the following factors, Capacity (amount of water that needs to be treated), feed (type of water being treated), method (how the desalination process works) pre-treatment (Method of feed pre-treatment) [17]. Depending on the needs, such as the wind farm capacity, the availability of water and the method of desalinization the energy consumption needed to produce hydrogen will vary. For the purposes of our model two factors have already been determined, the plant capacity and feed type. As mentioned earlier, the model capacity is 770 MW, and with a determined electrical efficiency, the amount of hydrogen in kilograms theoretically that can be produced can be determined. This in return can determine how much water is needed to be put through the desalination process. The minimum amount of water needed to produce 1 [kg] of hydrogen would be 9 [kg] of water [43]. By taking the electrical efficiency of 50 [kWh/kg H2] [33], a 770 MW plant would produce 15400 [kg] of hydrogen per hour. Then by using the minimum amount of water needed, the process would need 138600 [kg] of water or 138.6 Tonnes of water per hour equalling 138.6 cubic meters of water per hour. Now it would be possible to make energy consumption estimates based on the theoretical limits.

As the scope of the thesis focuses on the transportation losses of each scenario, the fine details of the desalination process such as looking specifically at the different methods of desalination is outside the scope and instead the average estimates for a Reverse Osmosis using sea water ranges on average 4.3 - 4.4 [kWh/m^3] [17]. Depending on the type of method of desalination, the energy consumption would vary. By multiplying the average energy consumption with by 138.6 [m^3], the energy consumption for the plant would range from 596.0 to 609.8 [kWh]. Its important to note this is using theoretical minimum amount of water needed in the process and realistically the amount of energy needed would be higher depending on multiple factors such as electrolyzer properties and the desalination units. Also, the process of desalination becomes cheaper in terms of energy consumption when using brackish water if the hydrolysis process were to happen onshore.

Now the power for the pumps need to be calculated. This is a relatively straight forward equation and is written as,

$$P = qh\rho/(6116 * 10^3 * \mu) \tag{B.1}$$

where P is the power needed to pump water h meters, where q is the flow rate in liters per minute, ρ

is the density of water in terms of kilogram per cubic meter and μ is the efficiency of the pump [52]. By assuming an efficiency of the pump .9 [47], the distance between the deck where desalination takes place and the location where the entrance of the pipe where the water gets pumped from is always submerged in water is taken as 20 meters. The density of water is taken as 1025 [kg/m^3]. The flow rate is calculated by dividing the hourly amount of liters of water needed by 60. By solving the equation, the minimum power needed to operate the pump is 6.80 [kW]. This is for when the plant operates at rated power. When it comes to wind farms there are fluctuations in total power output and in return less power would be needed to power auxiliary units when the wind farm produces below rated wind power. Regardless, this is a fraction of the power compare to the energy needed to operate the desalination unit. Again depending on conditions, the power needed for the pump is subject to change but ultimately it is shown that the power needed is quite small compared to the desalination process.

An alternate method is proposed to account for the desalination and pump energy costs. The electrical efficiency can be modified to accommodate for the energy needed for the pump and desalination units. By lowering the efficiency, making it require more energy to produce a kg of hydrogen, this can account for energy that needs to be used to power the auxiliary devices. Assuming that it costs 1 MW in total for both the pump and desalination units, that means the total plant power to be used for hydrogen production is 669 MW instead of 770 MW. By assuming the same electrical efficiency of as before (50 [kWh/kg H2]), the 669 MW plant produces 20 [kg] of hydrogen less than at full 770 MW. By modifying the electrical efficiency to compensate for the power needed for auxiliary units and produce the same amount of hydrogen for the 669 MW case while keeping the plant size the same, 770 MW, the new electrical efficiency is 50.07 [kWh/kg H2]. This is a relatively small change because the power needed to power the auxiliary units compared to full plant capacity is very small. According to [33] the electrical efficiency of a PEM electrolyzer can range 47-66 [kWh/kg H2], hence it is a safe assumption to make that the electrical efficiency of 50 [kWh/kg H2] already takes into account the power for auxiliary units.

C | Continued Economic Study and Resources

Figure C.1 is used to estimate the costs of the pipeline for different radius values. The line of best fit was used to estimate the .25 [m] and the .1[m] pipeline.

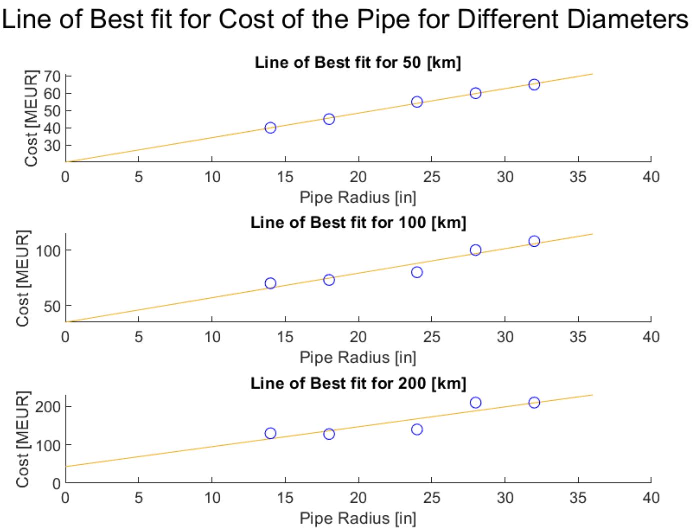

Figure C.1: Line of best fit for different distances and diameters

The sensitivity study that was implemented in the thesis revolved around taking the original parameter values and changing the parameter individually. Two parameters of the model that was changed was the diameter and the distance to shore. These parameters were changed one at a time and not both at the same time. This meant that the when the diameter was changed, the distance to the shore stayed at 50 [km] and when increasing the distance to the shore, the original diameter of .25 [m] was used. The goal of the sensitivity study was to see the effect that changing a single parameter has on the model. By changing two or more parameters, it could have a more significant effect on the losses and the economic difference in payback. By expanding on the sensitivity study by increasing/decreasing multiple parameters, the lifetime difference payback can be calculated based on the input parameters and the corresponding losses are also measured.

It was shown that pipeline favors distances compared to the electrical cables when comparing losses. In the economic feasibility study, it was shown that increasing the diameter or the distance to the shore increased the cost benefit, up to a point, but the losses themselves were never visualized or shown. The model is updated by setting the distance to shore and the pipe diameter respectively to 150 [km] and 0.35 [m].

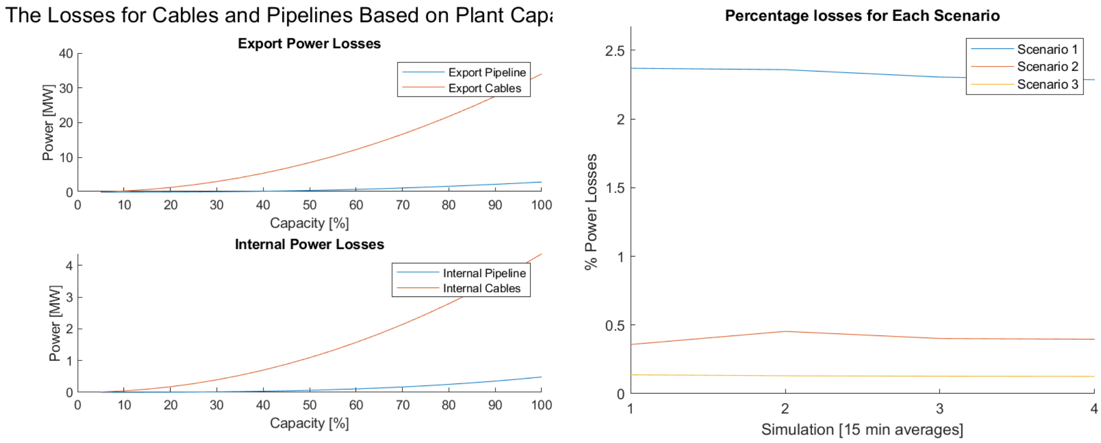

(a) Capacity Losses (b) Power Losses

Figure C.2: Setting the distance to the shore to 150 [km] and export diameter to .35 [m]

As seen from Figure C.2, it shows that the difference in losses effects are considerable. In addition to the change of diameter and distance to shore, the model is also up-scaled to 1050 [MW] and the results are shown in Figure C.3. By looking at the difference in losses for each scenario, the losses for 2 and 3 increased slightly while scenario 1 has increased significantly and shows how well the pipeline can handle the losses. For the difference in payback, that also benefits with the use of pipelines to about 181 [MEUR].

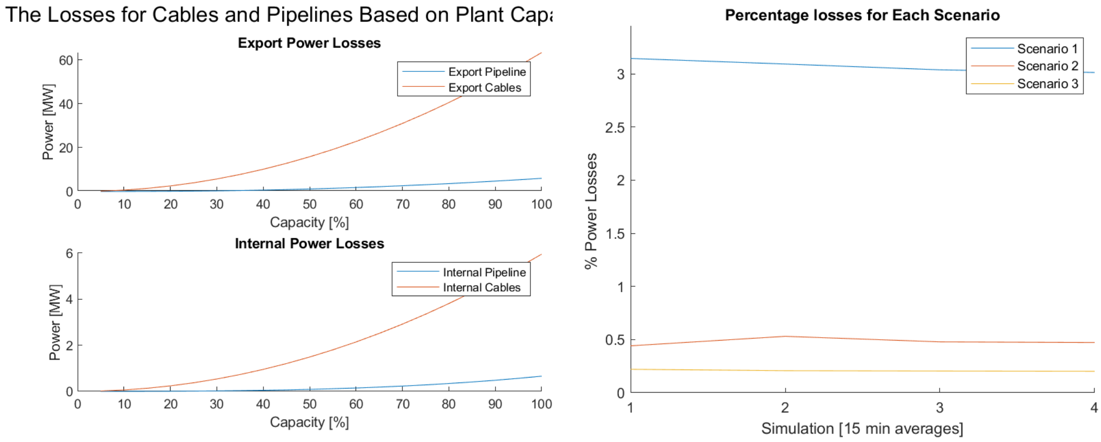

(a) Capacity Losses (b) Power Losses

Figure C.3: Up-scaling model to 1050 [MW]

D | CAPEX Considerations

When looking at the economics in chapter 7, the overall payback after a lifetime was not analyzed. Instead, the difference in payback for the different scenarios was compared. The difference when it came to capital costs for the different scenarios was only for the transportation. It was assumed that all other aspects would be kept the same, such as the support structures, desalination units etc. and the cost of maintenance was also considered the same since the topic of the thesis was specifically looking at transportation losses for the different production methods of hydrogen. For a more robust economic study, these considerations should have to be analyzed.

Different Combinations

To keep the model consistent and be able to compare the different losses for the scenarios, PEM electrolyzer has been used for each method of hydrogen production, even for onshore hydrogen production. PEM is more expensive per unit than an Alkaline electrolyzer[33]. As mentioned before, PEM electrolyzers needs maintenance less than Alkaline electrolyzers which would make it preferable to use for offshore purposes. For onshore hydrogen production, it could be advantageous to use alkaline electrolyzers as maintenance would be less of an issue onshore than offshore. Using a PEM electrolyzer would be 200-400 [USD/kW] (For 10 MW stacks) more than the Alkaline electrolyzer counterpart. A 770 MW of PEM electrolyzes plant would initially cost 15.4-30.8 million more USD than the Alkaline equivalent. By just looking at the lifetime difference in payback, that would be about the same price for a diameter of 0.25 [m] and a coastline distance of 50 [km]. This doesn't include the costs of maintenance. The prices of desalination units have not been mentioned, just the power consumption however there is a relation to the cost and power. When power increases so does the costs. As mentioned in appendix B, the desalination unit for brackish water would use less power and would result in lower costs. By having hydrogen production onshore, the use of this type of water becomes a possibility and would reduce the overall costs [17].

Each of the different methods of hydrogen productions explored in the thesis is assumed that just hydrogen is the product even for onshore hydrogen production where 100% of available power is used in the electrolysis process. When producing hydrogen on shore, the end product could be either electricity from the offshore wind farm or using the electricity to convert water into hydrogen if there is a demand for it. This system is called a hybrid system [34].

Pipeline prices

The costs of pipelines was based on [27] and is an estimate based on the main factors that contribute to the price besides the material type, the diameter and the length. The trend that was seen in the economic sensitivity study was that making the pipeline longer reduced the overall distance in payback and the normalized price [EUR/m] was cheaper for longer distances. The economic feasibility only focused on a single type of material and the uses of different materials could result in a cheaper a pipeline such as poly-ethylene. It was also assumed that were no obstacles in the way that the pipeline had to avoid resulting in either bends or increased distances which would impact the overall costs and losses.

Pipe Thickness

Another aspect that was not considered for the model was the thickness of pipes which would also play a role in the costs. The pipe should be handling both the design pressure and if the pipe was buried, the pressure of the environment has on the pipe. An example for the thickness calculation for a pipe to withstand internal pressures is written as, where t is the wall thickness, P is the design pressure, F is the design factor, D is the outer diameter, S is the minimum Yield Strength and E is the longitudinal joint factor. If the economic model were to continue, the thickness should be defined.

$$t = P * D / (2 * F * S * E) \tag{D.1}$$

Modifications to support structures

For the economic sensitivity study, it was assumed that the support structures were the same for each of the different scenarios. This might not be the case. The equipment for the needed electrolyer process adds extra weight for the support structure to compensate meaning that the support structure might have to be modified. This in result would cause an increase in costs. For the centralized offshore production, the individual support structures for each wind turbine would not have to be modified since there would be no extra weight, but for the case individual hydrogen productions, support structures might have to me modified to withstand the increased weight of the overall structure.

Bibliography

[1] N.O Jensen. 'A note on Wind Generator Interaction'. In: *Riso national laboratory* (Nov. 1983).

[2] M. Chaczykowski A. Osiadacz. 'Comparison of isothermal and non-isothermal pipeline gas flow models'. In: *Chemical Engineering Journal* (June 2000).

[3] S. Hamdi et al. 'Method of Lines'. In: *Scholarpedia* (Apr. 2009).

[4] A. et al Bergen. 'Transient electrolyser response in a renewable-regenerative energy system'. In: *International Journal of Hydrogen Energy* (Jan. 2009).

[5] Bart Ummels. 'Wind Intergration'. MA thesis. Tu Delft, 2009.

[6] G.Sieros et al. 'Upscaling wind turbines: theoretical and practical aspects and their impact on the cost of energy'. In: (Jan. 2012), pp. 1–17.

[7] C.Zheng et al. 'An overview of global ocean wind energy resource evaluations'. In: *Journal of Marine Science and Engineering* (Mar. 2015).

[8] Ibrahim Dincer et al. 'Review and evaluation of hydrogen production methods for better sustainability'. In: *Hydrogen Energy* (Jan. 2015).

[9] R. Getreuer. 'Preferred offshore power grids for wind energy'. MA thesis. Tu Delft, Aug. 2015.

[10] A. Benito et Al. 'Steady-state non-isothermal flow model for natural gas transmission in pipes'. In: *Applied Mathematical Modelling* (July 2016).

[11] J.Gonzales and R. Lacal-Arantegui. 'Technological evolution of onshore wind turbines—a market-based analysis'. In: (2016).

[12] M.Leimeister. 'Rational Upscaling and Modelling of a Semi-Submersible Floating Offshore Wind Turbine'. In: (May 2016).

[13] M. P. C. Bontekonig. 'Analysis of the Reduced Wake Effect for Available Wind Power Calculation During Curtailment'. MA thesis. Tu Delft, 2017.

[14] Wind Europe. 'The European offshore wind industry'. In: (Jan. 2017).

[15] M. Esteban et al. 'Gravity-Based Foundations in the Offshore Wind Sector'. In: *Journal of Marine Science and Engineering* (Mar. 2019).

[16] Y. Kikuch et al. 'Upscaling and levelized cost of energy for offshore wind turbines supported by semi-submersible floating platforms'. In: *Journal of Physics* (June 2019).

[17] M. Antonyan. 'Energy Footprint of Water Desalination'. MA thesis. University of Twente, June 2019.

[18] A. Bluis. *The Atmosphere: Getting a Handle on Carbon Dioxide*. 2019. URL: https://climate.nasa.gov/news/2915/the-atmosphere-getting-a-handle-on-carbon-dioxide/.

[19] Abu Dhabi. 'Future of wind: Deployment, investment, technology, grid integration and socio-economic aspects'. In: (2019).

[20] Y. Murakami. *Metal Fatigue*. 2019.

[21] D.Caine M.Liffe K.Kinsell W.Wahyuni and L.Bond. 'Dolphyn Hydrogen Phase 1- Final Report'. In: (2019).

[22] C.Kurrer. 'The Potential of hydrogen for decarbonising steel production'. In: *EPRS* (2020).

[23] C. Delbert. *2022 Toyota Mirai*. 2020. URL: https://www.popularmechanics.com/flight/airlines/a33768744/ammonia-as-jet-fuel/.

[24] Hugo Díaz and Carlos Guedes Soares. 'Review of the current status, technology and future trends of offshore wind farms'. In: *Ocean Engineering* 209 (June 2020). DOI: 10.1016/j.oceaneng.2020.107381.

[25] Office of Energy Efficiency. *Hydrogen Storage*. 2020. URL: https://www.energy.gov/eere/fuelcells/hydrogen-storage.

[26] Cummins Inc. *Electrolyzers 101: What they are, how they work and where they fit in a green economy*. 2020. URL: https://www.cummins.com/news/2020/11/16/electrolyzers-101-what-they-are-how-they-work-and-where-they-fit-green-economy.

[27] Miralda van Schot. 'A vision on hydrogen potential from the North Sea'. In: *North Sea Energy* (June 2020).

[28] M. V. Sickler. 'A Comparison of Performance between Regular and Irregular Wind Turbine Layouts'. MA thesis. Tu Delft, 2020.

[29] TNO. *From grey and blue to green hydrogen*. 2020. URL: https://www.tno.nl/en/focus-areas/energy-transition/roadmaps/towards-co2-neutral-industry/hydrogen-for-a-sustainable-energy-supply/.

[30] A. Elberry et al. 'Large-scale compressed hydrogen storage as part of renewable electricity storage systems'. In: *Elsevier* (Feb. 2021).

[31] M. Shields et al. 'Impacts of turbine and plant upsizing on the levelized cost of energy for offshore wind'. In: *Applied Energy* (June 2021).

[32] S. Ben-Achour. *How close are hydrogen planes, really?* 2021. URL: https://www.marketplace.org/2021/10/28/how-close-are-hydrogen-planes-really/.

[33] F.Camera. 'Green Hydrogen Cost Reduction'. In: (2021).

[34] G.Calado and R.Castro. 'Hydrogen Production from Offshore Wind Parks: Current Situation and Future Perspectives'. In: (2021).

[35] J. Jaeger. *Explaining the exponential growth of renewable energy*. 2021. URL: https://www.greenbiz.com/article/explaining-exponential-growth-renewable-energy.

[36] B. et al Pakenham. 'A Review of Life Extension Strategies for Offshore Wind Farms Using Techno-Economic Assessments.' In: *Energies* (Mar. 2021).

[37] Toyota. *2022 Toyota Mirai*. 2021. URL: https://www.toyota.com/mirai/features/mpg_other_price/3002/3003.

[38] E. Christantonis. 'Tri-Suction Pile Caisson Analysis of Soil-Structure Interaction'. MA thesis. TU Delft, Feb. 2022.

[39] Bart Ummels. Jan. 2022.

[40] N.E Woning. 'Application of Nacelle-based LiDARs for Model Validations of Wake and Blockage Effects in Offshore Wind Parks'. MA thesis. Tu Delft, Feb. 2022.

[41] Netherlands Enterprise Agency. *Operational wind farms in the North Sea*. URL: https://english.rvo.nl/subsidies-programmes/sde/offshore-wind-energy-sde/existing-wind-farms-north-sea.

[42] J. Kollwitz et al. 'DEFINING THE WAKE DECAY CONSTANT AS A FUNCTION OF TURBULENCE INTENSITY TO MODEL WAKE LOSSES IN ONSHORE WIND FARMS'. In: ().

[43] Herib Blanco. *Hydrogen production in 2050: how much water will 74EJ need?* URL: https://energypost.eu/hydrogen-production-in-2050-how-much-water-will-74ej-need/.

[44] Brunel. *The pros and cons of onshore and offshore wind*. URL: https://www.brunel.net/en/blog/renewable-energy/onshore-offshore-wind.

[45] *Calculating the Pressure Drop in a Pipe*. URL: https://www.pipeflow.com/pipe-pressure-drop-calculations.

[46] EnggCyclopedia. *Power and Efficiency Equations for Compressor Calculations*. URL: https://www.enggcyclopedia.com/2011/11/compressor-power-efficiency-equations/.

[47] Joe Evans. *Pump Efficiency—What Is Efficiency?* URL: https://www.pumpsandsystems.com/pump-efficiency-what-efficiency.

[48] IEA. *Offshore wind outlook 2019*. URL: https://www.iea.org/reports/offshore-wind-outlook-2019.

[49] Iha. *Pumped hydro*. URL: https://www.hydropower.org/factsheets/pumped-storage.

[50] Yuka Kikuchi. *Upscaling and levelized cost of energy for offshore wind turbines supported by semi submersible floating platforms*. The University of Tokyo.

[51] The Investopedia Team. *What Are the Types of Capital Expenditures (CapEx)?* URL: https://www.investopedia.com/ask/answers/112814/what-are-some-examples-main-types-capital-expenditures-capex.asp.

[52] The engineering Toolbox. *Pumping Water - Required Horsepower*. URL: https://www.engineeringtoolbox.com/pumping-water-horsepower-d_753.html.

[53] U.S.NRC. *Capacity factor (net)*. URL: https://www.nrc.gov/reading-rm/basic-ref/glossary/capacity-factor-net.html.

[54] David E. Watson. *Wind Turbine Power Coefficient*.